DEVELOPMENT OF AUTOMOBILE DISK BRAKE PADS USING ECO-FRIENDLY PERIWINKLE SHELL AND FAN PALM SHELL MATERIALS

BY

GABRIEL SIMON AMAREN

DEPARTMENT OF MECHANICAL ENGINEERING

FACULTY OF ENGINEERING

AHMADU BELLO UNIVERSITY,

ZARIA, NIGERIA

FEBUARY,2016

DEVELOPMENT OF AUTOMOBILE DISK BRAKE PADS USING ECO-FRIENDLYPERIWINKLE SHELL AND FAN PALM SHELL MATERIALS

BY

Gabriel SimonAMAREN B.Eng. (Uni Port) 1999M.Eng(Uni Port) 2007
Ph.D./ENG/14150/2007/2008

A THESIS SUBMITED TO THE SCHOOL OF POSTGRADUATE STUDIES,

AHMADU BELLO UNIVERSITY, ZARIA

IN PARTIAL FULFILLMENT OF THE REQUIREMENTS FOR THE AWARD OF THE DOCTOR OF PHILOSOPHY (Ph.D.) IN MECHANICAL ENGINEERING

DEPARTMENT OF MECHANICAL ENGINEERING,

FACULTY OF ENGINEERING

AHMADU BELLO UNIVERSITY,

ZARIA, NIGERIA

FEBUARY, 2016

DECLARATION

I declare that the work in this thesis titled“Development of Automobile Disk Brake Pads using Eco-friendlyperiwinkle shell and fan palm shellmaterials”has been performed by me in the Department of Mechanical Engineering under the supervision of Prof. S.Y. Aku, Prof. D.S. Yawas, and,Dr. M. Dauda. The information derived from the literature has been duly acknowledged in the text and a list of references provided. No part of this thesis was previously presented for another degree or diploma at this or any otherinstitution.

Gabriel Simon Amaren	_____	_____
Name of Student	Signature	Date

CERTIFICATION

This Thesis titled "Development of Automobile Disk Brake Pad using Eco-friendly Periwinkle shell and fan palm shellmaterialsby Gabriel Simon Amarenmeets the regulations governing the award of the degree of Doctor of Philosophy of Ahmadu Bello University, Zaria and is approved for its contribution to knowledge and literary presentation.

Prof. S.Y.Aku _____ _____ _____
Chairman, Supervisory Committee Signature Date

Prof. D.S. Yawas _____ _____ _____
Member, Supervisory Committee Signature Date

Dr. M. Dauda _____ _____ _____
Member, Supervisory Committee Signature Date

Dr. M. Dauda _____ _____ _____
Head of Department Signature Date

Prof. KabirBala _____ _____ _____
Dean School of Postgraduate Studies Signature Date

ACKNOWLEDGEMENT

I first thank God for continuous guidance from the beginning to the end of this research. I am extremely grateful to my supervisors; Professor S.Y. Aku the Chairman Supervisory committee, Professor. D.S. Yawas and Dr. M. Dauda for their willing cooperation and thorough supervision that finally led to the successful completion of this work. My appreciation also goes to Dr. Victor Aigbodion of University of Nigeria, Nsukkaand Engr. Omorogbe of Chemical Engineering Department of ABU, Zaria, for theircontribution to the experimentation.

I am grateful to all members of staff of the Department of Mechanical Engineering, Ahmadu Bello University, and Zaria for their assistance in one way or the other throughout the duration of this undertaking.

My sincere appreciation goes to all members of my family for their love, prayers, understanding and encouragement. My virtuous wife, Jessica Amaren, stood by me during this period. Our children Tirimwet, Awyn, Boaz (late), Mbehwmanaand Mbwehyau, -also stood with me to this point, I am grateful to them. I am also grateful to my parents Mr Simon Maren and Mrs Rifkatu Simon (Late) who have been my source of encouragement.

ABSTRACT

This research was conducted to produce asbestosfree automobile disk brake pads using eco-friendly; Periwinkle and Fan palm shells materials. The use of asbestos fiber is being avoided due to its carcinogenic nature that might cause health risks. A new brake pad was produced using agro waste materials (periwinkle shell and fan palmshells)with thermoset resin as a binder to replace asbestos with thermoset as a binder. Two sets of brake pad composites were produced using periwinkleshell and fan palm particles by varying the particlesizes from 125µm to 710µm. The morphology, physical, mechanical and wear properties of the brakepads werestudied. The mechanical properties upon addition of the agro waste improved. Theresults showed that the uniform distribution of the periwinkle shell and the fan palm particles in the microstructure of the brake pad composites is the major factor responsible for the improvement in themechanical properties,though the periwinkle shell pad had better properties. Taguchi technique was used to arrive at 65 % periwinkle or fan palm and 35 % resin as the optimal formulation, with thecorresponding manufacturing parameters as; (moulding pressure41 Kpa, moulding temperature 150 ºC, curing time 10 mins, and heat treatment time1hr.).Design expert software 6.0.8 was employed to on investigate the effect of particle size, speed, temperature and load the coefficient of friction. The design expert analysisshowed thatthe particle size, speed, temperature, loadshave significanteffect on friction coefficient.Brake pads developed from 125µm formulation for both periwinklesand fanpalm shell particlesexhibited better thermal and mechanical properties than those of fan palm shells andcompared favourably with that of commercial brake pad. Hence this research indicates that both periwinkles shell and fan palm particles can be effectively used as replacement for asbestosin the development of automobile disk brake padindicating 14.28%, 15.5 %, and 33.63 % increase in coefficient of friction, hardness, and compressive strength respectively than that of Mercedes Benz 230E salon car.

TABLE OF CONTENTS

LIST OF FIGURES

LIST OF TABLES

LIST OF PLATES

NOMENCLATURE

ASTM	American Society of Testing and Materials
($BaSO_4$)	Barium Sulphate
$CaCO_3$	Calcium Carbonate
Cc	Cubic Centimetre Cube
Cu	Copper
Cu_2S	Copper Sulphide
Cr_2O_3	Chromium Oxide
Cs	Coefficient of fluctuation
DTA	Differential thermal Analysis
EDX / EDS	Energy dispersive X –ray microscopy
FTIR	Fourier transform infra-red spectrometer
HBN	BrinellHardness Number
HRB	Brinell hardness tester on “B"
HRC	Brinell hardness tester on “C"
kg	Kilogram
Kα	K shell alpha electron
km	Kilometre
kN	Kilo Newton

kV	Kilovolts
kW	Kilowatt
mg	milligram
F&R	fade and recovery
(Fe_2O_3)	Iron oxide
NAO	Non asbestos Organic
Na_2O	Sodium Oxide
MgO	Magnesium Oxide
Mo	Molybdenum
N	Newton
MoS_2	Molybdenum disulfide
PAN	Poly-acrylo-nitrile
Pb	Lead
PbO	Lead oxide
PbS	Lead sulphide
(PKS)	Palm kernel shell
R	Radius of gyration
RPM	Revolution per minute

S	sliding distance in m.
SAE	Society of Automotive Engineers
Sb	Tin
SEM	Scanning Electron Microscopy
S/N	Signal to Noise Ratio
SRM	Standard Reference Material
TGA	Thermo-Gravimetric Analysis
µm	Micro metre
$\boldsymbol{\omega}$	Mean angular speed
µ	Miu
$\Delta \boldsymbol{E}$	Maximum fluctuation energy
ΔW	weight difference of the sample before and after the test in Kg
Wt	Weight
W_1	weight after immersion
W_o	weight before immersion
XRD	X-ray diffractograms
XRF	X-Ray Fluorescence
ZnO	Zinc Oxide
$ZrSi0_4$	Zirconium silicate

CHAPTER ONE

INTRODUCTION

1.1 BACKGROUND OF THE STUDY

Brake pads are important part of braking systems for all types of vehicles that are equipped with disc brakes. They are considered as one of the key components for the overall performance of a vehicle and as heterogeneous materials, they are usually made from more than 10 ingredients. An ideal brake friction material should have constant coefficient of friction under various operating conditions such as applied loads, temperature, speeds, mode of braking and in dry or wet conditions so as to maintain the braking characteristics of a vehicle. In addition, it should also possess various desirable properties such as resistance to heat, low water and oil absorption, low wear rate and high thermal stability, exhibits low noise, and should not damage the brake disc.

According toAnderson (1992), brake pads are steel backing plates with friction material bound to the surface facing the brake discBrake pads convert the kinetic energy of the vehicle to thermal energy by friction. During the application of brake, friction between brake pads and rotating disc causes a vehicle to stop by converting kinetic energy of the vehicle into heat energy, with a transfer of smallamounts of friction material to the disc, (that is why a brake disk has dull grey colour).The brake rotor and disk (both now with friction material on), will then "stick" to each other to provide stopping power, and it is this action of friction material against the disk that is responsible for stopping the vehicle. There are two types of brake systems, the disc and the drum. In disc brake applications, there are usually two brake pads per disc rotor, held in place and actuated by a caliper affixed to a wheel hub or suspension upright and are grouped into three viz: metallic, semi – metallic and organic.

Generally, brake pad consists of a composition of reinforced fibers, binder, fillers, and friction additives. All these constituents are mixed or blended in varying composition and brake pad material is obtained using different manufacturing techniques. Reinforced fibers increase mechanical strength of the friction material,the binder maintains the brake pads structural integrity under mechanical and thermal stresses. It holds the components of a brake pad together and to prevent its constituents from crumbling apart. Fillers in a brake pad improve brake pad's manufacturability as well as reduce the overall cost of the brake pad. Abrasives and lubricants are considered as friction additives; abrasives increase the friction coefficient, and remove iron oxides from the counter friction material as well as other undesirable surface films formed during braking. Lubricant stabilizes friction coefficient at high temperature. In addition to the function of these constituents, is the design of the brakes whichaffects heat flow, reliability and noise characteristics Chapman *et al.*,(1999)

In past years'(1908 -1960's), asbestos dominated the industry as the best friction material Blau (2001).Its content in vehicle brakes varies from 30%-70%. The positive characteristics of asbestos are thermal stability, and good strength and flexibility. But asbestos causes carcinogenic effects on human health.

Due to the increasing trend in the development of asbestos free brake pads, several research works have been carried out in the area of development of asbestos-free brake pads. The use of bagasse (Aigbodian*et al.,* 2010), palm kernel shell Dagwa and Ibhadode (2006) and palm oil clinker (Zamri*et al.,* 2011) have been investigated in order to replace the asbestos-free brake pad material. Current trend in the research field is the utilization of industrial or agricultural wastes as a source of raw materials for composite development (Leman *et al.,* 2008). This will provide more economical benefit and also environmental preservation by utilizing the waste of natural fiber. Thus it is in line with this trend that this work based on the development of automobile disk

brake pads using eco-friendly periwinkle shell and fan palm shell materials which are agricultural waste.

1.1.1 Periwinkle Shells

Periwinkle shell Plate 1.1 is a waste product generated from the consumption of a small greenish-blue marine snail periwinkle (*littorea*), housed in a V shaped spiral shell, found in many coastal communities within Nigeria and othertropical swampyregions of the world. The shell is a very strong, hard and brittle material. It is found in the lagoons and mudflats of the Niger Delta between Calabar in the South East and Badagry in the West of Nigeria. The edible part of periwinkle is eaten as sea food while the shell is disposed off as a waste, though few people utilize the shell as coarse aggregate in concrete in areas where neither stones and granite are not readily available for purposes such as; paving of water logged areas, for homes, soak-away, slabs and road construction. However, a large amount of these shells are still disposed off as waste and withthe disposal already constituting a problem in areas where they cannot find any use, the use of this material in the development of an automobile disk brake pad will reduce or eliminate this environmental nuisance.

Plate1.1Photograph of periwinkle shells

1.1.2 Fan Palm (*hyphaenepetersiana*)

Fan palm shown in Plate1.2a belongs to the family of (*Hyphaene*) found in savanna habitats of Africa. It has large gray- green, leaves with stiff segments that are held in a rounded crown atop a massive trunk that can reach 25 m (80 ft.) tall and is usually swollen in the middle. Mature plants carry large round seed see Plate 1.2 andit is highly drought resistant and very adaptable to most weather conditions.Mats, hats and baskets are made from the leaves, the hard white kernel of the seed, termed vegetable ivory, are carved into small ornaments and buttons.

(a) Fan palm Tree (b) Fan Palm Fruit

Plate 1.2Photograph ofFan palm tree and fan palm fruit

1.2 STATEMENT OF THE PROBLEM

The problem identified by this research is health risk associatedwith the use of asbestos as a friction material and theincompatibility of thenumerous materials currently used in the development of an asbestos free brake pads. Some of these health risksinclude; Asbestosis, Lung cancer, Mesothelioma (a cancer of the linings around the lungs and abdomen), non-cancerous diseases that affect the linings around the lungs and abdomen (commonly called 'benign pleural diseaseas identified by Dagwa and Ibhadode, (2005).Although several alternative materialssuch as; mineral fibers, cellulose, aramid, poly-acrylo-nitrile (PAN), chopped glass, steel and copper fibers have been used to developed asbestos free brake pads,however, the incompatibility the numerous used in the replacement of asbestos brakes is also a challenge.

Consequent upon the health risk associated with the used of asbestos and the incompatibility of thenumerous ingredients used in the replacement of asbestos as a friction material, the need to develop an asbestosfree brake pad with only 2 ingredients and still maintaining the recommended physical, thermal and mechanicalproperties of a brake pad still remains a challenge to the engineer which the works sought to address.

1.3 THE PRESENT RESEARCH

The present research has been able to overcome the health risk associated with use of asbestos in the development of friction material by using only two (2) materials to develop an eco-friendly brake pad and still achieve the recommended (0.3 to o.35) range of coefficient of friction.

1.4 AIM AND OBJECTIVES OF THE STUDY

The aim of this research is to widen the scope of locally sourced eco-friendly materials that may be used for production of asbestos – free brake pads.

The specific objectives of this study are:

i. To determine physical thermal and chemical properties of periwinkle and fan palmshells using characterization techniques such as thermo gravimetric analysis (TGA), Scanning electron microscope (SEM), X-ray diffractograms (XRD) and X-Ray Fluorescence (XRF).

ii. To determinetheoptimum periwinkle or fan palm particle size for the formulation of brake pad

iii. To employ Taguchi method to optimize the friction material formulation and the manufacturing parameters.

iv. To determine the physical, mechanical; (hardness, compressive stress friction and wear), chemical and thermal properties of the formulated brake pads.

v. To carry out laboratory and vehicle performance test for the developed brake pad and compare the results with those of a commercial brake pad for the Mercedes Benz 230E salon car

1.5 SCOPE OF THE STUDY

Experiments were conducted under laboratory conditions to determine the mechanicalproperties (coefficient of friction, wear,compressive strength, hardness strength, oil and water/absorption), thermal properties (thermo gravimetric analysis), the elemental composition of the base materials by using and characterization of the developed brake padsby using Scanning electron microscope (SEM), X-ray diffractograms (XRD) and X-Ray Fluorescence (XRF) of the.The laboratory and vehicle performance test for the developed brake pads were carried out and the resultswere compared favorably withthose in the literature and of the commercial brake pad for the Mercedes Benz 230E salon car.

1. 6 SIGNIFICANCE OF THE STUDY

The significance of the study is enormous but most importantly it is:

I. To encourage the development of small scale industries in Nigeria. Small scale industries play a vital role in the socio- economic development of any country. They strengthen the economy of a nation by utilizing its productive resources with minimum capital investment. The main objective of such a process lies in the absorption of the surplus amount of labour which would not have been absorbed by capital intensive industries. This in turn, helps in scaling down the level of unemployment as well as poverty.

II. To increase Nigerian local content, in the automobile industry: local content means the development of skills, technology transfer, use of manpower and local manufacturing techniques. All the present day industrialized nations are what they are because they have been able to develop skills, apply technology transfer, and use local man power and local manufacturingtechniques and materials Thus the

production of brake pads material from locally sourced raw materials will encourage local content development in Nigeria.

III. To produce cheaper brake pads: With locally sourced raw materials it is expected that both the cost of materials and production will be low resulting tocheaper brake pads.

IV. *Economic and Weight Reduction:* Periwinkle shells and Fan palm shells can be obtained at a lower cost compared to the present materials used in the manufacture of brake pads. In addition, their low density of 1.12 (g/cm^3) and 0.99 (g/cm^3) has the potential of reducing the weight of the brake pad which will lead to the reduction of vehicle weight. This in turn will reduce fuel consumption resulting in less carbon dioxide emission, lower greenhouse effect and reduction in global warming.

V. *Health Risk:* It is known that asbestos is carcinogenic. However available literature and results obtained from the XRD tests show that both periwinkle shells and fan palm shells do not contain any harmful substances Amaren*et al.*,(2013).

VI. *Added Value:* The use of the aforementioned materials in the production of brake pads will encourage the breeding of periwinkles for food, meat and their shells, which have been an environmental nuisance, will be of value.

VII. *Renewable Resources:* Periwinkles and fan palms shells are renewable and have high potential availability.

CHAPTER TWO

LITERATURE REVIEW

2.1 HISTORICAL DEVELOPMENT OF BRAKES

2.1.1 MechanicallyOperated Brakes

The history of brakes dates back much further than those of today's internal combustion engine. Even the early Phoenicians made use of simple devices for slowing down their war chariots. Also, the coaches of the 18th and 19th centuries used brake shoes or wedges on chains Keon*et al.*, (2008). However, in the earliest days of the automobile industry and at the end of the 19th century, brakes tended to be regarded as an insignificant item of auxiliary equipment with the engineers of that time devoting all their energies in developing more powerful internal combustion engines without considering their braking systems.For instance, WilhelmMaybach used most of his energy in boosting the speed of the four-stroke engine from 180rpm to 600rpm without considering the braking system Bert and Karlheinz, (2006).

In 1885, the Reitwagen built by Maybach and Gottlieb Daimler had a maximum speed of 12km/h. Friction in the drive chain was so high that it slowed vehicles without brakes. Against this background, nobody considered braking a steering axle or a steered wheel, because of the design complexity involved. As a result of these, early day vehicles were dominated by band brakes, block brakes, or wedge brakes, which the driver operated manually using cranks, levers, rods, or cables. Such devices were not specially designed; they were simply carried over from the horse-drawn carriages of the time, with the brake acting on the rigid, driven rear axle (Blau, 2001, and Kim *et al.*, 2003).

In 1887, the three-wheel patent motor car used by Carl Friedrich Benz employed brakesband brakes, block brakes or wedge brakes. However, in 1902, other wheel brakes were developed although still purely mechanically actuated, were far more efficient and met rapid acceptance among the pioneer automobile manufacturers. Lanchester invented the disk brake, and the drum brake as a result of the Louis Renault internal shoe brake and the Mayback external band brake. However, it took some 50 years for the disc brake to be used on vehicles in the form of the hydraulic partial contact disc brake (Kim *et al.*, 2003). Up to 1950, drum brakes were the main type of brakes installed in vehicles with the internal shoe brake increasingly replacing the external band brake.

According to Nicholson (1995) Herbert Froodis credited with inventing the first brake lining materials in1897.It was a cotton-based material impregnated with bitumen solution and was used for wagon wheels as well as early automobiles. His invention led to the founding of the FerodoCompany, a firm that still supplies brake materials today. The first brake lining materials were woven, but in the 1920's these were replaced with molded materials that contained chrysotile asbestos fibers. These plentiful mineral resin-bonded metallic linings were introduced in the 1950sand by the 1960s the so-called 'semi-metals'were developedBertand Karlheinz (2006).

The mechanical internal shoe brake used an expander lever to push the brake shoe against the inside of the drum, which was directly connected to the road wheel. However,with the increase in engine performance and speed, rear axle brakes and transmission breaks were no longer efficient. Thus in 1920, the first vehicle with four-wheel brakes appeared in the market. This complex system had up to 50 joints, 20 bearings and 200 components Tatarzicki and Webb (1992). The complexity of the system led to uneven braking forces on the vehicle wheels. In spite of this draw back many automobile manufacturers

continued to use the mechanical four-wheel drive leading tothe gradual development of various brake materials as shown in Table 2.1

Table 2.1 HistoricalDevelopment of Automotive Friction Brake Materials (Nicholson, 1995)

Material description	Application (s)	Approximate year
Cast iron on steel	Railroad car brake blocks and tires	Prior to 1870's
Hair or cotton belting (limited by charring at about 300^0F)	Wagon wheels and early automobiles	ca. 1897
Woven asbestos with brass and other wires for increased strength and performance	Automobiles and trucks	ca. 1908
Molded linings with shorter chrysotile fibers, brass particles, and low-ash bituminous coal	Automobiles and trucks	ca. 1926
Dry-mix molded material to replace cast iron brake blocks that produced metallic dust that shorted electric train rails	London underground	ca. 1930
Flexible resin binders developed along with more complex formulations	Brake drum linings	1930's
Resin-bonded metallic brake linings	Industrial and aircraft applications	1950's
Glass fibers, mineral fibers, metal fibers, carbon and synthetic fibers to provide semi-metallic with higher performance than asbestos (beginning of safety issues with asbestos)	Automotive and trucks	1960's
Non-asbestos (fiberglass) materials	Brake drums on original equipment cars	1980's
Suggested use of carbon fibers	Automotive brakes	1991

ca - usedwithadate to approximatetimee.g., around, near or about that time.

2.1.2 The Hydraulically Operated Four-Wheel Brake

It was the California-based mining engineer Malcolm Loug Head(who later changed his name to Lockheed) that originally invented the hydraulically operated four-wheel brake. In 1917, he patented a hydraulic wheel brake cylinder for cars thatwere operated with brake fluid (Tsang *et al.,* 1985, Nicholson, 1995).

This wheel brake cylinder and the foot operated master brake cylinder for which Loug Headreceived a patent in 1920 formed the crucial elements of the “hydraulic brakes” that are in use today. In this system, foot pressure on the brake pedal causes hydraulic fluid to be displaced from the master cylinder by a piston andis transmitted to the wheel cylinders by pistons and hoses. In accordance to Pascal principles the fluid transmits the muscular forces from the driver evenly throughout the closed brake tube system in the form of hydraulic pressureBert and Karlheinz, (2006).. This vastly reduces the risk of brake pull associated with the mechanically operated brakes. A further advantage over mechanical brakes lies in the considerably improved efficiency of actuation between 0.8 and 0.9 as compared to 0.4 to 0.5 obtained in the mechanically operated brakes. The first car to use this braking system was Chrysler 70 in 1924. The deficiencies of mechanically operated four wheel brakes brought a number of competing systems since the early 1920s alongside hydraulic brakes. For instance, there were the combined hydraulic/mechanical brakes which used hydraulic equipment in place of mechanical equipment to balance the braking force Tatarzicki and Webb (1992).

2.1.3 Brakes with Internal Amplification

Although the greater efficiency of the hydraulic brake reduced the pressure needed to operate it compared than the mechanical systems, but the fact that cars were constantly becoming heavier and faster meant that the engineers were still faced the challenge of developing an effective braking system. In their efforts to develop better braking systems, different designs of self-servo and servo assisted brakes that required less pressure at the pedal, were produced Nicholson(1995).

As a solution to this ineffective braking system, ATE Reynolds brake was developed in 1927/1928. In their construction, the brake fluid acted on the pistons of one-wheel brake cylinder and was transmitted over the brake shoe to a second wheel cylinder whose piston

again multiplied the braking force. In 1936, the duplex brake was developed. This system featured two wheel cylinders that introduced the braking force independently, thus making it possible to have two leading shoes and thereby increasing the braking efficiently in one direction (forward). However, when reversing, the braking efficiency was reduced as the system resulted in two trailing brake shoes. This problem was surmounted by the duo duplex brake featuring two dual cylinders Kato and Soutome (2001). Next was the servo brake introduced in 1950 which was based on the simplex brake with a single wheel cylinder which transmitted the frictional force of the leading brake shoe to the trailing shoe over a support that moves over in one direction only, thus achieving lower actuation forces coupled with greater breaking efficiency Gudmand-Hoyer *et al.*,(1999).

2.1.4. Multi-Circuit Braking System

The hydraulically operated braking system undoubtedly was more advanced compared to the mechanically operated brakes. But in the early years, their lack of thermal stability was a significant short coming. When placed under heavy loads, for instance during long downhill stretches, it was possible for the brake fluid which could not be compared with present high performance fluids, to develop vapor bubbles that were able to be compressed. In the 1920's, brake circuits were not the split types, thus pressing the brake pedal had no effect as insufficient hydraulic pressure or no pressure at all was transmitted to the wheel brakes. This situation ushered in the split circuit braking system in the 1930's which ensured that at least two wheel brakes remained operationalif one circuit fail Gudmand-Hoyer *et al.*,(1999).

2.1.5 Full Power Brakes

After World War II, cars became heavier and faster, and despite advances in the field of wheel brakes the forces required to operate mechanical brakes continued to increase.

Thus, there was the need to search for ways of improving the braking force generated by the driver in the hydraulic system. To achieve such objective, generators were developed that generated excess pressure using either hydraulic or pneumatic means. The driver then introduces this pressure to the breaking system gradually by pressing the brake pedal without actually using his muscle power to generate the braking force. All these brakes were mostly made from steel Gudmand-Hoyer *et al.*,(1999,).

2.2 BRAKEMATERIALS AND ADDITIVE FUNCTIONALITY

Brake pad materials and shoe additives serve a variety of functions and their composition is important to the performance of a braking system. According to Nicholson (1995) it is conventional to list compositions of brake additives, but not all authors do so. Brake materials and additives can be grouped based on their expected functions as follows; abrasives, friction modifiers, fillers, reinforce and binder materials.

2.2.1 Abrasives

Abrasives as shown in Table 2.2 help maintain the cleanliness of mating surfaces and control the build-up of frictionfilms. They also increase friction, particularly when initiating' a stop (i.e., they increase "bite") (Nicholson, 1995).

Table 2.2 Some Common Abrasives Used in Brake Pad(Nicholson, 1995)

Abrasive Material	Description	Reference(s)
Aluminum oxide	when in ;(1) hydrated form it is added as a polishing agent and for wear resistance, (2) in anhydrous form it is more abrasive,	Nicholson (1995)
Iron oxides	When in; (1) Hematite (Fe_2O_3) form can act as a mild abrasive; (2) magnetite (Fe_3O_3) form mildly abrasive	Nicholson (1995)
Quartz	Crushed in mineral particles (SiO_2) form is abrasive	Eriksson and Jacobson (2000)
Silica	May be natural or synthetically-produced (SiO_2)	Hooton (1969)
Zirconium silicate	(ZrSi04)	Jang and Kim (2000)

2.2.2 Friction Producers / Modifiers

These materials lubricate, and increase the friction properties, or react with oxygen to help control interfacial films. The list of common friction producers/modifiers are shown in table 2.3.

Table 2.3 Lists of common friction producers/modifiers(Oak ridge National laboratory- USA)

Material	Description/Comment	Reference(s)
Carbon (graphite)	Cheap and widely-used; but there are many forms and sources, some of which can contain abrasive contaminants; burn in air at >700^{0}C, friction level is affected by moisture and structure	Spurr(1972), Nicholson (1995)
Ceramic "microspheres"	Special product consisting of alumina-silica with minor iron or titanium oxides; size 10-350 μm, low-density filler said to reduce rotor wear and control friction; claimed to also absorb rotor dust; 5-10% vol. leading type.	PQ Corporation (1993)
Copper	Used as a powder to control heat transfer but can cause excessive cast iron wear	Nicholson (1995)
Friction dust	Commonly consists of processed cashew resin, may have a rubber base; some additives used to reduce spontaneous combustion or help particle dispersion.	Nicholson (1995)
Friction powder	May consist of Iron (Fe) sponge, e.g. for semi-metallic brake pads; a number of different particle grades (sizes) are available depending on requirements for surface area, light-medium-heavy duty vehicle applications.	Heogenaes (1990)
Lead oxide	Lead oxide (PbO) has been used as a friction modifier, but has toxicity concerns	Nicholson (1995)
Metal-fluxing compounds	Lead (Pb),Tin(Sb), Bismuth (Bi),Molybdenum (Mo), as fluxing compounds serve as oxygen getters to stabilize friction-induced films and help to keep them from getting too thick	Hooton (1969)
Metal oxides	Magnetite (Fe_3O_4) improves cold friction; Zinc oxide (ZnO) lubricates but can cause drum polishing; Chromium oxide ($Cr_2O_{3)}$ raises friction	Nicholson (1995)
Metal sulfides-various	Copper sulphide ($Cu_2S_{1)}$ Tin sulphide ($Sb_2S_{3),}$Lead sulphide (PbS); studies show the effect of additives on disc brake pads with and without metal fibers; modify and stabilize the friction coefficient; highest μ for Tin (Sb) 0.47-0.49, next Tin sulphide(PbS) 0.40-4, most variable forCopper (Cu) 0..36-0.52) – wear worst for copper sulphide(Cu-S)	Gudmand-Hoyer, *et al*. (1999)
Mineral fillers	Causes the coefficient of friction (μ) to be roughly proportional to Mohs hardness which has a maximum index of 10, however, too much mineral filler tends to wear the counter-face	Spurr(1972)
Molybdenum disulfide	Molybdenum disulfide (MoS_2), a typical layer-lattice-type lubricant	Spurr (1972)
Petroleum coke	Low-cost, can lower friction, low ash	Nicholson (1995)

2.2.3 Fillers, Reinforcements and Miscellaneous

Fillers are used to maintain the overall composition of the friction material, and some have other functions as well. They can be metals, alloys, ceramics, or organic materials. The list of common fillers and reinforcementsis shown in table 2.4.

Table 2.4 Lists of common fillers and reinforcement used in brake pad(Oak ridge National laboratory- USA)

Material	Description/Comment	Reference(s)
Anti-oxidants	Help to maintain the proper oxide film thickness on aircraft brakes – too much oxide leads to unstable friction (high at low speeds) and thick films that can wear off too readily, graphite is common in metal ceramic composite brakes	Hooton (1969)
Asbestos	Most common filler in early brake materials	Spur (1972), Rhee (1974), Nicholson (1995)
Barium sulfate ("barites")	(BaSO4) basically inert, but increases density and may aid in wear resistance, stable at high temperature	Nicholson (1995)
Calcium carbonate	CaCO3 is a lower cost alternative to barites, but not quite as stable at high temperatures	Nicholson (1995)
Cashew nut shell	Resilience in the binder system and reduces brake noise (See friction dust in Table 2.3)	Nicholson (1995)
Cotton	Reinforcing fiber for the matrix	Spurr (1972)
Fibers-mixed oxide	Reinforcement fibers, produced from a base slag glass mineral wool, can contain, for example, a mixture of silica (40-50 wt%) alumina (5-15wt.%), calcia (34-42wt%), magnesia (3-10 wt%), and other inorganics (0-7 wt%); function is to control fade and increase braking effectiveness	Sloss (1996)
Lime	Ca(OH)2 is used to control corrosion in Fe-additives, and , brake fade at high temperatures	Nicholson (1995)
Potassium titanate	Inert filler material; also, an insulator and structural participant to replace the role of asbestos	Jang and kim(2000)
Rubber-diene, nitrile	Used as stabilizers to promote cross-linking and increase wear resistance in polymer composite brake materials containing asbestos fibers; rubber also modifies the compressibility (modulus/stiffness)	Gong *et al.*,(1985)
Rubber scrap	Ground up tires ("tire peels"), decreases cost, must not contain road dirt	Nicholson (1995)
Sea coal	General low-cost particulate filler, may contain harmful ash; not good for high temperatures	Nicholson (1995)
Zinc oxide	ZnO imparts some wear resistance, but can polish drums	Nicholson (1995)
Palm Kernel shell	A reinforcement, use to maintain the overall composition of the friction material	Ibhadode and Dagwa (2008)
Bagasse	A reinforcement, use to maintain the overall composition of the friction material	Aigbodion*et al.*, (2010)

2.2.4 Binder Resin (matrix)

The purpose of a binder is to maintain the brake pads' structural integrity under mechanical and thermalstresses. Typical binder materials are shown in table 2.5

Table 2.5 Resin used in brake pad formulation(Nicholson, 1995)

Resin	Description	Reference(s)
Phenolic Resin	Common binder; too little material weakness ;if too much is used, there is a friction drop-off at high temperatures; the degree of polymer cross-linking affects behavior	Spurr(1972
Metallic alloys of Cu,Fe, Ni	Use in Aircraft brakes due to their high-temperature characteristics	Hooton (1969); Tatarzyck*et al.*,(1992)
Modified resins	Modified resins improve bonding characteristics of binderand increase temperature resistance. Examples include;cresol, epoxy,Novolacresins.	Borden (1994)

2.3 REVIEW OF PAST WORKS

Seong and Ho (2000) in their study of friction and wear of friction materials containing two different phenolic resins reinforced with aramid pulp, they investigated the friction and wear characteristics of automotive materials containing two different phenolic resins (a straight resin and a modified novalac resin) using a pad-on- disk type friction tester. Two different test modes were employed to examine the friction characteristics concerning accumulated thermal history (a constant initial temperature test model I) and a constant interval test model II. Friction characteristics such as friction stability and wear resistance changed significantly according to the type of phenolic resin and the amount of aramid pulp. Friction materials with modified novalac resin showed better friction stability than those with unmodified novalac resin. In particular, the friction materials that were reinforced with 10% of aramid pulp showed substantial improvement on friction stability regardless of the resin type. However, the friction materials with the modified

resin showed significant reduction in wear resistance. The study did not compare theresult obtained with the recommended range for coefficient friction ofcommercial brake pads.

Blau.(2001) worked on friction layer formation in a polymer composite material for brake applications. The characterization of the properties of polymer matrix composite friction layer was carried out. It was shown that the friction layer character determines the friction performance of the investigated composite material. The structure and chemical composition of the friction layer generated on the friction surface differs significantly from the bulk material. Mechano-chemical interactions occurring in the friction process were compared to a “non-friction” situation where equivalent apparent temperature and compressive loading respectively were applied to the same material. No simple relationship existed between the composition of friction layer and bulk materials formulation. However, phase stability and kinetics of interactions for friction and equivalent non-friction loading conditions differ significantly. The test condition (temperature, speed, and load) at which the friction layer of the composite material was investigated seem not to have been considered.

El-Zahraa*et al.,* (2003) used metallic powders of iron, copper and aluminum to develop new composite friction materials. The frictional behavior of the composite materials as well as wear resistance was investigated at a load of 15N with a rubbing velocity of 5m/s. The effect of braking time on friction and wear was studied. It was found that the composite containing 45% wt of phenolic resins, and 1% wt of aluminum as well as composite containing 50% wt of phenolic resins and 22.5% wt of iron displayed higher friction coefficient than asbestos based materials. However, the drawback of using steel fibers is that they will rust especially if the vehicle has an extended rest period or its operating near costal area.

Gopal*et al.*,(2003) used a chase friction material testing machine in studying fade and wear characteristics of a glass fiber-reinforced phenolic friction material. At low counter facetemperature, the friction material showed relatively high friction range of 0.4 to 0.5. However, during the fade test the coefficient of friction dropped to about 0.18 at 343^0C. Reconditioning the surface at the end of fade tests altered the frictional behavior during subsequent fadetests. The wear test showed that the specific weight loss per unit load and sliding distance decreases with increasing applied load and speed, but increase with increase in bulk drum temperature. At high temperature, thermochemical degradation and fiber pull-out appear to contribute to higher specific wear rate. The worn surface of the specimen were observed by scanning electron microscopy and analyzed by energy-dispersive x-ray analysis. The results were consistent with low friction coefficients due to film formation on the worn surface of glass fiber at high temperature.However,the drop of friction from 0.5 to 0.18 at temperature of 343^oCwhich is lower than the average breaking temperature of 450^oCshow that at normal brake pad operating temperature the coefficient of friction drops.

Jiaand Ling (2003) carried out an investigation of friction materials reinforced by brass fibers, and the influence of the organic adhesion agent, cast-iron debris, brass fiber, and graphite powder on the friction-wear characteristics were studied. Friction and wear tests were carried out on a block-on-ring tribometer. The friction pair consisted of the friction material and gray cast iron. The worn surface layers formed by sliding dry friction were examined using scanning electron microscopy (SEM), X-ray energy-dispersive analysis (EDX), and differential thermal analysis-thermogravimetric analysis (DTA-TGA). The experimental results showed that the friction coefficient and the wear loss of the friction materials increase with the increase of cast iron debris, but decrease with the increase of graphite powder content. The investigation also showed that friction coefficient and wear

loss also increased slightly when the mass fraction of brass fibers was over 19%. However, when the mass fraction of organic adhesion agent was about 10-11%, the friction materials had excellent friction – wear performance. The study did consider the effect of the particle size of the material used on the performance of the developed friction material.

Satapathyand Bijwe (2004), carried out a study of the friction materials based on the variation in the nature of organic fibers, fade and recovery behavior. They investigated the influence of four selected organic fibers viz, aramid (AF) and poly-acrylo-nitrile (PAN) on the N-fade and N-recovery behavior. It was observed that the carbon fiber based composite showed the highest resistance to N-fade whereas the composite base cellulose fiber showed the least resistance. The recovery behavior of all the composites were more than 100% and the extent depended on the type of fiber inclusion. The composites containing AF and SF showed the highest and lowest resistance, respectively, while the lowest friction coefficient were recorded for SF and CF based composites, respectively.

Dagwa and Ibhadode (2005) developed asbestos free friction lining material from palm kernel shell. In their study the mechanical and physical properties as well as the static and dynamic performance compared well with commercial asbestos-based lining materials.However, more pad wear was observed on the PKS pad at high vehicular speeds beyond 80km/hour which suggest thatPKS is not suitable in the formulation of brake pads meant for high speed cars.

Bhabani and Jayashree (2006) worked on sensitivity of friction and wear on composite friction materials made of organic fibers. The sensitivity of friction and wear behavior of selected composites based on variation in inclusion of organic fibers, viz: aramid, PAN,

carbon and cellulose to braking pressure and sliding speed were investigated. The sensitivity of coefficient of friction and wear to the operating variables (temperature, breaking force, and speed)were carried out on a subscale brake rig. The results showed that the inclusion of cellulose fiber increased the friction coefficient, while aramid fiber improved the wear resistance. The values of friction and wear of the developed composite material were not compared with the recommended values and the quantities of the cellulose fibre and aramid added were not optimized.

Shaoyang and Fuping (2006), compared the friction and wear performances of some brake material dry sliding against two aluminum matrix composites reinforced with different sizes (3.5 and 34 μm) of SiCp particles respectively, in place of the conventional cast iron drum for a chase machine. It was shown that the friction coefficient decreased with the increase in load and speed. It was also shown that friction fade took place at high temperatures, followed by excellent recovery upon cooling. The specific wear rate was found to increase with increase in load. The study did not specify the composition friction materials in question.

Zmago*et al.,* (2007) studied the friction and wear of sintered metallic brake linings on a carbon/carbon-silicon carbide (c/c-sic) composite brake disc. The friction characteristics were examined by a dynamometer on two different commercial motorcycles – brake systems. The influence of components such as graphite and abrasive in the metallic matrix on the formation of the friction layer was investigated using a scanning electron microscope (SEM) equipped with energy dispersive X –ray microscopy (EDX). The Friction layer formed on the pads sliding surface by oxidation wear, which consisted mostly of iron and copper oxide was confirmed. The friction properties of the sintered metallic brake pads were determined and related to the composition and structure of the

brake lining. These results needed to be compared with the recommended values for commercial brake pads

Ganguly and George (2008), carried out a study on an asbestos free friction material composite containing fibrous reinforcing constituents, friction imparting and elastomeric additives, the composites showed high wear resistance and good thermal conductivity. However,study was not carried out on the friction behavior of the composite..

Ibhadode and Dagwa (2008) developed an asbestos – free friction lining material from palm kernel shell. Taguchi optimization technique was used to achieve optimal friction material formulation and manufacturing parameters. The laboratory brake pads were tested for wear and effectiveness on a car and when compared with premium asbestos – based commercial brake pad they were found to perform satisfactorily. However, the study recommended that PKS particle of size lower than the 125µm could be used to develop brake pads for vehicles with higher vehicular speed. Also the use of copper chip as one of the ingredients poses some health challenges as itis known to be associated copper toxicities.

Dilip*et al.,* (2008) carried out the analysis of load- speed sensitivity of friction composites based on various synthetic graphites. The sensitivity of coefficient of friction of composites containing synthetic graphite with different particle sizes to braking pressure and sliding speed was investigated. The studies were carried out on a subscale brake testing machine following 4 loads x 3 speeds experimental design. The best performance was obtained from composites containing synthetic graphite having average passive size of 410µm. Other particle sizes which resulted in good performance were 38 and 169µm. Very fine particle size was not beneficial for desired combination of performance properties. The regression analysis coefficient of friction on orthogonal L9 (3x3)

experimental design method revealed that the first order influence of sliding speed and braking pressure were significant. The study is not in conformity with the Hall- Petch law which states that the strength of materials increases as the particle size decreases as it is evident that friction composite with particle size of 410μm performed better that those with 169μmRajiv et el., (2006).

Jayashree*et el.,* (2008), studied the effect of brass fibers in increasing amounts on the friction and wear performance of non-asbestos organic (NAO) friction composites. Four friction materials based on parent composition and with varying amounts of brass and barite were developed as brake pads, and characterized for physical, chemical and mechanical properties. They were further tested for their friction and wear behavior in the fade and recovery (F&R) modes on a Krauss machine as per ECE R90 schedule. In addition, small specimen (24mm x 24mm) of the brake pads were evaluated by studying their friction sensitivity for loads and speeds in a simulated braking condition against a commercial disc on a reduced scale prototype (RSP). Results showed that composites with 8 % brass fiber where thermal conductivity (TC) was not highest proved exhibited the best combination of performance parameters related to friction and wear in both testing modes. The study was limited to friction sensitivity and did not consider wear sensitivity at loads and speed.

Adewuyi and Adegoke (2009): Carried out a study on the potentials of periwinkle shell as a coarse aggregate for concrete. It was discovered that design mix with compressive strength of 26.67 N/mm^2, 19.50 N/mm^2 and 19.83 N/mm^2 at 28 days' dehydration period, met the ASTM – 77 recommended minimum strength for structural weight concrete. The study is limited to compressive strength of mix rather than the requirement of friction material.

Kukutschova*etel.*, (2009) investigated the wear mechanism in automotive brake materials, wear debris and its potential environmental impact. A model semi metallic brake lining was subjected to a full scale automotive brake dynamometer test. The structural properties and surface topography of brake linings were analyzed at different stages of wear testing and correlated to frictional performances. The characteristic of wear particles were investigated. A combination of abrasive and adhesive wear with oxidative processes dominated the friction process. It was observed that the characteristics of the layer depend mostly on surface temperature, normal pressure and sliding speed. It was also shown that wear rates and friction levels depend on the chemistry, structure and hardness of the friction layer covering the surface of the pad or the disc. The various friction materials used in this study were not mentioned; hence it became difficultto know how the various material constituents influence the wear mechanism.

Gurunath and Bijwe (2009), worked on the potential exploration of novel green resins as binders for non-asbestos – organic (NAO) friction composites in severe operating conditions. In the study, four NAO friction composites based on these resins were developed. Results obtained showed that the new composites were remarkably better. It was concluded that apart from eliminating problems such as; emission of harmful volatiles, possibility of voids, cracks and shrinkages associated with traditional phenolicfor friction materials, the novel green resin binders exhibit better properties from the friction material point of view in severe operating conditions. The study is limited to effect of resins on the performance of non-asbestos – organic (NAO) friction composites;the influence of reinforcing materials on the performances of the friction material was not investigated.

Olufemiand Joel (2009), undertake a study on the suitability of Periwinkle shell as a partial replacement of River gravel in concrete. Physical and mechanical properties of the shells and well graded river gravel were determined and compared. Concrete cubes with periwinkle shells and alone as coarse aggregate were lighter and of lower compressive strengths compared to those with periwinkle shells and gravels. This study limited to the suitability of Periwinkle shell as a partial replacement of River gravel in concrete and not as a friction material.

Zamri*et el.*, (2011); Investigated thepotential of **p**alm oil clinker as reinforcement in aluminium matrix composites for tribologicalapplicationsPalm oil clinker particle (POCp) reinforced aluminium matrix composites at different weight % of POCp (0 –20%) were fabricated via powder metallurgy technique. Sliding wear behaviour of the composites was studied against mild steel mating surface using Pin-On-Disc configuration at different applied load (3 –51 N), sliding distances (0 –500 m) and sliding velocities (0.55 m/s). The analysis of worn surface and subsurface was studied using a scanning electron microscope (SEM). The results indicate that the composites exhibited better wear resistance at applied load below than 11 N.However the study did not consider the effect of temperature on the tribological of the composite.

Festus*et el., (*2012) carried out a study on assessment of the suitability of Periwinkle shell ash (PSA) as a partial replacement for ordinary Portland cement (OPC) in concrete. In the study, Periwinkle shell cleaned and dried in an electric furnace at 1000^{o}C and thereafter sieved through BS (75microns) to fine ash. Hardened concreate was obtained from this sieve size, the result showed that compaction factor increased with increase in Periwinkle shell ash (PSA), while the slump and compressive strength of the mix decreased with its increase. The study also showed that PSA has lower specific density compared with

ordinary Portland cement (OPC).Again the studydoes not show that Periwinkle shell ash (PSA) isa suitable replacement of friction material.

Kolapo and Akaninyene. (2012); Investigated the effect of periwinkle shell ash (PSA) as a substitute cement on concrete. Specimens were prepared from mixwith strengthof 25N/$mm^{2,}$a total of 180 specimens were casted and tested for compressive and tensile strength for 7 to 180 days. The results revealed that compressive strength increased with the increase in curing time, but decreased as the PSA contents increased. The optimal strength was attained with 10% PSA content at 28 days compared was in agreement with the conventional concrete. The study concluded that 10% PSA content is adequate as cement substitution for structural concrete.However, the study is limited to the use of periwinkle shell as a substitute for cement on concrete.

Fono-Tamo, and Koya (2013);evaluated the mechanical characteristics of friction Lining developed from palm kernel shell. The study showed that the bonding strength of the friction material to the back plate was 3375 N/s, while the hardness value, the mean Shear Strength and the coefficient of friction were of 32.34MPa and 40.95 MPa and 0.43 respectively. Although these values fall within the recommended limits for automotive friction material, the bonding strength of the developed brake pad was 26% lower than that of asbestos brake pad. However material optimization was not carried out.

Ikpambese*et al.*, (2014); carried out a study on the possibility of using palm kernelfibres (PKFS) for the production of asbestos free brake pads. It was concluded that brake pad having a composition of 40% epoxy-resin, 10% palm wastes, 6% Al_2O_3, 29% graphite, and 15% calcium carbonate gave better properties than other compositions. The result was compared with those of commercial brake pad and was found to be within the acceptable range. However the study did determine the optimal (PKFS) particle size.Also Tsang etal.,(1985) had observed that pure epoxy resin unless modified at temperatures

above 260ºC,typical epoxy resin binders decomposes by charring and evaporation. This process decreases the density of the brake friction material at the wear surface, increases porosity, thereby losing its structural integrity.

Elakhame*et el., (*2014);carried a study on the development and production of brake pads from palm kernel shell composites. The PKS were sieve into sieve grades of 100μm, 350 μm, 710μm and 100 μm. The sieved PKS was used in production of brake pad in ratio of 20% resin, 10% graphite, 15% steel, 35-55% PKS and 0-20% SiC using compression moulding. The properties examined were microstructure analysis, hardness, compressive strength, density, and flame resistance, water and oil absorption. The microstructure reveals uniform distribution of resin in PKS. The results obtained showed that the finer the sieve size the better the properties. The results obtained in their work were compared with that of commercial brake pad (asbestos based)and were in close agreement. Hence PKS can be used in production of asbestos-free brake pad. However, the study did not show how the formulation and manufacturing parameters were arrived at.

Mayowa*et el.,(*2015) investigated the effect of palm kernel shell and cow bone as reinforced polymer composites in brake pad production by adding palm kernel shell and cow bone at different sieve grading into an epoxy resin and hardener at 100, 100 and 120 sieve grades respectively. The formulated brake pads were characterized based on the requirements for brake pad and the result show that;the impact test for PKS and cow bone were 1.0 J and 1.5 J, the hardness test 55.7 HRB and 46.0 HRB values for PKS and cow bone respectively. The water absorption test for PKS was 5.05% and cow bone was 5.53%. Oil absorption test for PKS was 2.2% and 4.1% for cow bone. The values of thermo-gravimetric analysis (TGA) were measured in terms of highest percentage weight loss and for PKS it was 57.14% and 63.24% for cow bone. While the values of coefficient of friction for PKS and cow bone were 0.735 and 0.677 respectively. Wear rate for PKS

was 9.57E-7 and 1.44E-6 for cow bone. Crushing strength for PKS was 23N/mm² and 21N/mm² for cow bone. However, the study recommended that further research should be carried out in order to improve the oil and water absorption properties of PKS and cow bone formulated brake pads.

2.4. RESEARCH GAPS

The extensive literature survey showthe workdone on thevarious properties of friction materials; their selection, formulation, characterizations and comparison of test results with the recommended values, however, the literaturesurvey presented above stillreveals the following knowledge gap that helped to set the objectives of this research work:

1. There are too many constituents in the friction materials to make their behavior predictable.
2. There is no research on the use of periwinkle shell and fan palm shell as ingredients for the development of brake pads.

Against this background, the present work focuses on thedevelopment of an automobile disk brake pad using only 2 eco-friendly materials; periwinkle shell/fan palm shell as reinforce materials with thermoset resin as a binder for the replacement of asbestos brake pad and still maintain the recommended physical, thermal and mechanical properties of a brake pad

CHAPTER THREE

MATERIALS AND METHOD

3.1 MATERIALS

The materials used during the course of this work are: phenolic resin (phenol formaldehyde), periwinkle shells, fan palm shells, engine oil (SAE 20/50),and tapwater.

3 .2 EQUIPMENT

The equipment used for this work includes;

1. Vernier caliper Model ; 530-105
2. Digital Tachometer DT-838
3. Rockwell hardness tester Karl Frank 6MBH,Weinhem – Birkenau Mode; 38506
4. Tinius Universal Teastiing Machine Digital displl , Model; 390
5. Scanning Electron Microscope/EDS model ; JOEL JSM-700F
6. Energy Dispersive X-ray Fluorescence Spectrometer (ED-XRFS) Model; Mini Pal – 4
7. Denver Jaw Crusher. Model; BDA 15571,type A
8. Denver Cone Crusher model; A003,Type 12
9. Bico Ball Milling Machine, model; 69012 (USA)
10. Endecott Test Sieve Shaker, model; EFL2mk11(5471
11. A set of sieves of sizes 125µm, 250µm, 355µm, 500µm and 710µmm (ISO3310-2:1990 R20/3, R20, R40/3 series standard.)
12. Thermo-gravimetric analyzer (TGA/DTA) ,
13. Camry digital balance pin on disc machinemodel; TR-201CL
14. Fourier transform infra-red spectrometer (FTIR

15. X-Ray Diffractometer (XRD), model; PANanalytical-X
16. Constructed brake pad test rig
17. Digital tachometer and infrared thermometer (-50ºC to 500ºC) model DT8500,
18. Thermocouple Model C900KO2-M*AN, range 0-600ºC,
19. Smits tachometer (up to 20,000rpm)
20. Mercedes Benz 230 E brake pad (standard)
21. Used brake pad back plate for Mercedes Benz 230E-

3.3 METHOD

3.3.1 Procedure for determining physical and mechanical properties of periwinkle and fan palm shells

The length L (mm),thickness t (mm), volume (mm^3), mass (kg), Moisture content (%), Hardness ,Compressive strength (N/mm^2, Specific gravity and Density g/cm^3 of the Periwinkle and Fan palm shells were determined at National Metallurgical Development Centre Jos. These values were obtained by taking the average of three readings. These values are shown in tables A 25 and A26(Appendix A).

3.3.2 Determination of the elemental composition of periwinkle and fan palm shells

The chemical composition of the sample was determined using Energy Dispersive X-ray Fluorescence Spectrometer (ED-XRFS), Mini Pal – 4 model . Before the analysis the sample was first milled to -75 µm, pressed into powder briquettes standard as required by the machine for proper mineral count and analysis. Each sample was placed in the machine for one hour thirty minutes (thirty minutes for major elements and one hour for the trace elements).The software used analyzed all elements in the periodic table between Sodium (Na) and Uranium (U). But only elements found above the detection limits were reported. All major elements were expressed as oxides and analyzed in percentage (%) composition.

However, for trace elements analyses, the samples were mixed with polyvinyl alcohol (PVA) binder and pressed into a pellet using a 10 ton press. The sequential XRF with WinXRF software was used for analysis. The elemental composition of the periwinkle and fan palm shells as shown in tablesA 27 andA 28 (Appendix A) were obtained from National Metallurgical Development Centre Jos

3.3.3 Production of periwinkle and fan palm shells powders

The dried periwinkle and fan palm shells consisting of 50 kg each were sun dried for five (5) days, followed by oven drying at 105^{o}C for 5 hours to eliminate most of the moisture as obtained in the industry. These were then charged into a Denver cone crusher and reduced to a size of 3mm to 4mm wide. They were further charged into a roll crusher that further reduced the size of shells between 1mm to 2mm.

(a) Periwinkle shell powder **(b) Fan palm shell powder**

Plate 3.1: Photograph of Periwinkle and fan palm shells powder

The products from the roll crusher were transferred into a ball milling machine and left in the mill for two (2) hours; after which they were transferred into a set of sieves of sizes; +710µm, +500µm, +355µm, +250µm, +125µm sizes, and sieved for 30 minutes using a sieve shaker machine. Sieve sizes above +710 µm were reprocessed and passed through the sieves again to obtain the powders (as shown in Plates(3.1a and b).

3.3.4Optimization of brake pad formulation and manufacturing parameters

a. Optimization of manufacturing parameters

Taguchi method was used to optimize the manufacturing parameters for the brake pad manufacture. This method provides a means to determine the optimal values of the characteristics of a product or process such as robust (insensitive to the source of variance), while requiring less experimentation.The effect of the four parameters; Moulding pressure, Moulding temperature, curing time, and post curing or heat treatment time were studied.The minimum number of experiments N_{tag} which is required to be conducted by Taguchi method is given by;

$$N_{tag} = \sum_{l=1}^{Nv} (Li - 1) \quad 3.1$$

whereN_v= number of variable

L = number of levels

The levels for the manufacturing were obtained based on the values used in the brake pad industry by creating equal interval between them. Table 3.1 shows the factor levels for the manufacturing parameters, while the orthogonal array for the experiment is in table 3.2

Table 3.1Factor levels for the manufacturing parameters

Manufacturing parameters	Level		
	Low	Medium	High
A: Moulding Pressure (kpa)	41	48	56
B: Moulding temperature (^oC)	100	130	160
C: Curing Time (Mins)	10	15	20
D: Heat treatment time (Hr)	1	1.5	2

Table3.2Orthogonal array for the experiment using Taguchi method is ($L_9 3^4$)

Experiment number	Moulding Pressure (kpa)	Moulding temperature (^oC)	Curing Time (Mins)	Heat treatment time (Hr)
1	1	1	1	1
2	1	2	2	2
3	1	3	3	3
4	2	2	2	3
5	2	3	3	1
6	2	1	1	2
7	3	3	3	2
8	3	1	1	1
9	3	2	2	2

Table3.3 shows the results of the experiment conducted towards identifying the optimum levels for the manufacturing parameters.

Table 3.3Experimental results and S/N ratio for coefficient of friction.

Experiment number	Moulding Pressure (Kpa)	Moulding temperature (^oC)	Curing Time (Mins)	Heat treatment time (Hr).	Average coefficient of friction	(S/N) for larger the better
1	1	1	1	1	.463	-1.914
2	1	2	2	2	.360	-4.102
3	1	3	3	3	.464	-1.898
4	2	2	2	3	.444	-2.280
5	2	3	3	1	.356	-4.199
6	2	1	1	2	.462	-1.935
7	3	3	3	2	.360	-4.102
8	3	1	1	1	.455	-2.068
9	3	2	2	2	.456	-2.049

In this study optimization was achieved by using the S/N ratio larger-the better quality characteristics. The largest coefficient of friction is required for effective brake performance. For the larger-the-better characteristics, the S/N ratio calculated as follows:

$$S/N = -10log\frac{1}{n}\sum_{l=1}^{n}\frac{1}{y^2} \quad 3.2$$

Where *n* is number of observations in the L9 orthogonal array and *yi*is the average of observed data. Thus from equation 3.2, the signal to noise ratio (S/N) for experiment 1 to 9 were determined as follows;

$S/N_1 = -10log\frac{1}{n}\sum_{l=1}^{n}\frac{1}{y^2}$

$= -10log\frac{1}{3}\sum_{l=1}^{n}\frac{1}{.463^2}.$

= -1.9143

$S/N_2 = -10log\frac{1}{3}\sum_{l=1}^{n}\frac{1}{.360^2}$

= -4.102

$S/N_3 = -10log\frac{1}{3}\sum_{l=1}^{n}\frac{1}{.464^2}$

= - 1.898

$S/N_4 = -10log\frac{1}{3}\sum_{l=1}^{n}\frac{1}{.444^2}$

= - 2.280

$S/N_5 = 10log\frac{1}{3}\sum_{l=1}^{n}\frac{1}{.356^2}$

= - 4.199

$S/N_6 = 10log\frac{1}{3}\sum_{l=1}^{n}\frac{1}{.460^2}$

= - 1.936

$S/N_7 = 10log\frac{1}{3}\sum_{l=1}^{n}\frac{1}{.360^2}$

= - 4.102

$S/N_8 = 10log\frac{1}{3}\sum_{l=1}^{n}\frac{1}{.455^2}$

= - 2.0685

$S/N_9 = \mathbf{10log}\frac{1}{3}\sum_{l=1}^{n}\frac{1}{.456^2}$

= - 2.044

The average effect of each factor on the quality of the brake pad is equal to the sum of the signal to noise ratio (S/N) corresponding to a factor at a parameter level divided by the number of repetition of the factor. Thus the average is as follows;

Effect factor A: Mouldig pressure

At low level $= \frac{-1.914-4.102-1.898}{3}$

= -2.638

At medium level $= \frac{-2.280-4.199-1.935}{3}$

= - 2.982

At high level $= \frac{-4.1027+2.0685+2.0493}{3}$

= -2.740

Effect factor B: Moulding temperature

At low level $= \frac{-1.9148+2.2809+4.1027}{3}$

= -2.766

At medium level $= \frac{-4.1020+4.1997+2.0685}{3}$

= -3.457

At high level $= \frac{-1.898+1.19359+2.20493}{3}$

= -1.766

Effect factor C: Moulding time

At low level $= \frac{-1.19148+1.9359+2.0685}{3}$

$=-1.732$

At medium level $= \frac{-4.1020+2.2809+4.1027}{3}$

$= -3.495$

At high level $= \frac{-1.898+4.1997+4.1027}{3}$

$= -2.721$

Effect factor D: Heat treatment / Reaction time

At low level $= \frac{-1.9148+4.1997+4.1027}{3}$

$= -2.711$

At medium level $= \frac{-4.1020+4.1027+1.9359}{3}$

$= -3.3802$

At high level $= \frac{-1.898+2.2809+4.1027}{3}$

$= -2.761$

The response to signal to noise (S/N) is shown in Table 3.4

Table 3.4 Response to signal to noise (S/N)

Factor	Average S/N db		
	Level 1	Level 2	Level 3
A: Moulding pressure	-2.638*	-2.982	-2.740
B: Moulding temperature	-2.766	-3.457	-1.766*
C: Moulding time	-1.732*	-3.495	-2.721
D: Heat treatment / time	-2.711*	-3.802	-2.761

* = Optimal Parameter.

The larger the better Signal to Noise ratio (S/N) for each factor is preferred because the higher the coefficient of frictionthe better. Hence, the optimum setting for the

manufacturing parameters is A_1, B_3, C_1 and $D_1$and the corresponding manufacturing parameters are as shown in Table 3.5 below.

Table 3.5 Optimum setting for the manufacturing parameters

Factor	Value
A_1 (Kpa)	41
B_3 (^oC)	150
C_1 (min)	10
D_1(Hr.)	1

b. Optimization of brake pad formulation.

Periwinkle shells and fan palm shells were mixedwith resin in the manufacture of brake pads. The optimum level settings for the ingredients were determined by using the procedure in the optimization of manufacturing parameters. L(2^2) factorial design used is shown in the Table 3.6, while brake pad formulation with their levels and the experimental results and S/N ratio for coefficient of friction are in Tables 3.7 and 3.8 respectively.

Table 3.6 Experimental design layout.

Experiment no	Periwinkle shell or Fan palm shell	Resin
1	1	1
2	2	1
3	1	2
4	2	2

Table 3.7 Brake pad formulation and their level

	Level	
Factor	1	2
A: Periwinkle Shell	35	65
B: Resin	35	65

Table 3.8Experimental results and S/N ratio for coefficient of friction.

Experiment No.	Periwinkle or Fan Palm shell	Resin	Friction
1	35	35	0.356
2	65	35	0.456
3	35	65	0.462
4	65	65	0.330

The Signal to Noise ratio (S/N) for Periwinkle shell and Fan palm shell and Resin was obtained from equation 3.3 below;

SN= $-\mathbf{10}\boldsymbol{log}\frac{\mathbf{1}}{\mathbf{3}}(\sum_{\mathbf{y}}\mathbf{2}$3.3

$SN_1 = -\mathbf{10}\boldsymbol{log}\frac{\mathbf{1}}{\mathbf{3}}(\sum_{\mathbf{y}}\mathbf{2}$

$= -\mathbf{10}\boldsymbol{log}\frac{\mathbf{1}}{\mathbf{3}}(0.356)^2$

= 13.74.

$SN_2 = -\mathbf{10}\boldsymbol{log}\frac{\mathbf{1}}{\mathbf{3}}(0.456^2)$

= 11.596.

$SN_3 = -\mathbf{10}\boldsymbol{log}\frac{\mathbf{1}}{\mathbf{3}}(0.462)^2$

= 11.46.

$SN_4 = -\mathbf{10}\boldsymbol{log}\frac{\mathbf{1}}{\mathbf{3}}(\sum_{\mathbf{y}}\mathbf{2})$

$= -\mathbf{10}\boldsymbol{log}\frac{\mathbf{1}}{\mathbf{3}}(0.33^2)$

= 14.400.

The average effect of each factor on one multiple quality characteristics at different levels were determined using the procedure in optimization of the manufacturing parameter. Table 3.9 shows the S/N ratio, while Table 3.10 shows the optimum setting for the brake pad formulation.

Factor A: Periwinkle shell at level 1 = $\frac{\mathbf{10.15+11.596}}{\mathbf{2}}$ = 10.87

Factor A: Periwinkle shell at level 2 = $\frac{\mathbf{13.74+11.46}}{\mathbf{2}}$ = 12.60

Factor B: Resin at level 1 = $\frac{\mathbf{11.46+14.400}}{\mathbf{2}}$ = 12.93

Factor B: Resin at level 2 = $\frac{\mathbf{13.74+11.596}}{\mathbf{2}}$ = 12.67

Table 3.9 The response table for the Signal to Noise ratio (S/N)

Factor	$Level_1$	$Level_2$
A: Periwinkle shell or Fan palm shell	10.87	12.60*
B: Resin	12.93*	12.67

Hence, from Table 3.9 above, the optimum settings for the brake pad formulation is A_2, B_1, and the corresponding composition is shown in the Table below 3.10.

Table 3.10 Optimum settings for the brake pad formulation

Factor	% Composition
Periwinkle or Fan palm shell	65
Resin	35

3.3.5 Production of brake pad samples.

The periwinkle shell and the fan palm shell sieve sizes of 125µm, 250 µm, 335µm, 500µm and 710µm, were used to produce the brake pads.The choice of the sieve sizes was based on the recommended sieve sizes for brake pads by the Standards Organization of Nigeria (SON) Ref; NIS:1997,andsimilar works by Ibhadode and Dagwa (2008) Test samples were made from optimal composition consisting of 65%wtof periwinkle shell particles and 35% wt. of resin as shown in Table 3.14. Thirty (30) test samples from each of the sieve sizes (Plate 3.2) were then produced using this composition. Each composition was blend(Ahmet 2011). The mix was thentransferred into a mold having an

inserted back plate and kept at pressure of 41Kpa at a temperature of 150^0C for 10mins. The samples were post cured at 140^oC for 1hours in an oven.

a. Periwinkle shell test samples **b. Fan palm test samples**

Plate 3.2: photograph of Periwinkle shell/Fan Palm shell test sample

3.4 CHARACTERIZATION OF PERIWINKLE AND FANPALM PARTICLES

3.4.1 X-Ray Fluorescence (XRF)

The elemental composition of the periwinkle shell and the fan palm shell particles were determined using X-Ray Fluorescence (XRF) analysis. The particles were formed into pellets in a pelletizer with a hydraulic press (Carver Inc Model 30- 12). The pellets were then sealed into the chamber of the Amptek Inc XRF detectorand allowed to run for 1000 s at a voltage of 30 kV, and a current of 50μA. The resulting spectrum measured the elemental composition of the material (Kato and Soutome,2001, Aigbodion *et al.*, 2010).

3.4.2 X-ray diffractograms(XRD)analysis

XRD analysis of the periwinkle shell and fan palm particles were carried out to determine the various elements and phase distributions in them. They were carried out on a Philips

X-ray diffract meter. The X-ray diffract gram was taken using CuKαradiationatscanspeedof30m/min (Handa and Kato, 1996). The samples were rotated at precisely one – half of the angular speed of the receiving slit, so that a contact angle between the incident and reflected beam is maintained. The receiving slit is maintained in front of the counter tube arm, and behind it, is usually fitted a scatter slit to ensure that the counter receives radiations only from the portion of the specimen illuminated by the primary beam (Kim *et al.*,2003). The intensity diffracted at the various angles was recorded automatically on a chart and the appropriate (Ɵ) and (d) values were obtained. The tests were carried out in the University of the Witwatersrand, Johannesburg, South Africa.

3.5 CHARACTERIZATION OF THE DEVELOPED BRAKE PAD

3.5.1. Scanning electron microscope

The microstructure and the chemical compositions of the phases present in the test samples were studied using a JOEL JSM 5900LV scanning electron microscope equipped with an Oxford INCA^{TM}energy dispersive spectroscopy system. The polished samples were firmly held on the sample holder using double-sided carbon tape before putting them inside the sample chamber. The SEM was operated at an accelerating voltage of 20 kV. The test was carried out according toStandard Reference Material (SRM)-484 which is a sample for calibrating the magnification scale of a Scanning Electron Microscope (SEM) in the University of the Witwatersrand, Johannesburg, South Africa.

3.5.2. Thermal analysis

Thermal decomposition was observed in terms of global mass loss by using a thermo gravimetric analyzer Model TGA Q50. The test was carried out in the University of

Witwatersrand, Johannesburg; South Africa. The apparatus detects the mass loss with a resolution of 0.1 as a function of temperature. The samples were evenly and loosely distributed in an open sample pan of 6.4 mm diameter and 3.2 mm deep with an initial sample weight of 8-10 mg. The temperature change was controlled from room temperature (25±3°C) to 900°C with a heating rate of 10 °C/min. High purity argon was continuously passed into the furnace at a flow rate of 60 mL/min at room temperature and atmospheric pressure. Before the starting of each run, the argon was used to purge the furnace for 30 min to establish an inert environment in order to prevent any unwanted oxidative decomposition. The TG and DTA curves were obtained from TGA runs using universal analysis 2000 software from TA Instruments Seong and Ho, (2000).

3.6. PHYSICAL AND MECHANICAL PROPERTIES

3.6.1. Density

Density measurements were carried out on the periwinkle and fan palm shell formulated brake pad test samples.Archimedes' principle which states that the buoyantforce on a submerged object is equal to the weight.The fluid displaced was used for determining the volume and therefore the density oftest samples by measuring its mass in air and its effective mass when submerged in water (density=1gram/cc). This effective mass under water was its actual mass less the mass of the fluid displaced. The difference between the real and effective mass therefore gives the mass of water displaced and allows the calculation of the volume of the samples. The mass divided by the volume thus determined gives the average density of the sample.

3.6.2 Water and oil soak test

The 24-hour water and oil soak test determined the water and oil absorption behaviour of the asbestos-free experimental brake pad and the effect of the absorbed water and oil on

its dimensions. After oven drying of the specimen (0 – 250˚C), its weight was measured. Subsequently, the dimensions (thickness) of the specimen were measured using a Vernier caliper. After twenty-four hours of submersion in water and engine oil, SAE 20/50 at 26˚C to 30˚C, thespecimens were weighed after the excess water and oil had drained off. The following formula was used Talib.,(2008):

$$\boldsymbol{Asorption}\ (\%) = \frac{\left(\boldsymbol{w_1 - w_0}\right)\boldsymbol{X}\ \mathbf{100\%}}{\boldsymbol{w_0}} \qquad 3.4$$

where:W_1= weight after immersion

W_o= weight before immersion

3.6.3 Hardness test

The Brinell hardness values were obtained using a digital hardness tester. Test samples of diameter 22.7mm were used to carry out the tests for the different sieve grades. The hardness values were determined according to the provisions in the American Society of Testing and Materials (ASTM E18-79) using the Brinell hardness tester on "B" scale (Frank Well test Brinell Hardness Tester, model 38506) with a1.56mm steel ball indenter, minor load of 10kg, major load of 100kg and hardness value of 101.2HRB for thestandard block Talib*et el.*,(2008).

Before the test, the mating surface of the indenter, plunger rod and test samples were thoroughly cleaned by removing dirt, scratches and oil and calibration of the testing machine was done using the standard block. The samples were placed on anvils, which act as supports for the test samples. A minor load of 10kg was applied to the sample in a controlled manner without inducing impact or vibration and zero datum position was established, and then the major load of 100kg was then applied.The reading was taken

when theload pointer came to rest or had slowed appreciably and dwelled for up to 2 seconds. The load was then removed by returning the crank handle to the latched position and the hardness value read directly from the semi-automatic digital scale.

3.6.4 Compressive strength test

The compression test was conducted on the Avery Denison strength testing machine of 500kN capacity at a strain of 0.002. The test pieces were machined to the standard shape and dimensions specified by the American Society for Testing and Materials (Talib*et el.*,2008). The sample was locked securely in the grips of the upper and lower crossbeams of the testing machine. A small load was initially applied to seat the sample in the grips and then the load was increased until failure occurred.

3.6.5. Wear and friction test

A pin-on-disc test apparatus was used to investigate the dry sliding wear and friction characteristicsof the samples as per ASTMG99-95 standards for wear test (Aigbodion*et al*, 2010). Wear sample 20 mm in diameter and 40 mm high were made and then polished metallographically. Wear tests were conducted for various loads and sliding speeds at 150^{o}C to 250^{o}C. Theloads and speeds ranged from 40 kg to 140 kg and 1.2 to 2.8m/srespectively.The tests were carried out in the University of Witwatersrand, Johannesburg, South Africa.

The initial weight of the specimen was measured using a single pan electronic weighing machine with an accuracy of 0.0001g. During the test, the pin was pressed against the counterpart rotating againstanEN32steel disc (hardness 65HRC) of counter surface roughness of 0.5µm by applying he load. The frictional traction experienced by the pin during sliding was measuredcontinuously by a PC-based data- logging system. After running through a fixed sliding distance, the sample was removed, cleaned with acetone,

dried, and weighed to determine the weight loss due to wear. The difference in weight measured before and after tests gives the wear of the sample. The formula used to convert the weight loss into wear rate is (Aigbodion*et al*., 2010):

$$\text{Wear rate} = \frac{\Delta W}{S} \quad 3.5$$

whereΔW is the weight difference of the sample before and after the test in Kg, and S is total sliding distance in m.The frictional force at the each of the sliding speeds and loads was measured by a calibrated strain gauge mounted on the load level holding the specimen and the coefficient was determinedfrom the equation 3.3.

$$\mu = f / N \quad 3.6$$

Whereμ is the coefficient of friction, f is the sliding force and$N$ the normal force

3.7. STATISTICAL DESIGN ANALYSIS AND DEVELOPMENT OF MATHEMATICAL MODEL FOR THE CO- EFFICIENT OF FRICTION PROCESS

Factorial design and linear regression techniques have been widely used in engineering analysis. These techniques consist of plan of experiments with the objective of acquiring data in a controlled way and executing experiments in order to obtain information about the behavior of a given process.

Representing the co-efficient of friction value by W, the response function can be expressed by equation below(Amaren*et al.,* 2013)

$$W = f(A, B, C, D), \quad 3.7$$

where A= Sliding speed

B= applied load

C= Temperatures

D= particles size

The model selected includes the effects of main variables first-order and second-order interactions of all variables. Hence the general regression equation is written as:

$$W= \beta_o + \beta_1 A + \beta_2 B+\beta_3 C+\beta_4 D+\beta_5 AB+\beta_6 AC+ \beta_7 AD+ \beta_8 BC+\beta_9 BD+ \beta_{10} CD+\beta_{11} ABC+\beta_{12} ABD+\beta_{13} ACD+\beta_{14} BCD+ \beta_{15} ABCD \quad 3.8$$

where β_o is average response of W and$\beta_1, \beta_2, \beta_3, \beta_4, \beta_5, \beta_6, \beta_7, \beta_8, \beta_9, \beta_{10}, \beta_{11}, \beta_{12}, \beta_{13}, \beta_{14}, \beta_{15},$ are coefficients associated with each variable A, B, C, D and their interactions. Cube plots were obtained based on the effect of the four factors to study their effects on the coefficient of friction for different conditions. In order to determine the developed model, experimental data were substituted in the model equation at various conditions.

3.7.1 Design expert 6.0.8

Design expertsoftware 6.0.8 used to on investigate the effect of particle size, speed, temperature and load the coefficient of friction as well analysis of variance (ANOVA). The use of this software involves the following steps.

1. Log on to the software
2. Select the factorial design to be used in this case $L2^4$ factorial was employed, since the two levels are low (-) and high (+)
3. Define the factors, and for this study; factor A is speed (m/s), factor B is load (kg), factor C is temperature ºC, and factor D is particle µ
4. The orthogonal array, ANOVA, effect on the response and the cube map will then be obtained.

3.8 DESIGN OF LABORATORY TEST RIG

A test rig was designed and constructed to evaluate the performance of the brake pads produced at the optimum manufacturing parameters and compositionin the laboratory.The test rig consists of the following components;

1. An electric motor which supplies the required power
2. Flywheel - an energy storage device use to control speed fluctuations (khurma and Gupta (2012).
3. Brake disc-a device which slows the rotation of a wheel by friction caused by pushing brake pads against it.Swapnil and Bhaskar(2014).
4. The drive shaft which carries the flywheel and the disc

3.8.1 Selection of prime mover

According to National Electrical Manufacturers Association (NEMA), for a special service where starting torque is not excessive, an electric motor of ratings between 0.3725 to 149kW is normally selected Erik *et el*., (2004). Thus for this work a 1.5 kW motor was found to be suitable for the rotational energy needed to turn the gear box, flywheel and the brake disc.

3.8.2 Design of the flywheel

The following were considered during the selection of the flywheel

1. The rated power of the electric motor = 1.5 kW
2. The rated speed of the electric motor= 300 rpm
3. Diameter of flywheel = 3000 mm

The density of flywheel material (gray cast iron) $\boldsymbol{\rho}$= 7200 kg/m^3

According khurma and Gupta (2012), Coefficient of fluctuation of speed $C_s$for electrical machines (belt driven) = 0.02

The mean angular speed of the flywheel was obtained from equation3.9

$$\boldsymbol{\omega} = \frac{\boldsymbol{2\pi N}}{\boldsymbol{60}} \qquad 3.9$$

$$= \frac{\boldsymbol{2\pi\ x\ 300}}{\boldsymbol{60}} \qquad \text{Where } \boldsymbol{N = speed\ (rpm)}$$

$$\boldsymbol{= 31.42}$$

The work done by the flywheel was obtained from equation 3.10

$$\text{Work done } = \frac{\boldsymbol{P\ x\ 60}}{\boldsymbol{N}} \qquad 3.10$$

$$= \frac{\boldsymbol{1.5\ x\ 10^3\ x\ 60}}{\boldsymbol{300}}$$

$$= \boldsymbol{300\ Nm}$$

According khurma and Gupta (2012),the maximum fluctuation of energy of the rim is given by;

$$(\Delta \boldsymbol{E})_{\boldsymbol{rim}} = \boldsymbol{mrR^2\omega^2} C_s \qquad 3.11$$

Where ;$(\Delta \boldsymbol{E})_{\boldsymbol{rim}}$ = maximum fluctuation of energy of the rim

$\boldsymbol{\omega}$ = Mean angular speed

$\boldsymbol{m}$ = $\boldsymbol{Mass\ of\ flywheel\ (kg)}$

$\boldsymbol{R}$ = Radius of the flywheel

C_s = Coefficient of fluctuation of speed

Substituting the values of $(\Delta \boldsymbol{E})_{\boldsymbol{rim}}$, $\boldsymbol{\omega}$, $\boldsymbol{R}$, and Cs in equation 3.11

$$300 = \boldsymbol{mx1.5^2\ \ x\ 31.42^2\ \ x\ 0.02}$$

$$m = 6.75(kg)$$

$$\sim 7(kg)$$

Thus a $7(kg)$ flywheel was selected.

3.8.3 Selection of brake disc

Since the developed brake bad is for Mercedes Benz 230E salon car, the standard brake disc of the same car was used for the work.

3.8.4Shaft design

Shaft design consist primarily the determination of the correct shaft diameter to ensure satisfactory strength and rigidity when the shaft is transmitting power under operating and loading conditions. Allen. *et al*.,(2002).Using ASME code for shaft under torsion, bending loads with little or no axial load, the shaft size is obtained from equation 3.12;

$$d^3 = \frac{16}{\pi_{ss}}\sqrt{(K_b M_b)^2 + (k_t\ M_t\ )^2} \quad 3.12$$

Where:

M_t = Torsional moment, Nm

M_b = Bending moment, Nm

d = Shaft diameter m.

K_b = Combined shock and fatigue factor applied to bending and for rotating shaft loaded gradually the value is between 1.5 to 2.0

K_t = combined shock and fatigue factor applied to torsional moment and for a shaft loaded gradually the value is between 1.0 to 1.5.

S_s = Allowable stress and for shafts without keyway the value is 55MN/mm^2

3.8.5Test rig load diagram

The loading diagram of the test rig is shown in Figure 3.1

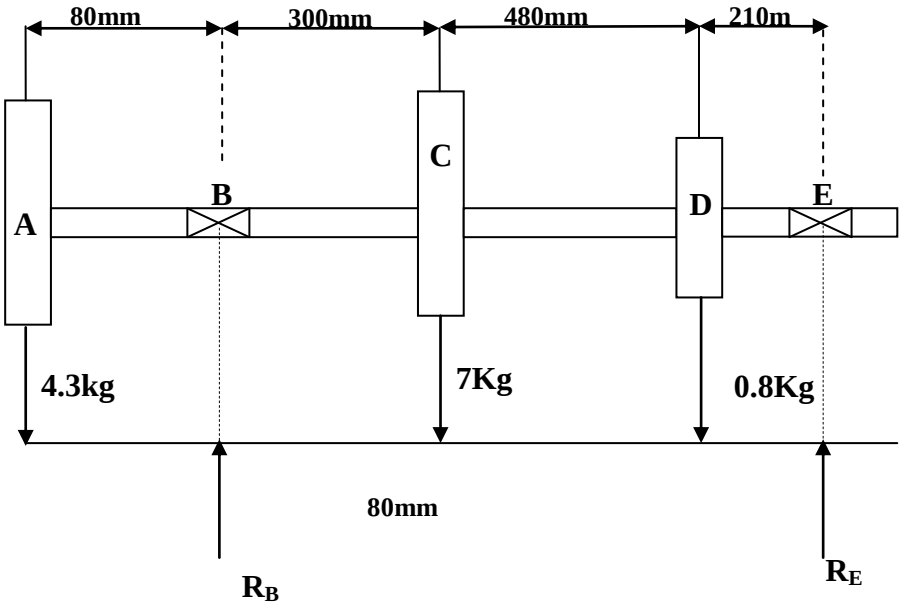

Figure: 3.1.Test rig load diagram

A = brake Disc $W_A = 4.3 \times 9.81 = 42.1N$

B = Bearing$W_C = 7 \times 9.81 = 68.67$ N

C = Fly wheel $W_D = 0.8x\ 9.81 = 7.8N$

D = Pulley where; W_A= weight of brake disk

E = Bearing. W_C= weight of flywheelW_D= weight of pulley

3.8.6 Bearing forces (R_B andR_E)

$$\sum f_v = 0$$

$R_B + R_E - W_A - W_C - W_D = 0$ 3.13

$R_B + R_E = W_A + W_C + W_D = 118.57$ N

$$\sum MR_E = 0$$

R_B x 0.99 – 42. 14 x 1. 07 – 68.67 x 0.69 – 7.84 x 0.21 = 0 3.14

R_B = 95.06 N. Thus from eqn. (3.7) R_E = 23.8

3.8.7 Force induced by pulley

The estimated torque induced by the belt was determined from equation (3.9) belowJoseph and Charles (1989) ;

$$\mathbf{T = \frac{P}{W}} 3.15$$

Where:

W = Angular velocity (Radians per second)

T = Torque P = power

According to ASME (American Society of MechanicalEngineers), the horse power of the selected V – belt is 6.5 Joseph and Charles (1989).

Thus from eqn. (3.15)

$$\mathbf{T = \frac{6.51 \text{ x } 745 \text{ x } 60}{325\ \pi} = 14\ Nm}$$

3.8.8 Test rig bending moment diagram

The force diagram and bending moment diagramis shown in Figure (3.2a and b).

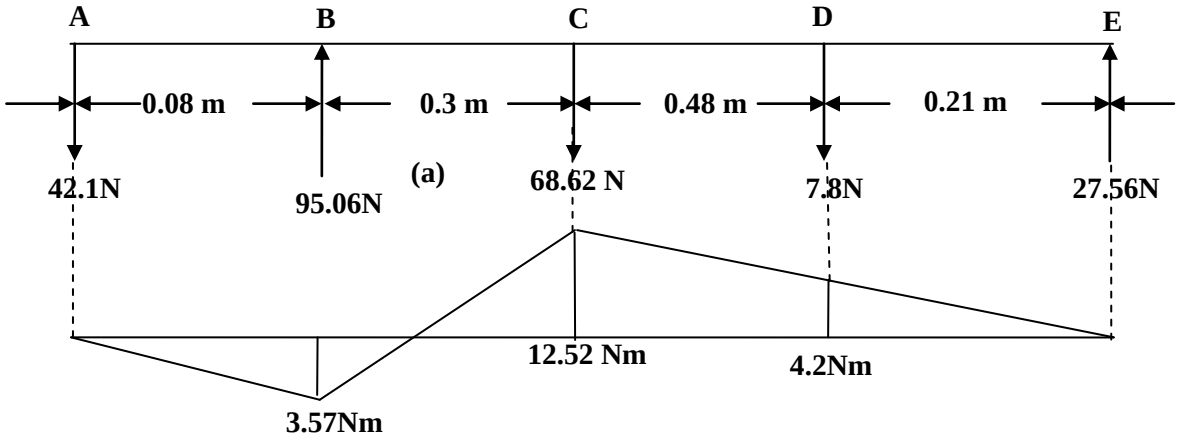

Figure: 3.2 Test rig free body and bending moment diagrams (a and b)

From fig 3.2b the maximum bending moment is 14.05Nm at point C

Since the shaft is driven by a vertical pulley, it induces an additional vertical moment of 14.0Nm from eqn. (3.15).

Total max bending moment M_b = 12.52 + 14.0 = 26.57 Nm

3.8.9 Torsional moment

According to Allen.*etal.*,(2002). The torsional moment acting on a shaft can be determined from equation 3.16.

$$\boldsymbol{M_t = \frac{9550\ X\ kW}{rev/_{min}}(Nm)} \quad 3.16$$

$$\boldsymbol{= \frac{955\ x\ 4.85}{325} = 142.52\ Nm}$$

From eqn. (3.9)

$$\boldsymbol{d^3 = \frac{16}{\overline{\pi}_{ss}}\sqrt{(K_b M_b)^2 + (K_t M_t)^2}}$$

$$\boldsymbol{= \frac{16}{\pi 55\ x\ 10^6}\sqrt{(1.5\ x\ 26.58)^2 + (2\ x\ 142.5\ )^2}}$$

$$\boldsymbol{d = 0.02664\ m}$$

$$\boldsymbol{= 26.64\ mm} \quad \approx 30\text{mm}$$

A shaft of 30mm was used.

3.8.10 Frame critical buckling load

When columns are subjected to compressive loads, they tend to fail by buckling when their critical load is attained. For a square iron column fixed at one end and free at the other end, the Euler's formula equation 3.17 is used to determine the critical buckling load of the rig frame.

$P_{critical} = \pi^2 EI_G / 4L_2^2$ 3.17

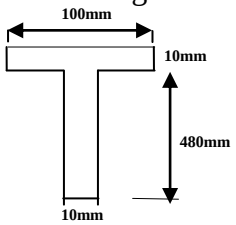

E for iron = 200GP$_a$

L = 0.6m

Figure 3.3: T-Section of the frame

$$I_g = \frac{bh^3}{12}$$

$$\bar{y} = \frac{(0.1x0.1)0.485 + (0.48 \times 0.01).24}{(0.01 \times 0.1) + 0.01 \times 0.48} = 0.02117m = 21.17\,mm$$

$$\bar{y} = 100 \times 10 \times 48$$

$$a_1 = 100 \times 10 = 100\,mm^2$$

$$y_1 = \frac{10}{2} = 5mm$$

$$a_2 = 480 \times 10 = 4800\,mm^2$$

$$y_2 = \frac{480}{2} = 240\,mm$$

The moment inertia of the T-Section about x – x

$$I_{xx} = \left[\frac{10 \times 480^3}{12} + 480(\bar{y} - y_2)\right] + [100 \times 10^3 + 100(\bar{y} - y_1)]$$

$$= \frac{10 \times 480^3}{12} + 480\,(218.83) + (100 \times 10^3 + 100(16.17)$$

$$= 92160000 + \frac{525192}{5} + 100,000 + 16.17$$

= 92,366,655.4

$$I_{yy} = \frac{480 \times 10^3}{12} + \frac{10 \times 100^3}{12} = 4,833,333.3\ mm^4$$

Euler's crippling load for one of fixed end and the other free, the Euler's formula (equation 3.14) is used determine the critical buckling load of the rig frame.

$P_E = \frac{\pi EI}{4l^2}$where the span $l = 600\ mm$

$$= \frac{\pi \times (200 \times 100^3) \times 4,833,333.3}{4(600)^2}$$

$$= \frac{200 \times 10^3 \pi \times 4,833,333.3}{4(600)^2}$$

= 210,921,281.750 KN

The total load on carried by the I-beam = w_t of disk + w_t of fly wheel + w_t of pulley (42.1+78.4+7.8)= 128.3NThis is far less than the buckling load

3.8.11 Selection of test rig pressure gauge

According to Mudd (1996) the maximum force needed at the pedal to fully operate the brakes should not exceed 180N. Therefore, applying Pascal's law (F = F/A), a pressure gauge ranging from 0 to 20 bar was found suitable

3.9 TEST RIG CONSTRUCTION PROCEDURE

The schematic diagram of test rigFigure 3.4was constructed with a 90mm X 5mm angle iron and 100mm X 50mm X 10mm channel as shown in Table 3.11

Table3.11Test rig construction procedure.

S/N	COMPONENT	MATERIAL	OPERATION PROCEDURE	TOOLS/ EQUIPMENT USED
1	Base frame	Mild Steel angle and Rectangular pipe	2 work pieces of angle iron with length, width and thickness of 1460mm/90mm/5mm and another 2 work pieces of rectangular pipes with length, width and thickness of 940mm/100mm/50mm/10mm were cut from stock and welded to form the base frame	Scriber, Vanier Calliper, Grinding Machine-cutting disk, file and drill, A/C welding machine, Electrode gauge 12, measuring tape
2	The Stand	Mild Steel Rectangular bar	2 work pieces of 480mm by 50mm by 15mm was cut from stock and welded to the base frame	Scriber, Vanier Calliper, Grinding Machine-cutting disk, file and drill, A/C welding machine, Electrode gauge 12, measuring tape
3	The Shaft	Stainless Steel Rod	A workpiece of length 1070mm of diameter 50mm was cut from stock and was machined to 30mm diameter	Scriber, Vanier Calliper, Lathe machine.

(The detailed drawings are attached at the appendix of this work)

3.10 LABORATORY BRAKE PAD TEST

Performance tests of the developed brake pad were carried out in a laboratory using a constructed test rig. It was carried out for wear (mass/thickness reduction), temperature rise and average stopping time for various conditions. A set of commercial brake pads for a Mercedes Benz 230E car were subjected to the same tests for comparison.The test rig consist of a 4 speed gear box with a reverse gear for speed variation, a diesel engine Model; CEALMAXIMUM RI75A,4.85kw, 2600rpm, a rotating shaft supported at both endsby bearings carrying a fly wheel, a brake disc with the caliper. The diesel engine provides the energy required to set the gear box, the fly wheel weights and the brake disc in motion. The schematic diagram of the system is shown in Figure 3.5 and the photograph in Plate 3.3

After installation of the pads in the brake caliper assembly, the engine was started and allowed to run to a stable speed of the selected gear. A manual force was then applied to the pedal to bring the system to rest. The disk temperature rise, the stopping pressure, and the wear in terms of (mass loss and reduction in thickness) for both the laboratory developed and commercial brake pads were then determined.

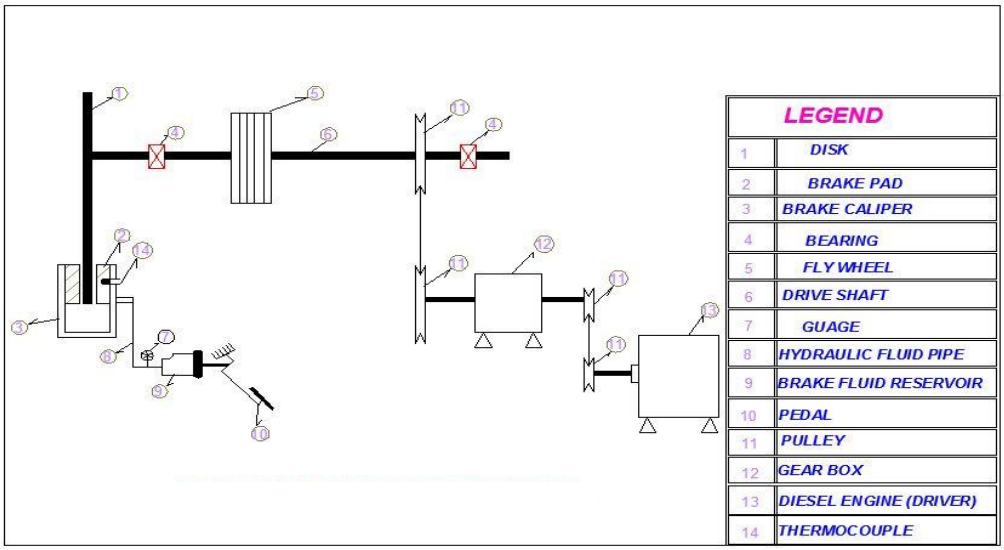

Figure 3.4: Schematic diagram of test rig

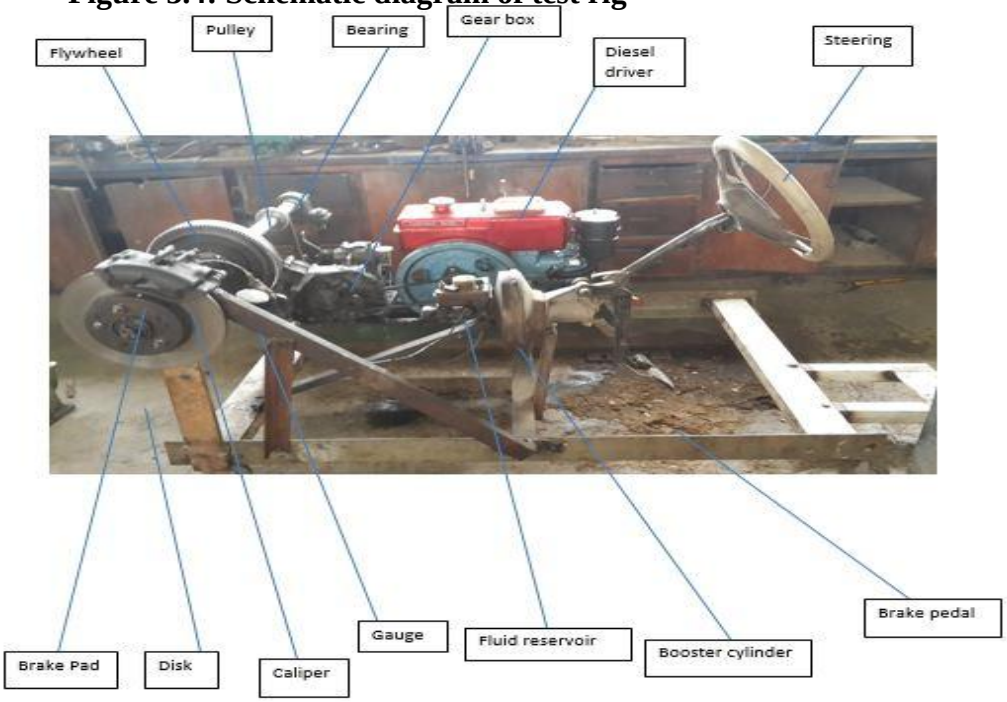

Plate 3.3: Photograph of the constructed Laboratory test rig

3.11 VEHICLE LIVE TEST

Live test of the developed brake pad was carried out using a Mercedes Benzsalon car model230E. Both the developed and commercial brake pads were installed onkm the front calipers at the same time with the car. The car was then accelerated from start and allowed to run for 5 minutes on each of these speeds; 20 km,30km,40km,50km,60km70km,80km,90km,100km,120km and 130 Km perhour. It was then brought to a stop at the end of each speed and the corresponding disk temperatures for both the developed and the commercial brake pad were measured with the aid of infrared thermometer (-50ºCto 500ºC).

CHAPTER FOUR

RESULTSANDDISCUSSION

4.1 CHARACTERIZATION OF PERIWINKLES/FAN PALM SHELL POWDER

The periwinkle shell and fan palm shell particles haddensities of 1.12 g/cm^3 and 0.99g/cm^3 respectively while asbestos has density of 2.8 *g*/cm^3. This means that, periwinkle shell and fan palm particles will be more suitable as filler material than asbestos on account of the overall weight of the brake pad.

The XRD patternsof periwinkle and fan palm shells are presented in Figures 4.1 and 4.2 respectively. Figure 4.1 reveals that the major diffraction peaks of periwinkle shell particles are 42.5, 16.15, 30.90, 34.47 and 54.08^{o}with theinter-planar distancesat 2.13, 5.49, 2.89, 2.58 and 1.69Å. The major compounds at these peaks aremagnesiumand manganese oxide, calcium silicate quartz and titanium oxide with the identified pattern list in Table 4.1. Figure 4.2 shows themajordiffraction peaksof fan palmshells as; 17.47, 21.03, 24.95, 42.09, 44.66 and 78.31^{o}and their inter-planar distance of 5.90, 4.90, 4.14, 2.49, 2.31 and 1.40Å.The major compounds andtheir phases at these peaks are $(C_{35}H_{25}N_3O_6)n$, silicon oxide, C_{11} H_{11} N O, Al_4 Si_3 C_6, Al Fe and Cr Si_2, andthe identified pattern list in Table 4.2. These analyses confirmed that the periwinkle shell and fan palm have similar characteristics with other agro-wastes presently used in brake pad composites Fono-Tamo, and Koya (2013).

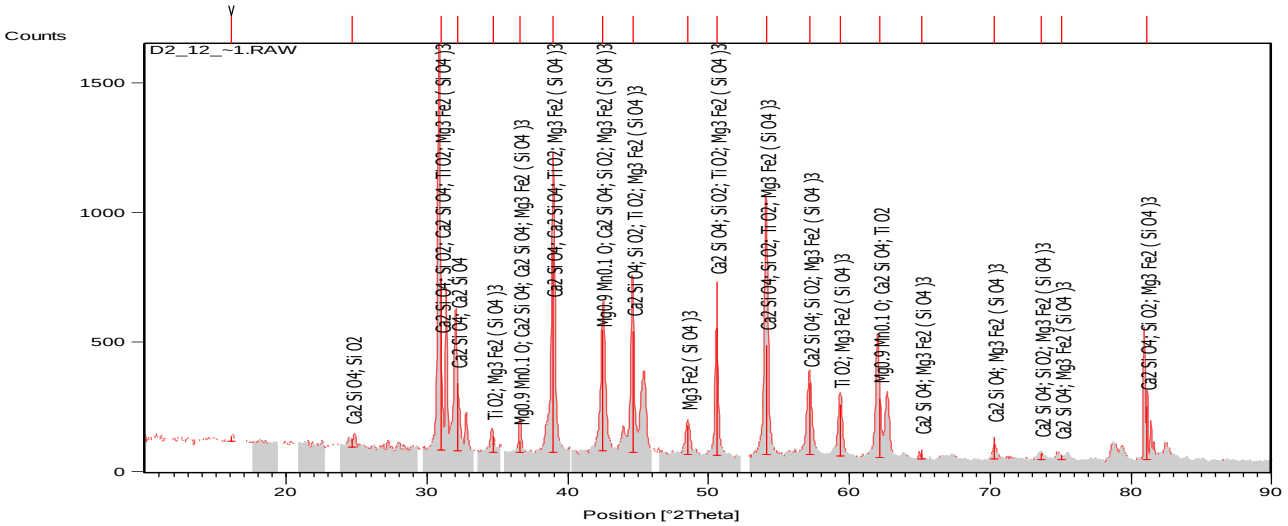

Figure 4.1: XRD spectrum of Periwinkle shell particles

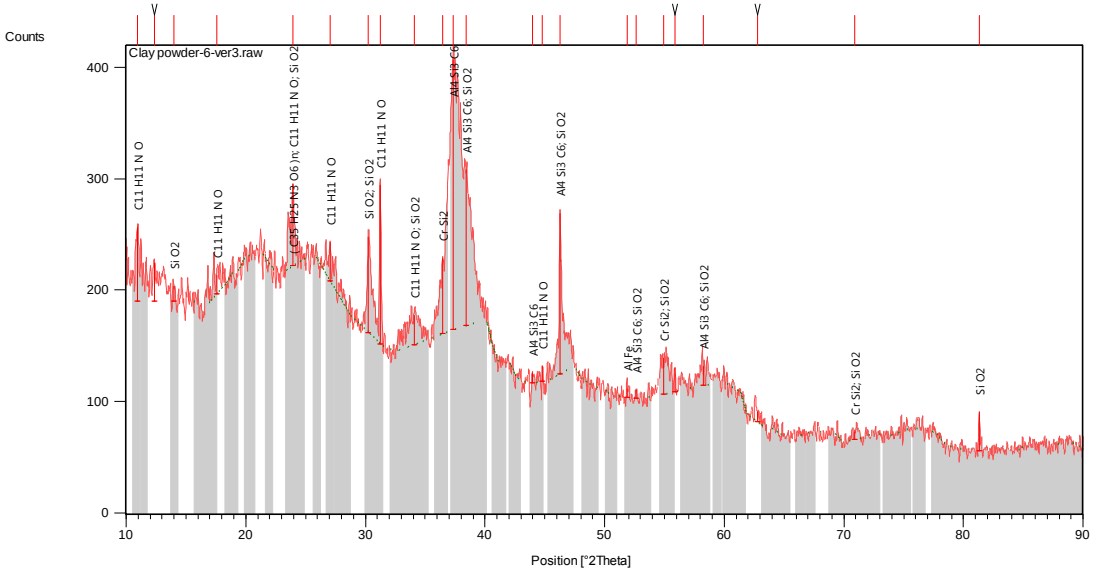

Figure 4.2: XRD spectrum of Fan palm particle

Table 4.1 Identified Patterns List of periwinkle shell particles

Visible	Ref. Code	Score	Compound Name	Displacement [°2Th.]	Scale Factor	Chemical Formula
*	00-036-1377	53	Magnesium Manganese Oxide	-0.011	0.286	Mg0.9 Mn0.1 O
*	01-077-0420	41	Calcium Silicate	-0.148	0.334	Ca_2SiO_4
*	01-080-2148	43	Quartz	0.132	0.979	SiO_2
*	00-024-0234	30	Calcium Silicate	-0.242	0.132	Ca_2SiO_4
*	00-048-1278	31	Titanium Oxide	-0.327	0.329	TiO_2
*	00-025-0843	33	Majorite	-0.223	0.245	$Mg_3Fe_2(SiO)_3$

Table 4.2 Identified Patterns List of Fan Palm

Visible	Ref. Code	Score	Compound Name	Displacement [°2Th.]	Scale Factor	Chemical Formula
*	49-2269	40	Poly(N-propyl-bisbenzoylamine 4,4'-diimido-diphenylethane)	0.000	0.230	$(C_{35}H_{25}N_3O_6)n$
*	16-0380	32	Silicon Oxide	0.000	0.318	$Si\ O_2$
*	34-1502	31	3-Acetyl-2-methylindole	0.000	0.305	$C_{11}\ H_{11}\ N\ O$
*	42-1172	17	Aluminum Silicon Carbide	0.000	0.605	$Al_4\ Si_3\ C_6$
*	01-1257	17	Aluminum Iron	0.000	0.043	Al Fe
*	81-0163	16	Chromium Silicon	0.000	0.153	$Cr\ Si_2$
*	83-1831	12	Coesite	0.000	0.240	$Si\ O_2$

The XRF chemical composition of the periwinkle shell and fan palm particle are representedin Table 4.3. XRF analysis confirmed that SiO_2, CaO, MgO, Cr_2O_3 and Fe_2O_3were found to be major constituents of the ash. Silicon dioxide, iron oxide, Cr_2O_3 and CaOare known to be among the hardest substances. Some other oxides viz. K_2O,

Na_2O and MnO were also found to be present in traces. The presence of hard elements like SiO_2, CaO, and Cr_2O_3 and Fe_2O_3 suggest thatperiwinkle shell and fan palm particles can be used as particulate material for brake pad production. This result of XRF is in agreement with the result of XRD obtained. Therefore, the present work shows the possibility of using periwinkle shell and fan palm particles as brake pad materials since the chemical composition has close similarity with the XRF analysis of palm kernel shell, bagasse and asbestos used in brake pad production (Dagwa and Ibhadode, 2006)

Table 4.3 XRF analysis of periwinkle and fan palm shell particles

Element composition / Material	% by weight								
	SO_3	CaO	Fe_2O_3	K2O	MgO	Na_2O	SiO_2	MnO	Cr_2O_3
Periwinkles shell	0.30	96.09	0.79	0.52	1.54	0.10	0.09	0.06	0.003
Fan Palm Shell	0.87	4.48	6.7	2.3	1.35	0.01	19.9	0.81	0.67

Surface morphology of periwinkle shell and fan palm particles is shown in back scattered electron (BSE) of Plate 4.1 and 4.2 respectively.The particle is observedto be solid in nature, but irregular in size. Some spherical shaped particles can also be seen in the Plates4.1 and 4.2.The chemical analysis show that the morphology of periwinkle shell particles consists mainly of Ca, Al, Si, Mg,Na and that of fan palm are C, H, Si, K, Mg as shown in the EDS scan (see Plate 4.1and 4.2). These results are consistent with XRD and XRF analyses of other biomass by Mayowa*et al.*, (2015).

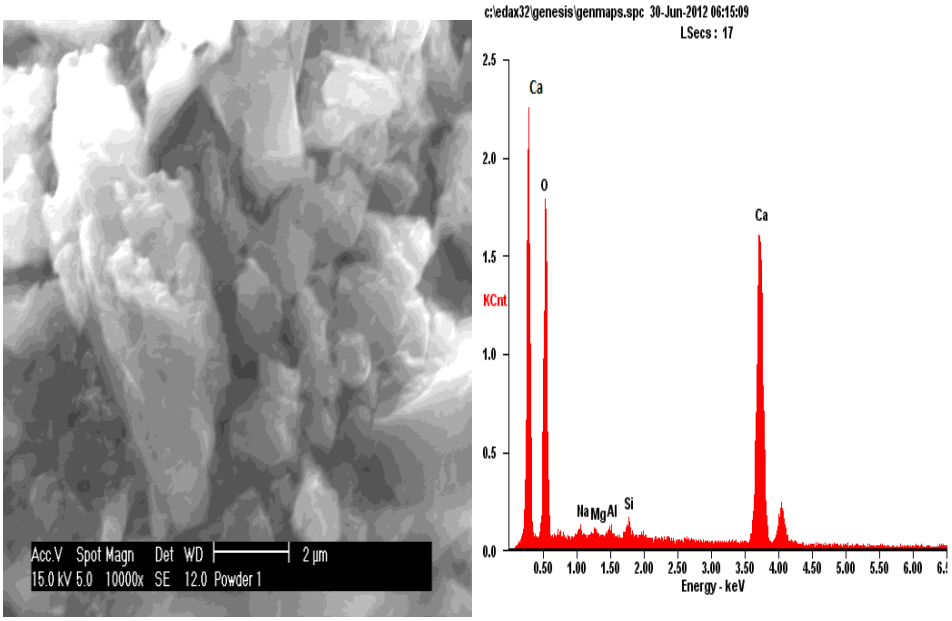

Plate4.1: SEM/EDS of the periwinkle shell particles

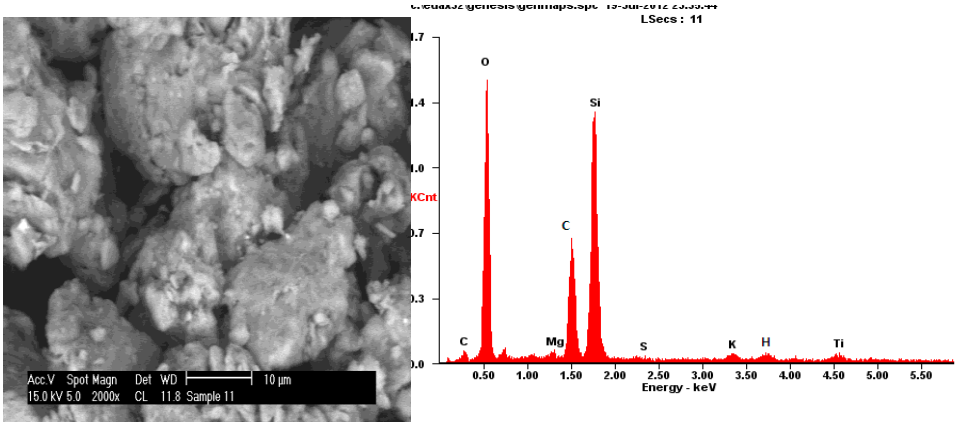

Plate 4.2: SEM/EDS of the fan palm particles

4.2 DENSITY OF THE SAMPLES

The result of density measurementsof periwinkle and fan palm brake samples for the various sieves sizes are shown in Figure 4.3 and Table A1 (Appendix A). From the Figure 4.3, the density of the samples increased as the sieve size is decreased from 710 to 125µm. In comparison, the corresponding values for asbestos are 2.8 kg/m$^{3.}$ The higher bulk density of periwinkle shell and fan palm particles implies that the particles are

closely packed, which reduces the possibility of air infiltration, which may initiate cracks in the manufactured product.

The increase in density as the particle sieve size decreased from 710-125µm can be attributed to the increases in bonding achieved i.e. increased packing of the particles. Resulting inreduction in porosity. Also the highest density which resulted to closer packing of particles creates more homogeneity in the entire phase of the brake pad composite body. The levels of density obtained are within the recommended values for brake pad application (Kim *et al.*, 2003).

The lower density shows that the periwinkle shell and fan palm based brake pad would be lighter than the asbestos brake pads. Consequently, periwinkle shell and fan palm shell particles are more suitable as filler material than asbestos on account of the overall weight of the vehicle. The result is in line with the earlier work of Ganguly and George (2008). The 125µm size has the highest density which is as a result of closer packing of the particles creating more homogeneity in the entire phase of the composite body.

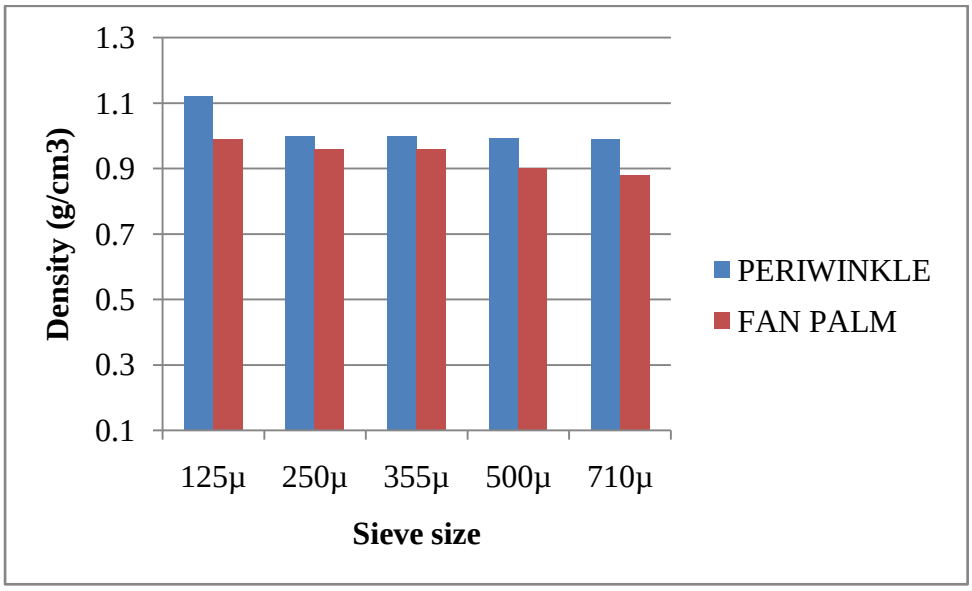

Figure 4.3: Effect of particle size on density of periwinkle and fan palm shells

4.3SURFACE MORPHOLOGY OF DEVELOPED BRAKE PAD

The surface morphology of theformulated brakepads was analyzed using SEM. Plates 4.3 to 4.7 shows the SEM Plates of the developed brake pad. The resin binder in the dark region can be seen in Plate 4.3 to 4.7 along with particles distribution in the white region. From the SEM study it can be postulated in general that microstructures of periwinkles shell based brake pad samples showed homogeneous distribution as the sieve size decreased (compare Plate 4. 3 with Plate 4. 7), while the microstructure of the fan palm based brake pad shows that particles are not well embedded in the resin. Fan palm particles are broken and there were voids around the particle indicating poor interaction.

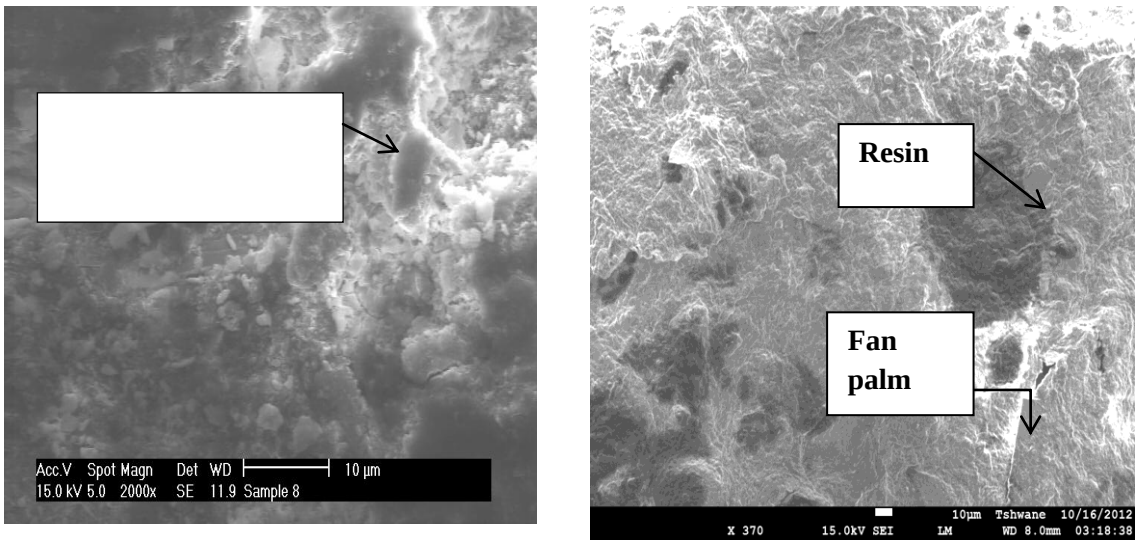

Plate 4.3: SEM microstructure of developed brake pad with 710µm particles size

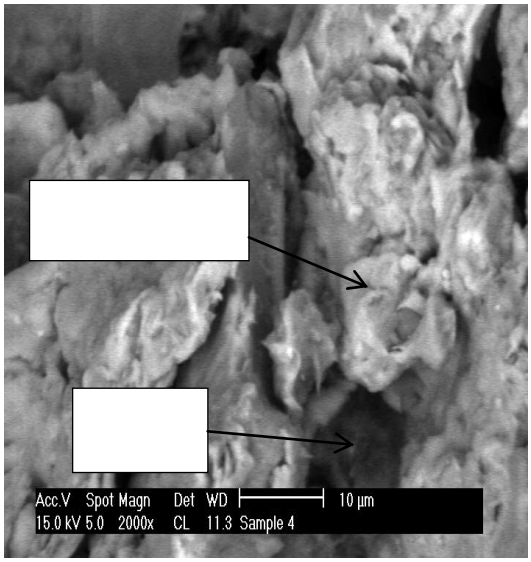

a) Periwinkle shell based brake pad

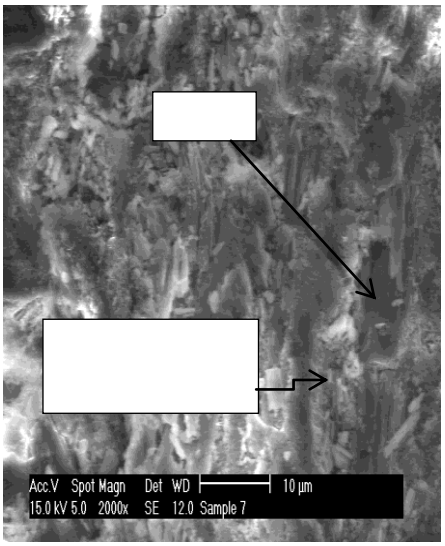

b) Fan palm based brake pad

Plate 4. 4: SEM microstructure of developed brake pad with 500µm particles size

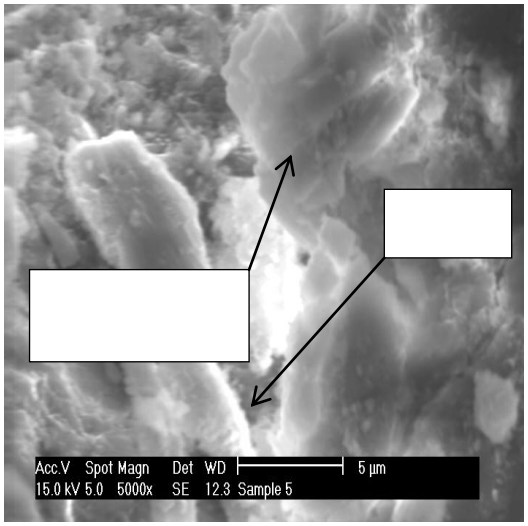

a) Periwinkle shell based brake pad

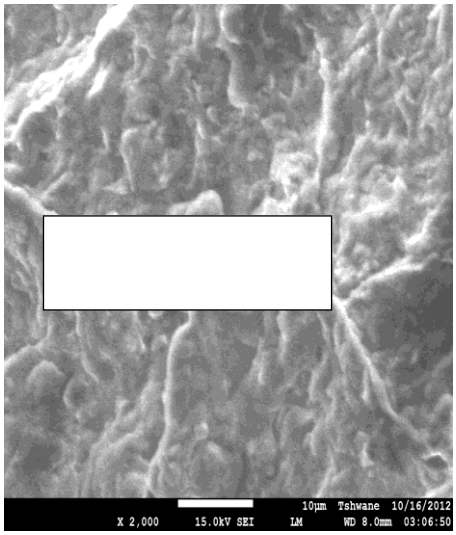

b) Fan palm based brake pad

Plate 4. 5: SEM microstructure of developed brake pad with 355µm particles

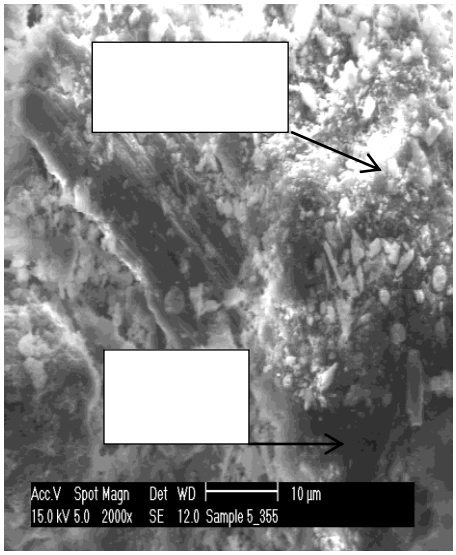

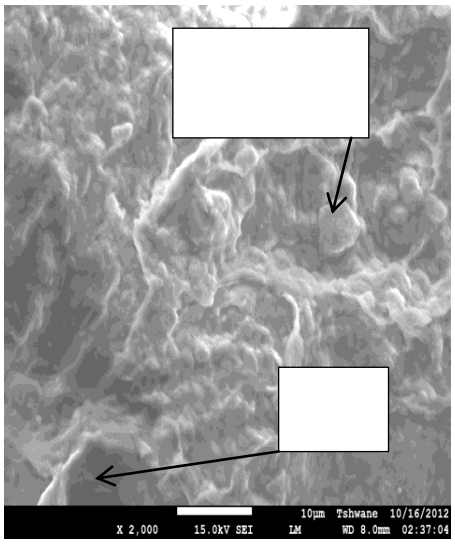

a) Periwinkle shell based brake pad **b) Fan palm based brake pad**

Plate 4.6: SEM microstructure of developed brake pad with 250µm periwinkle particles size

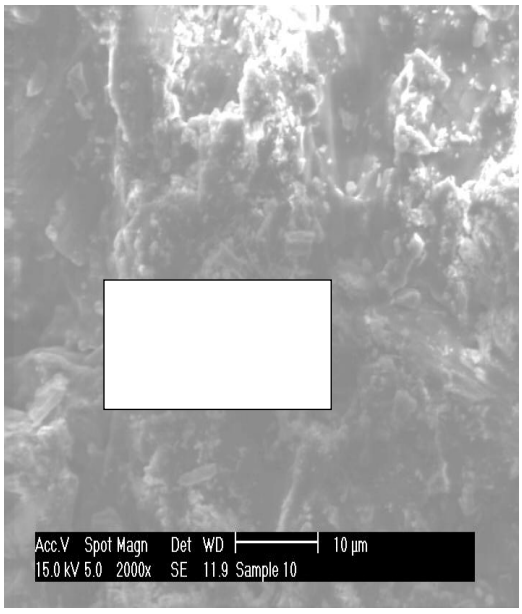

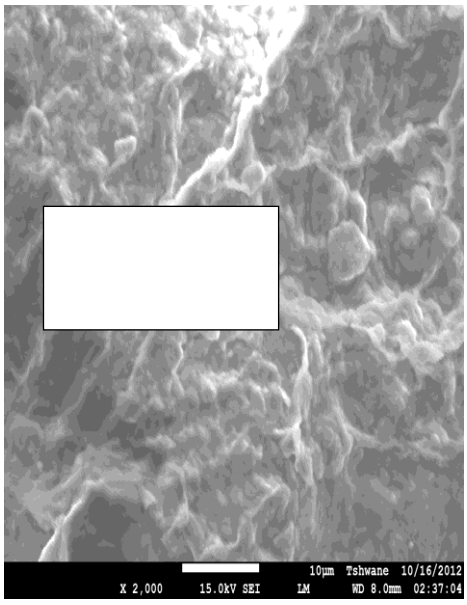

a) Periwinkle shell based brake pad **b) Fan palm based brake pa**

Plate 4.7: SEM microstructure of developed brake pad with 125µm particles size

4.4 EFFECT OF PARTICLE SIZE ON THICKNESS SWELL IN WATER AND SAE OIL

Figures 4.4to4.5 and Tables A2 to A3 (Appendix A) show the water and oil soak absorption of the developed samples. These properties decreased as the particle sizes decrease. This may be attributed to the decrease in pores because of the close interface packing achieved (see Plate 4.3to4.7). For the periwinkle shell based brake pad, increases in the interfacial bonding between the resin and the periwinkles shell particles led to decrease in the porosity level.

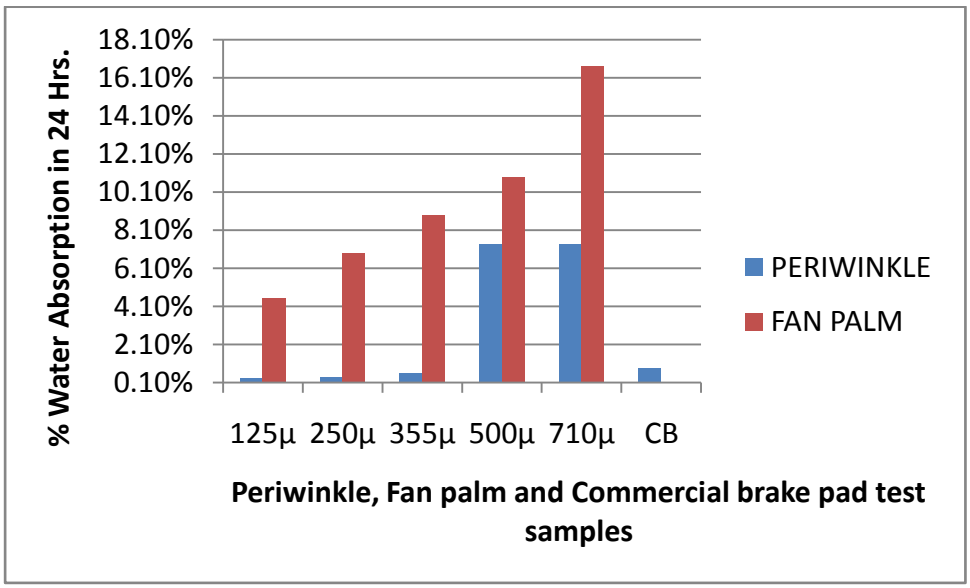

Figure 4.4: Effect of particle size on thickness swell in water for periwinkle shell, fan palm shell and commercial brake pad.

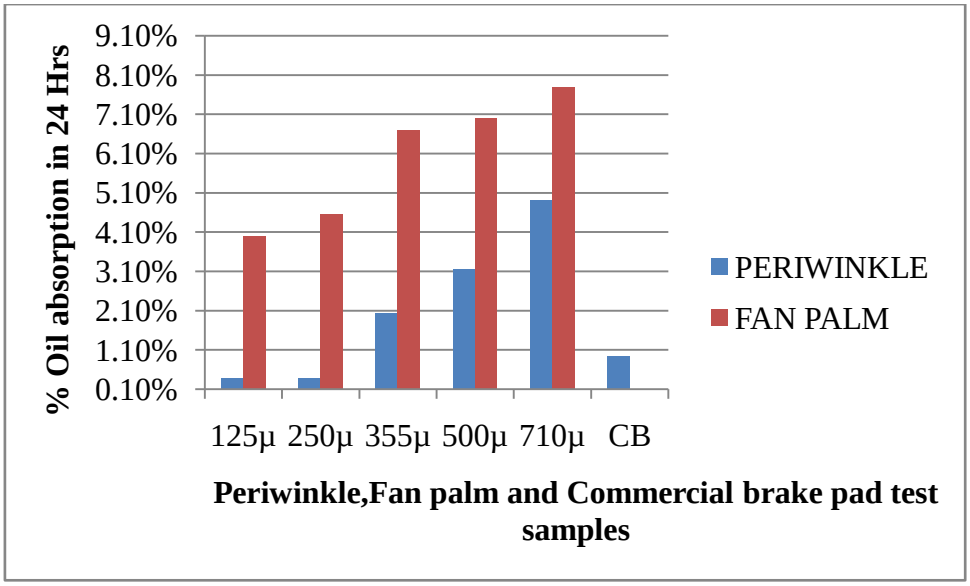

Figure 4.5: Effect of particle size on thickness swell in oil for periwinkle shell, fan palm shell and commercial brake pad.

The swelling that occurs during the water and oil absorption is the sum of two components, namely, swelling by hygroscopic particles and the release of compression stresses imparted to the brake pad composite during the pressing of material in the hot press.The release of compression stresses, known as spring back, is not recovered when the brake pad composite is in a dry state. From the Figures, the 125µm particles show lower values of both water and oil absorption than even the commercial brake pad. Higher sieve size resulted in more water absorption because more pores are observed. This result was influenced by porosity and voids formed in the brake pad samples. The water absorption decreased with decreasing particle sizes. Theoretically, lower water absorption by the brake pad will result in higher friction coefficient and wear rate due to higher contact area between the mating surfaces. The results obtained for the developed brake pad composites at 250-125µm periwinkle and fan palm shell particles are within the recommended standards.These results are at par with the earlier observations of the work of other researchersMathur*et al.*,(2004).

4.5 THERMAL ANALYSIS

The thermal analysis of the periwinkle shell particles, fan palm shell particles, commercial brake pad, the formulated brake pads for periwinkle and fan palm shells from sieve sizes of 125µm, 250µm, 355µm500µ and 710µm are shown in Figures 4.6 to 4.11

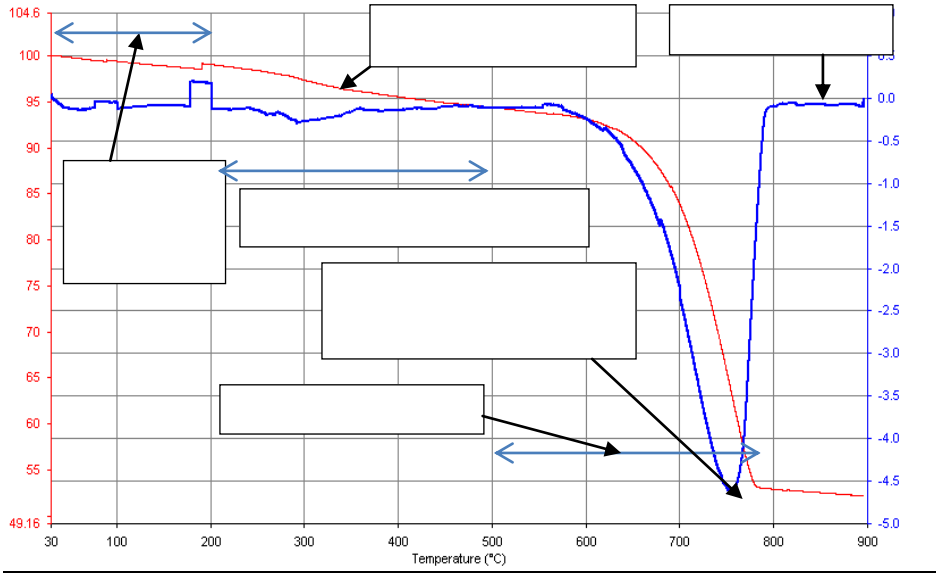

(a)TGA/DTG of Periwinkle shell particle

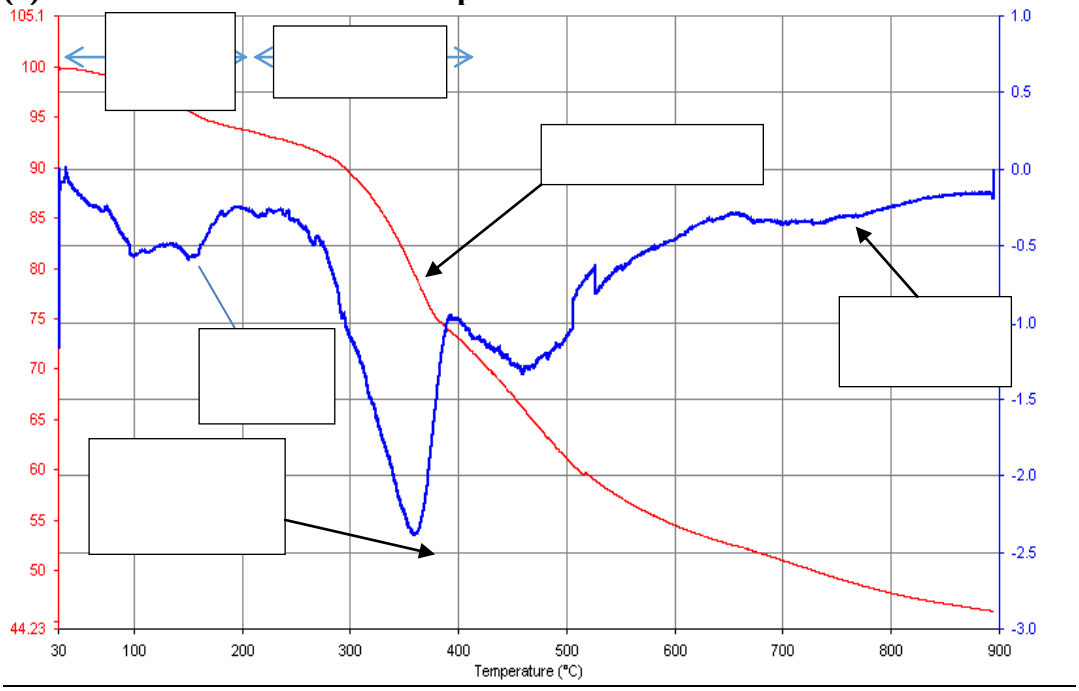

(b)TGA/DTG of Fan palmshell particles

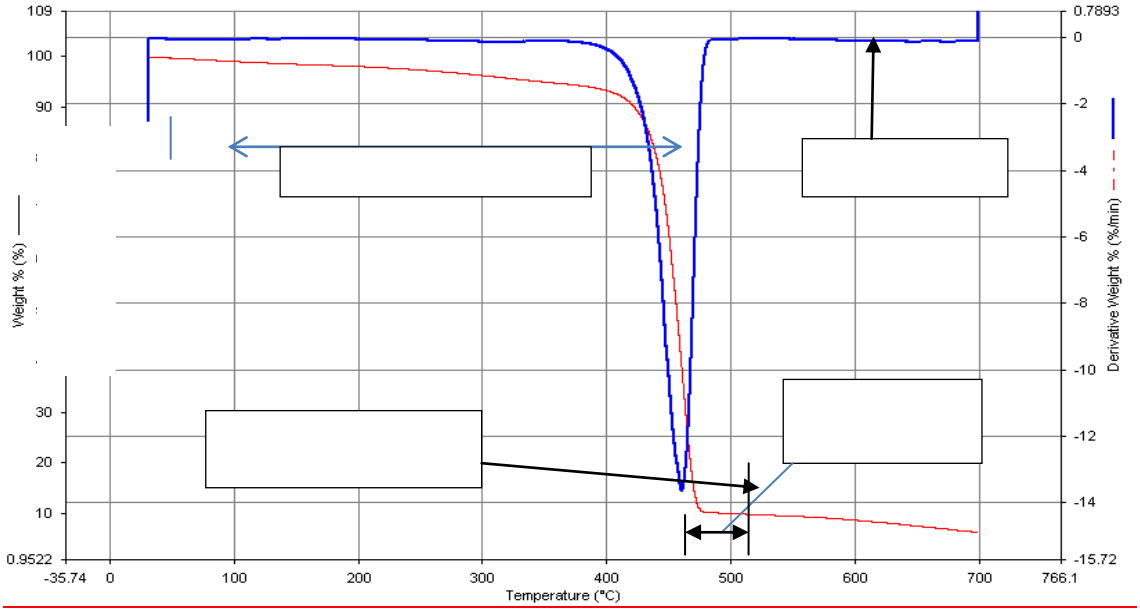

(c)TGA/DTG of Commercial brake pad Mercedes Benz

Figure 4.6 TGA/DTG pattern of periwinkle shell particles, fan palm shell particles and commercial brake pad.

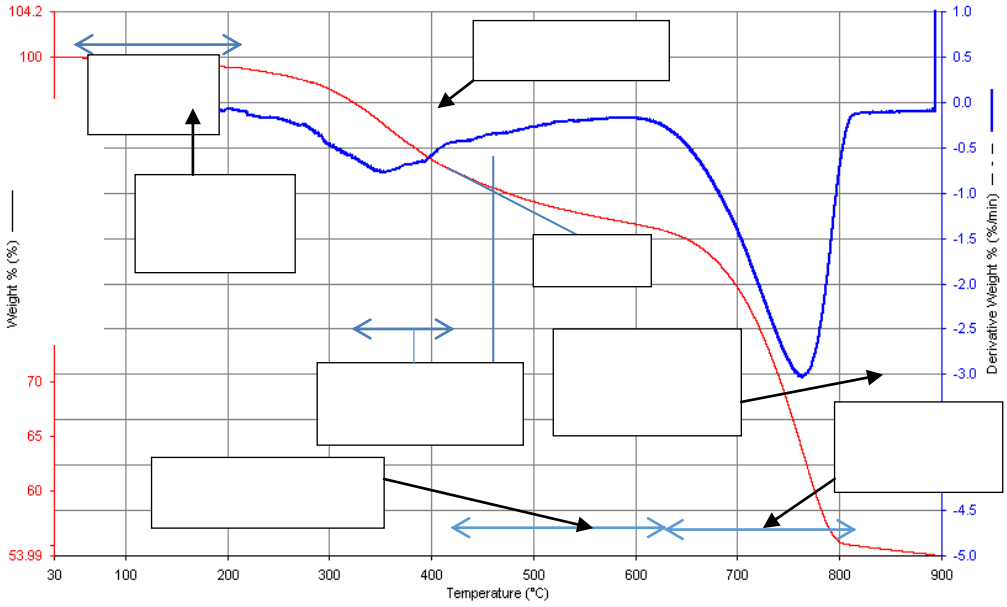

Figure 4.7a: TGA/DTG of developed brake pad from 125µm periwinkle shells

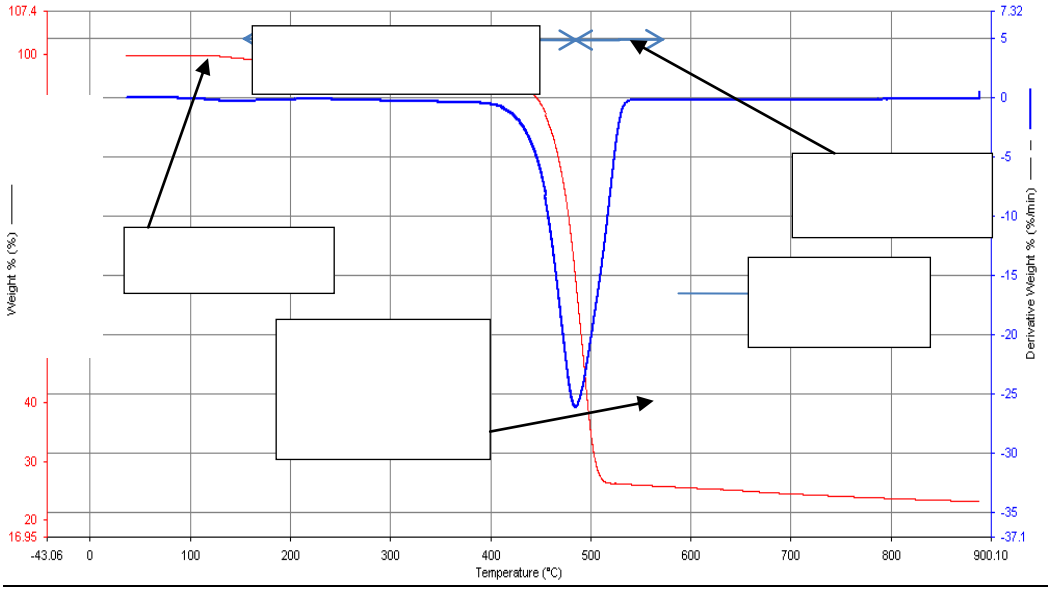

Figure 4.7b: DTA/TGA pattern of developed brake with 125µm fan palm particles

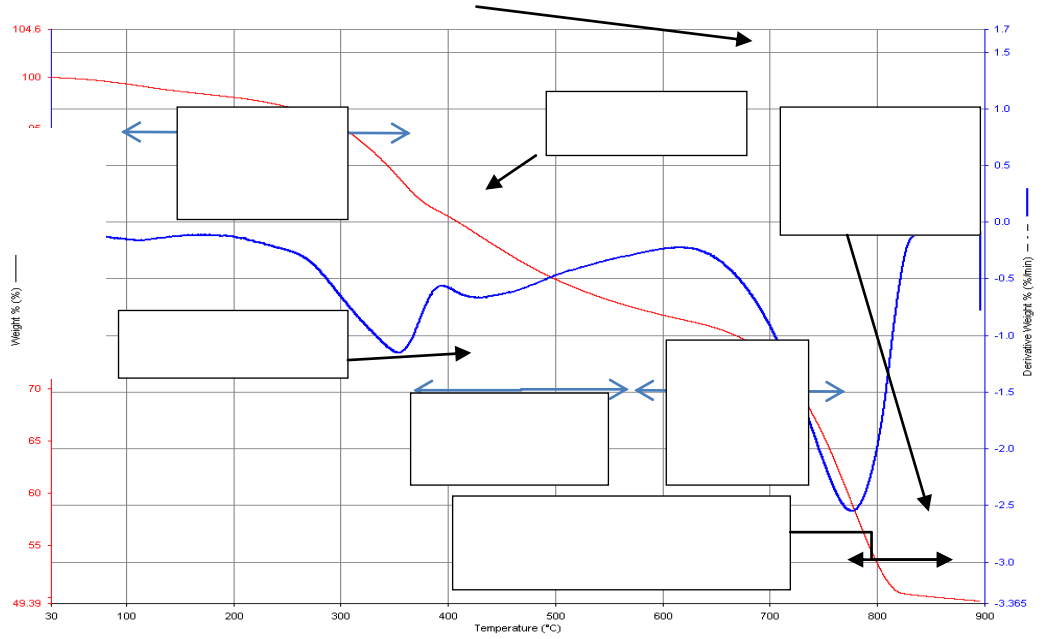

Figure 4.8a: TGA/DTG pattern of developed brake pad with 250µm periwinkle shell particles

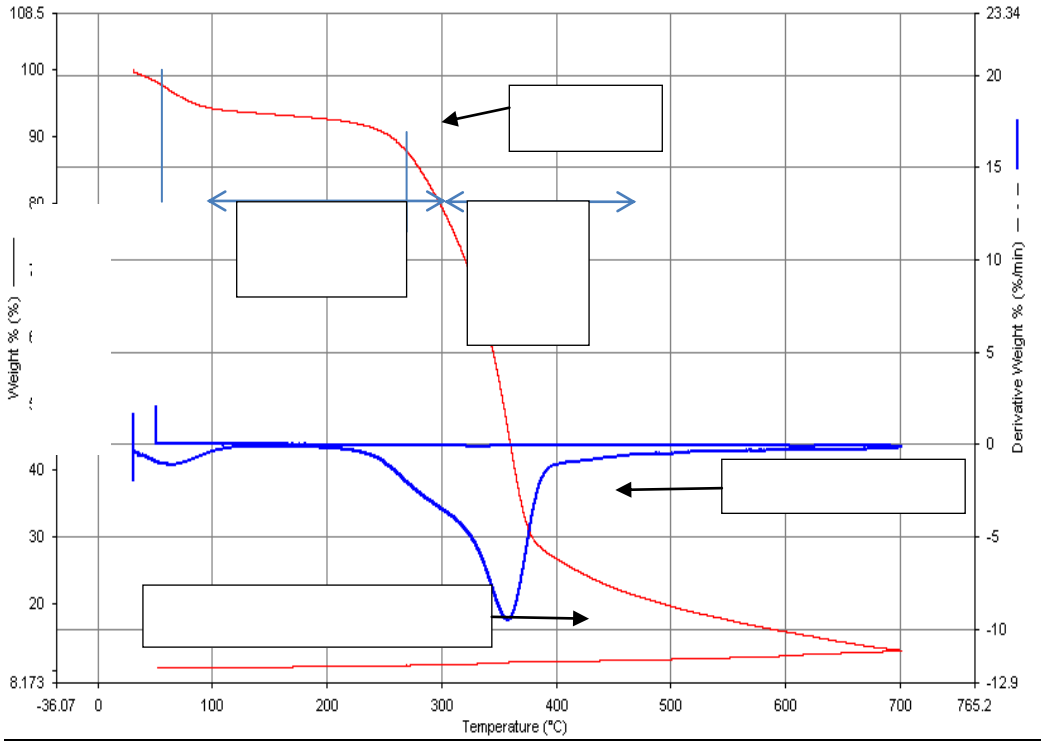

Figure 4.8b: TGA/DTG pattern of developed brake pad with 250µm fan palm shell particles

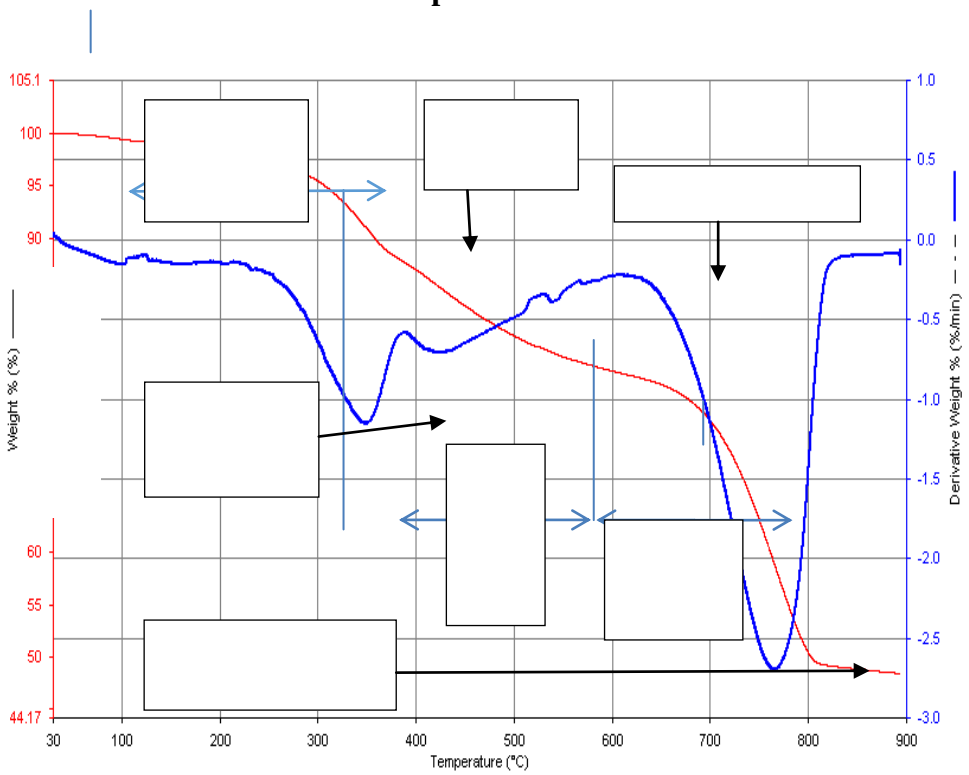

Figure 4.9a: DTA/TGA pattern of developed brake with 355µm periwinkle shell particles

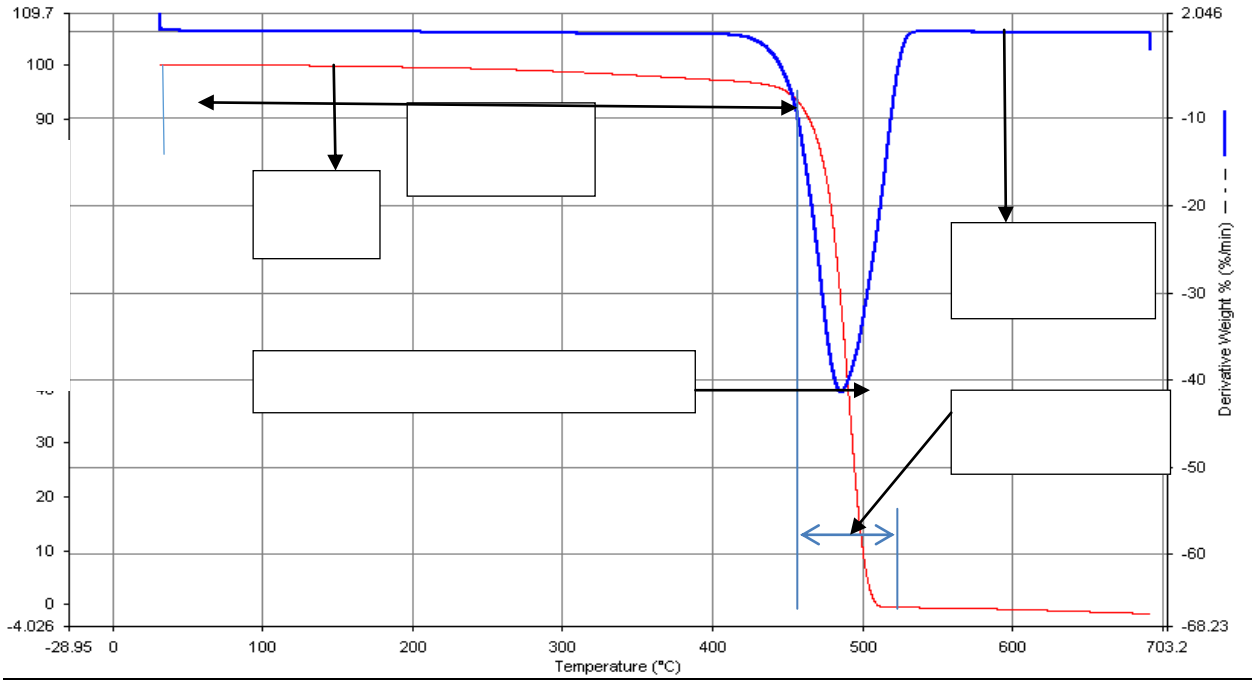

Figure 4.9b: DTA/TGA pattern of developed brake with 355µm fan palm shell particle

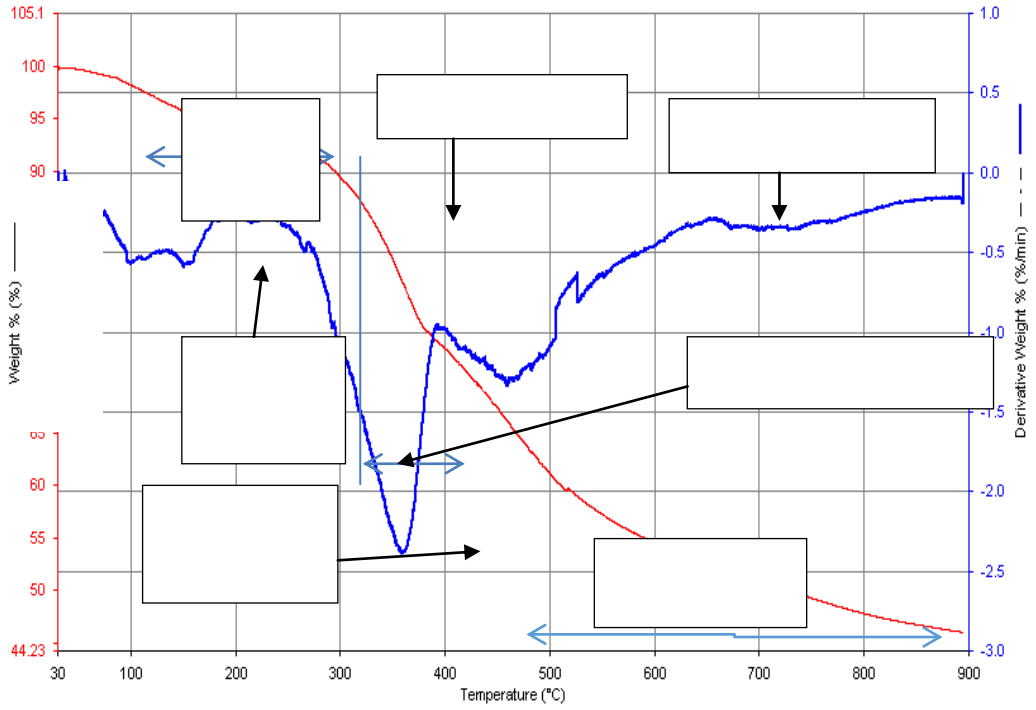

Figure 4.10a: DTA/TGA pattern of developed brake with 500µm periwinkle shell particles

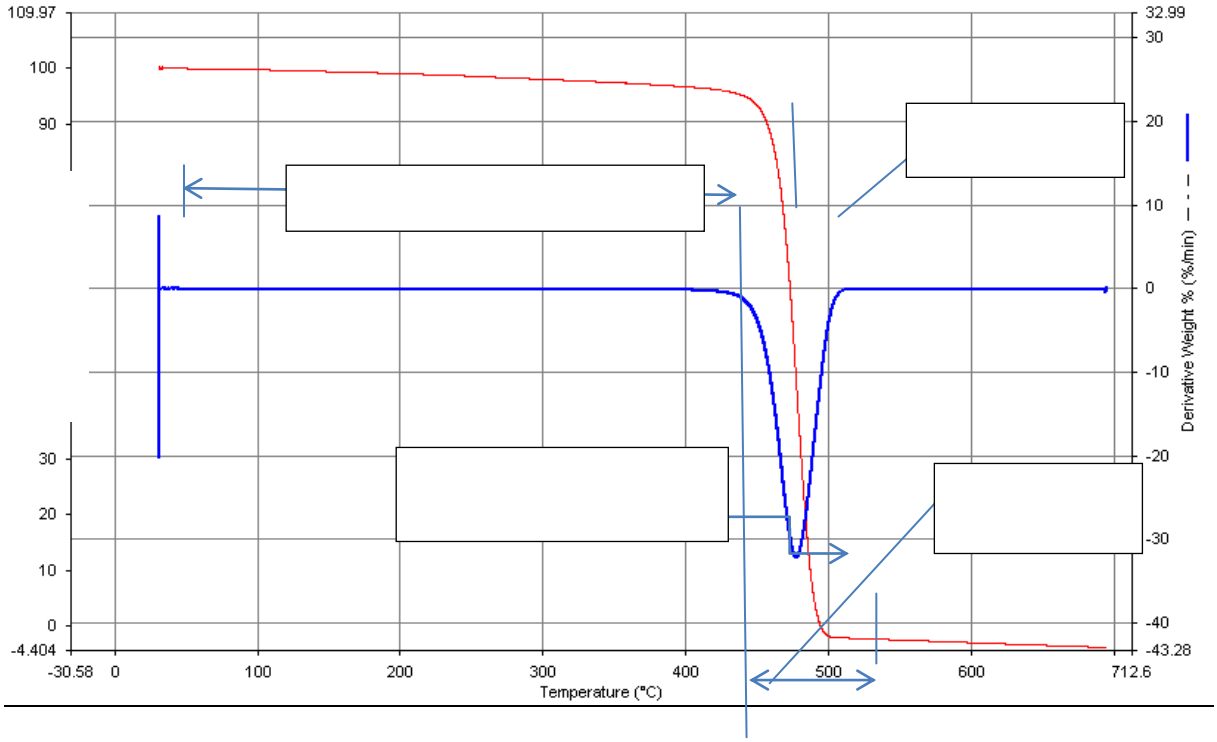

Figure 4.10b: DTA/TGA pattern of developed brake with 500µm fan palm shell particle

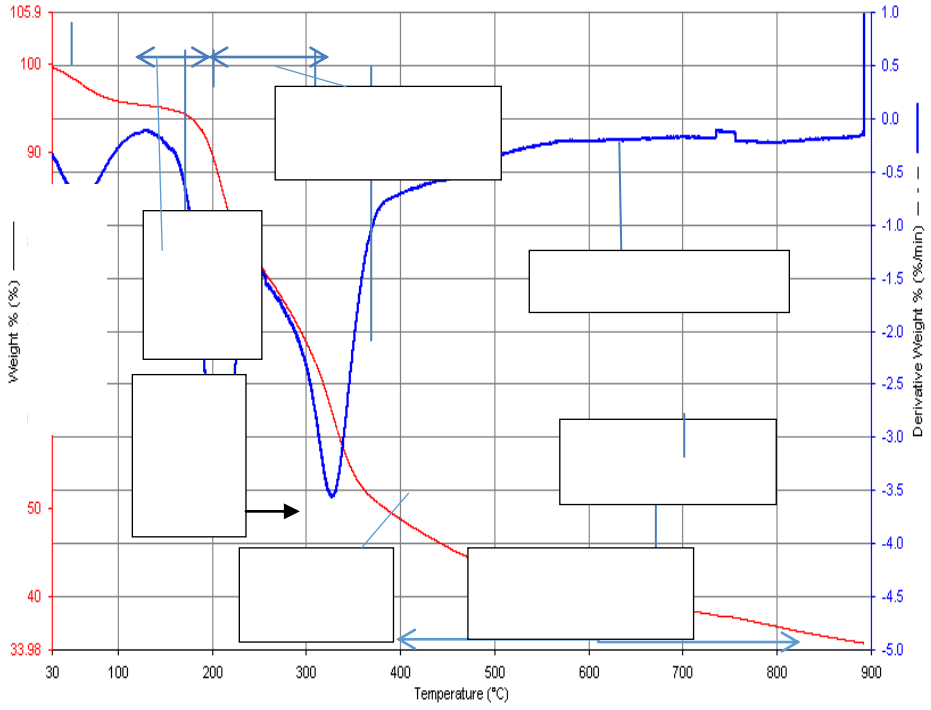

Figure 4.11a: DTA/TGA pattern of developed brake with 710µm periwinkle shell particles

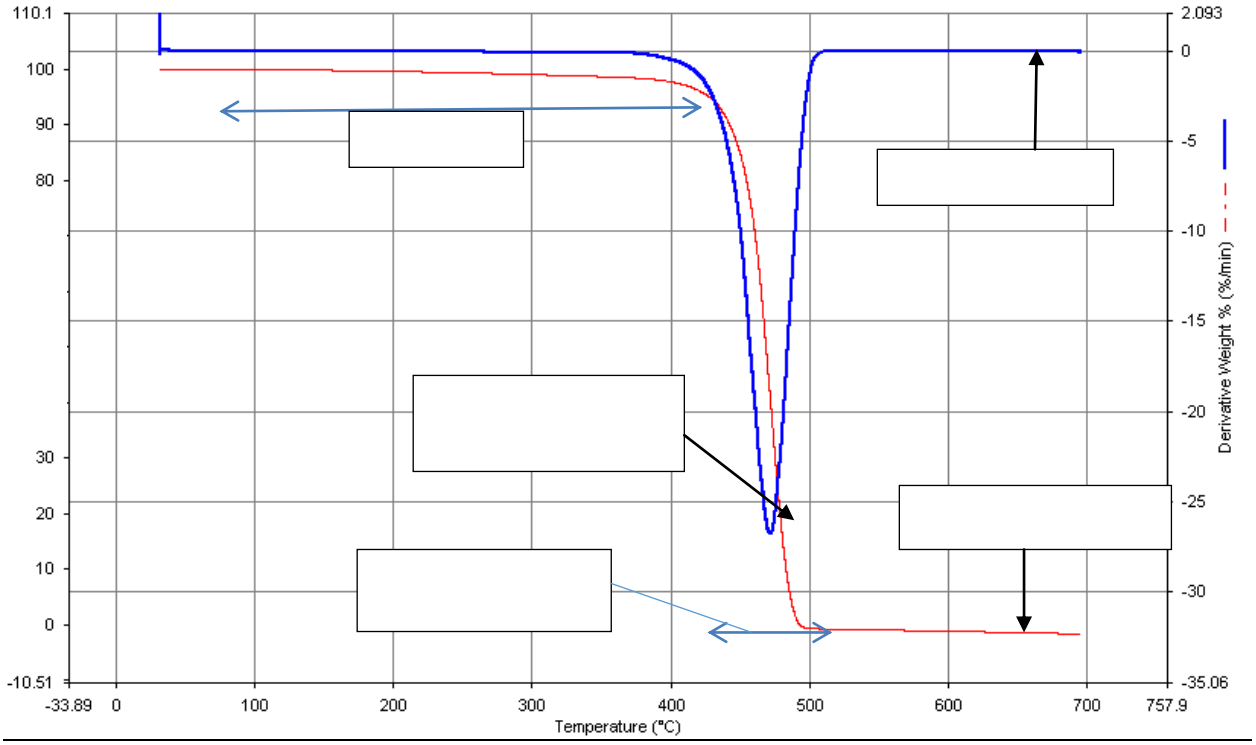

Figure 4.11b: DTA/TGA pattern of developed brake with 710µm fan palm shell particle

In Figure 4.6a, the DTG of the periwinkle shell shows that the occurs at 780°C, while the TGA curve shows three regions of weight loss; from 30°C to 200°C due to removal of moisture and light volatiles, 200°C to 500°C due to further removal of light volatiles and 500°C to 780°C due to pyrolysis.

In fig 4.6b the thermal analysis of fan palm shell particles, shows two stepswt. loss. The first weight loss between 30°C to 200°C corresponds to the removal of physically absorbed water and light volatiles with a maximum mass loss at 80°C as observed in the DTG curve. The second step between 200°C and 400°Cis due to active pyrolysis with maximum weight loss at 360°C as depicted by the DTG curve.

Figure 4.6c is the thermal analysis of the commercial brake pad. The maximum degradation occurs as 450℃, with the 1st mass lost occurring between 30 °C to 400°C, and the second mass loss is between 400°C to 480°C.

The comparative analysis of % weight loss of Figures; 4.6c,4,7a,4,8a,4.9a,4.10a and 4.11a for the different sieve sizes for the periwinkle and commercial brake pads are shown in Table 4.4 and Figure 4.12.The Figures,show that within the recommended brake pad operating temperature of 300ºC to 500ºC, the %weight loss of periwinkle brake pad formulation for the 125µm, 250µm,355µm,500µm, and 710µm, is 15%, 20%, 22%, 35% and 55%, while that of the commercial brake pad at the same operating temperature is 100%.Similarly, from Figures 4.6c, 4, 7b, 4, 8b, 4.9b, 4.10b and 4.11b, the comparative analysis of % weight loss for the different sieve sizes for the fan palm and commercial brake pads are shown in Table 4.5 and Figure 4.13. The Figures, show that within the recommended brake pad operating temperature of 300ºC to 500ºC, the %weight loss of fan palm brakepad formulation for the 125µm, 250µm, 355µm, 500µm, and 710µm, is 70%, 77%, 100%, 100% and 100%, while that ofthe commercial brake pad at the same operating temperature is also 100%. The low % weight loss for the periwinkle shell may be due the presence of CaOwhich has a very highdegradation temperature of~ **800**℃(Aku*et al.*, 2012)and also as shown in Figure 4.6a. Thus periwinkle and fan palm shells can be used in the development of an automobile disc brake pad.

Table 4.4comparative % weight loss for periwinkle shell brake pad formulation and commercial brake pad

Temperature °C / Sieve size	30°C.	100° C.	200° C.	300° C.	400° C.	500° C.	600° C.	700° C.	800° C.	900° C.
125µm	0%	0%	2%	3%	12%	17%	18%	20%	48%	55%
250µm	0%	2%	4%	7%	15%	20%	23%	26%	40%	66%
355µm	0%	3%	5%	7%	17%	22%	24%	32%	42%	55%
500µm	0%	4%	8%	10%	31%	39%	45%	51%	55%	58%
710µm	0%	4%	10%	30%	52%	57%	63%	66%	65%	70%
CB	0%	0.50 %	1%	1.50 %	3%	100 %	100 %	100 %		

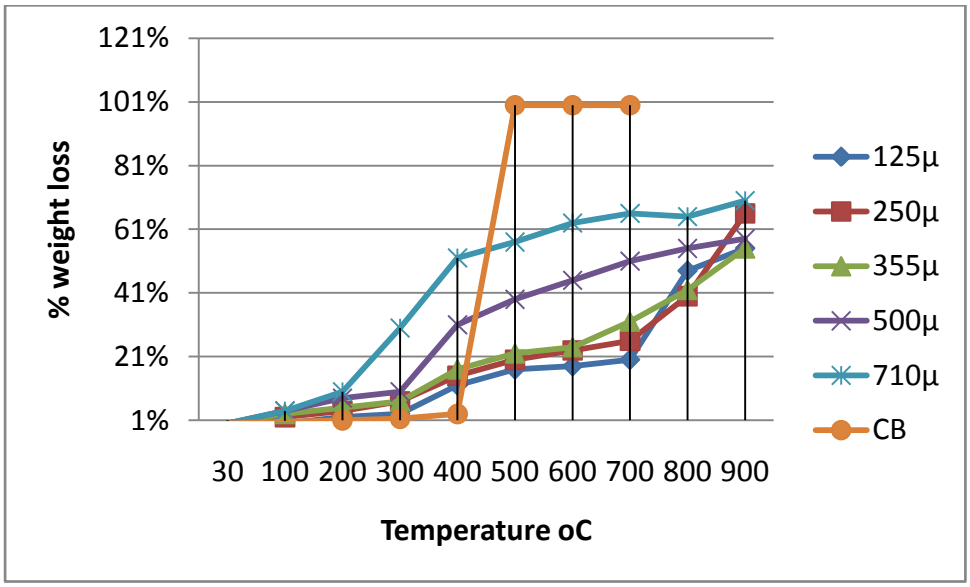

Figure 4.12; comparative % weight loss for periwinkle shell brake pad formulation and commercial brake pad.

Table 4.5comparative % weight loss for FanPalm shell brake pad formulation and commercial brake pad

Temperature °C	30°	100°	200°	300°	400°	500°	600°	700°	800°	900°

sieve size	C.	C.	C.	C.	C.	C.	C.	C.	C.	C.
125µm	0%	0%	10%	10%	12%	70%	73%	78%	78%	79%
250µm	0%	3%	4%	7%	73%	77%	80%	100%		
355µm	0%	0%	0%	0%	2%	100%	100%	100%		
500µm	0%	1%	2%	2%	3%	100%	100%	100%		
71µm	0%	0%	0%	0%	2%	100%	100%	100%	100%	
CB	0%	0.50 %	1%	1.50 %	3%	100%	100%	100%		

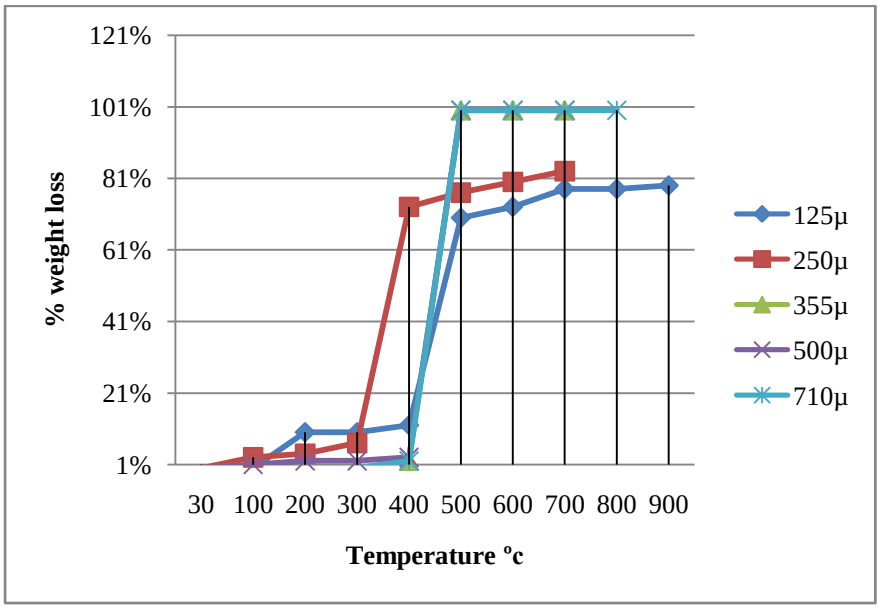

Figure 4.13: comparative % weight loss for Fan palmshell brake pad formulation and commercial brake pad

4.6 HARDNESS VALUES

The hardness values of the samples are shown in Figure 4.14 and Table A4 (Appendix A). From the results it is clear that the hardness increased with decrease in particles size. This is in agreement with Harald, *et al.*, (2010). The sample of 125µm sieve size has the highest hardness values of 116.7 and 95.7HBN for periwinkle shell and fan palm particle brake pads respectively. A sharp drop in hardness was observed in the samples with higher sieve grades (250, 355, 500 and 710µm). The high hardness for the 125µm sieve grade which much higher than that of the commercially used brake pad (CB) isas a result

its high bonding ability with the resin. The hardness value for this material was compared with other materials from other researches. Thus the hardness values of periwinkle shell and fan palm particle based brake pads at 125µm size is higher than that of the commercial brake bad (CB). Thisis probably due to the presence of $Fe2O_3$, CaO and SiO_2 in the periwinkle shell particles.

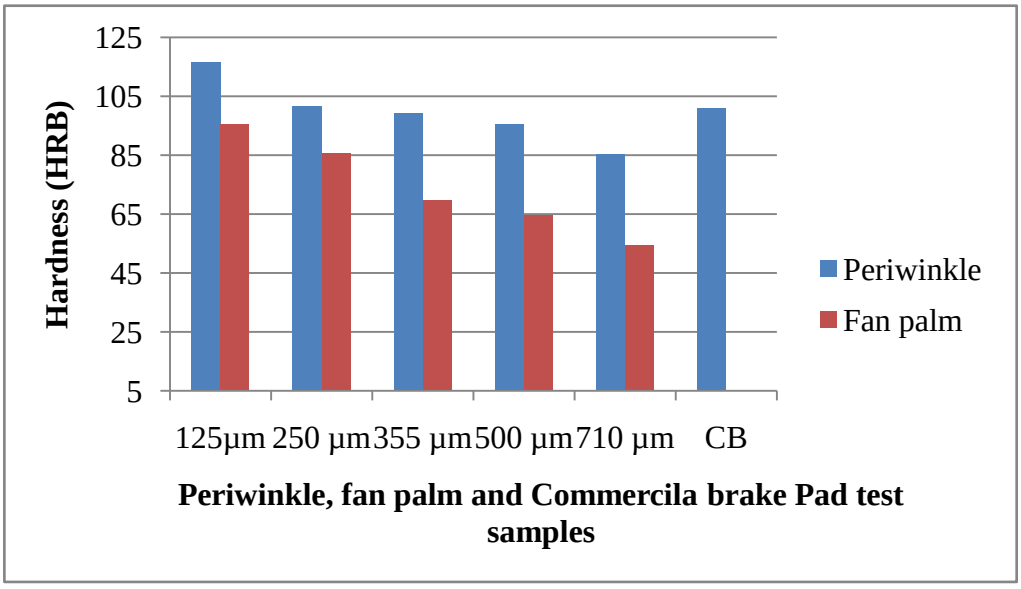

Figure 4.14: Effect of particle size on hardness values for periwinkle shell, fan palm shell and commercial brake pad

4.7 COMPRESSIVE STRENGTH

Compressive properties of the samples are presented in Figure 4.15 and Table A5 (Appendix A). It is clear that the compressive strength of the developed brake pad increased as the particle size decreased for both materials.This may be due to the hardening of the resin by particles. Brake pad formulation with 125µm periwinkle shell particles showed the highest compression strength compared to the commercial brake pad (CB), and the other sieve size used. The smaller the pores,the more thecompaction andthehigher the compression strength as shown by the 125µm periwinkle brake pads.

The decrease in compressive strength as the particle size increased is due to the interference of particles in the mobility or deformability of the resin. This interference is

created through the physical interaction and immobilization of the resin by the presence of mechanical restraints, thereby reducing the strength (Mahanty and Cough, 2007; George and Arnab2007).Also, the decrease in compression strength of the fan palm brake pads may be attributed to decreasing inthe interfacial area as the particles size increases resulting to weak interfacial bonding between the particles and resin (Plate 4. 3 to 4.7)

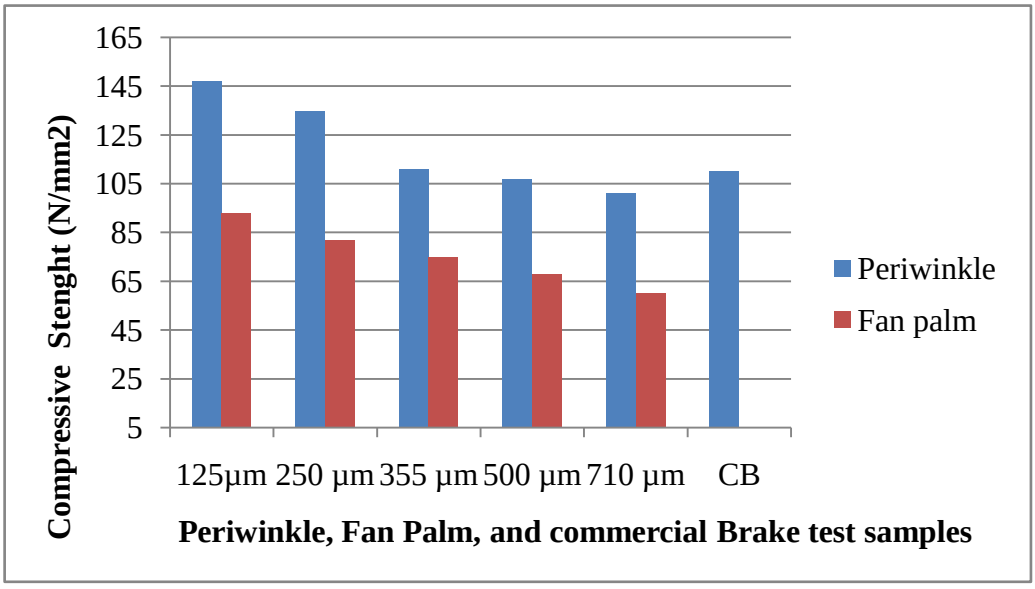

Figure 4.15: Effect of particle size on compressive strength values for periwinkle, fan palm and commercial brake pads

4.8 WEAR CHARACTERISTICS OF DEVELOPED AND COMMERCIAL BRAKE PADS

Figures4.16to4.19 and Tables A6 to A13 (Appendix A) show the variation of wear rate with applied loadsliding speed, and temperatures of the developed and commercial brake

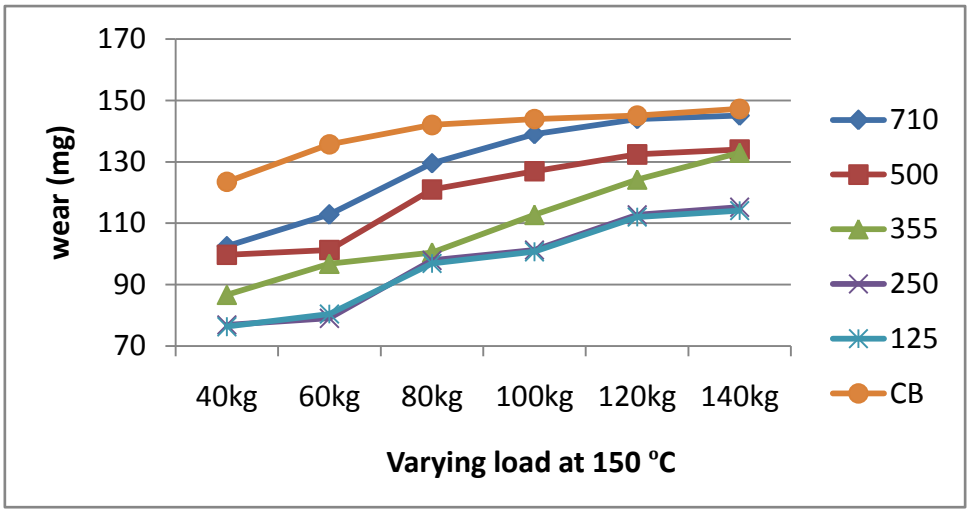

(a) Periwinkle shell and commercial brake pad

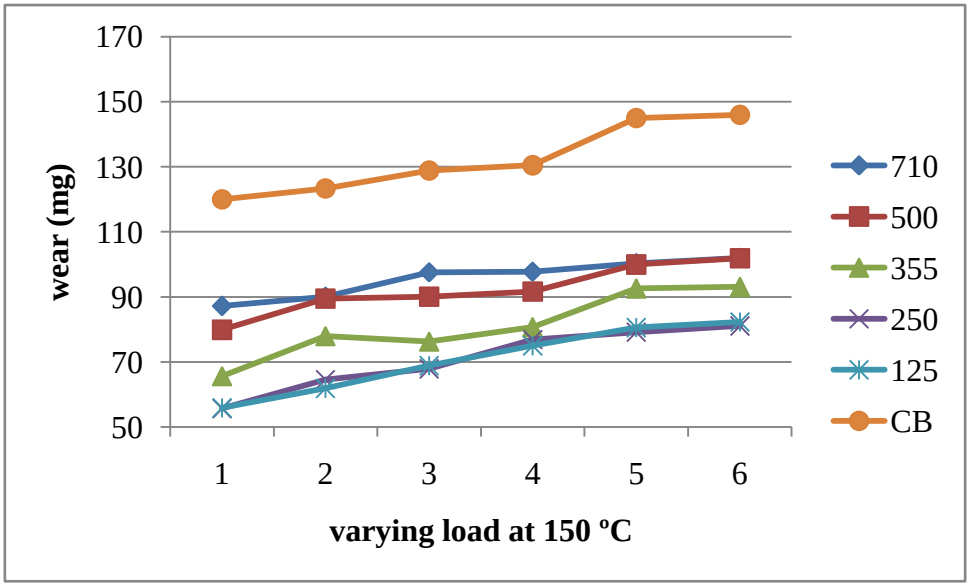

(b) Fan palm shell and commercial brake pad

Figure 4.16: Effect of load on wear (mg) of developed fan palm brake and commercial brake pad at varying load at constant speed 2.4m/s, time 45min at 150°C.

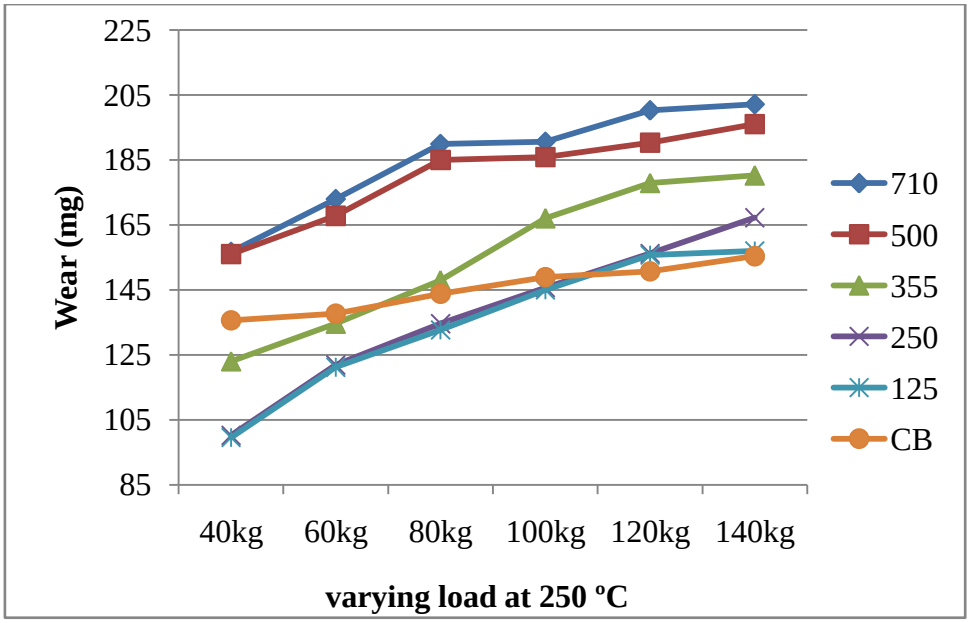

(a)Periwinkle shell and commercial brake pad

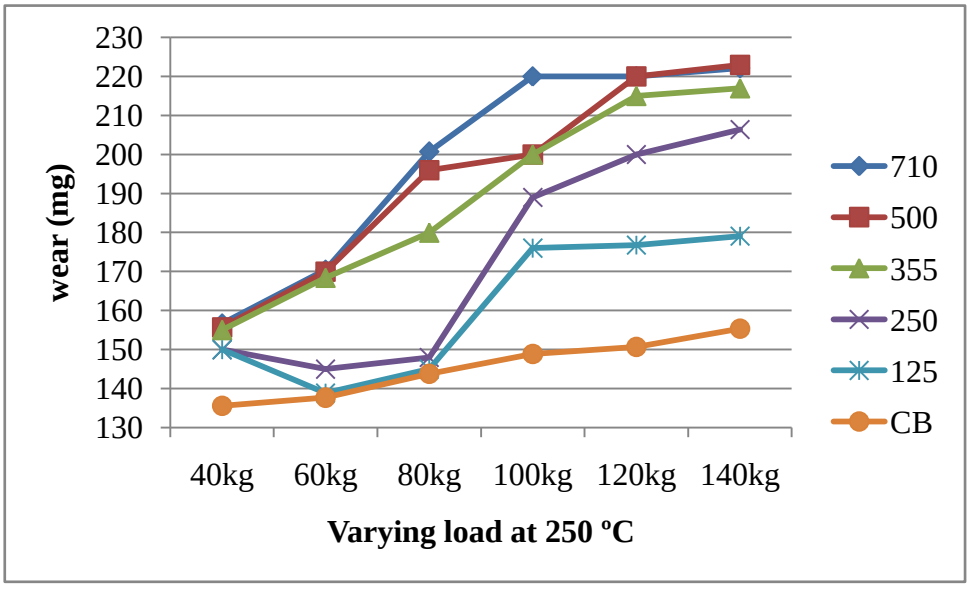

(b)Fan palm shell and commercial brake pad

Figure 4.17: Effect of load on wear (mg) of developed fan palm brake and commercial brake pad at varying load at constant speed 2.4m/s, time 45min at 250^{o}C

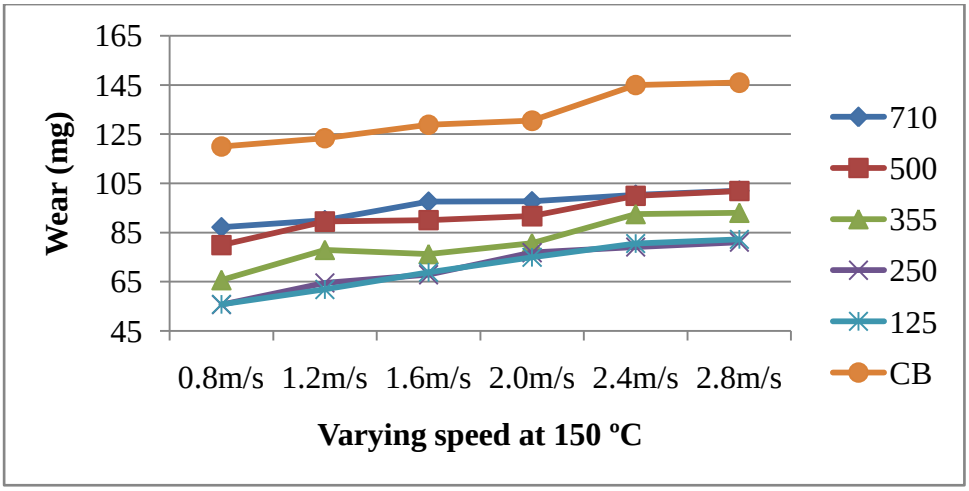

(a) Periwinkle shell and commercial brake pad

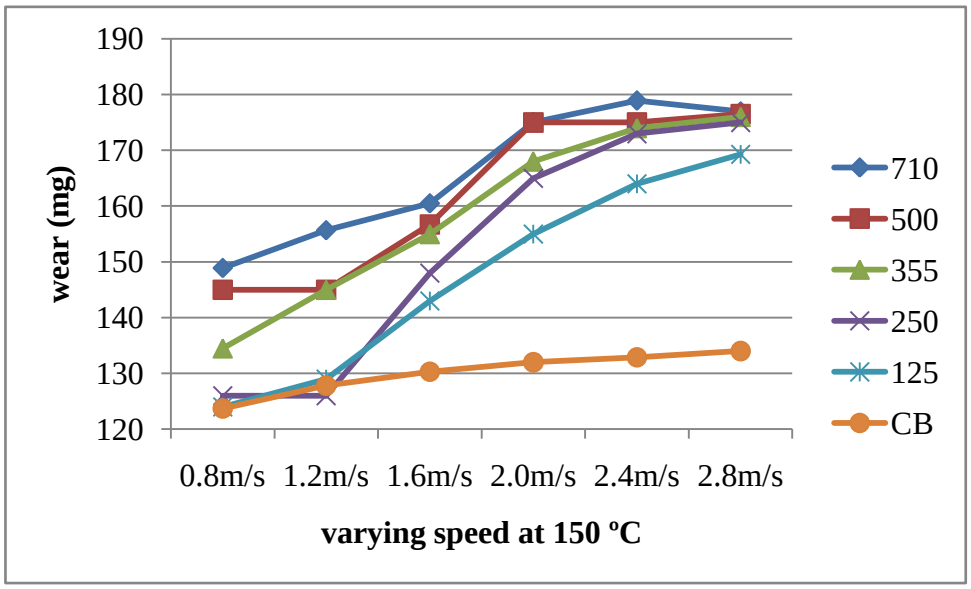

(b) Fan palm shell and commercial brake pad

Figure 4.18: Effect of sliding speed on wear (mg) of developed fan palm brake and commercial brake pad at varying speed at constant load 120kg, time 45min at 150^{o}C

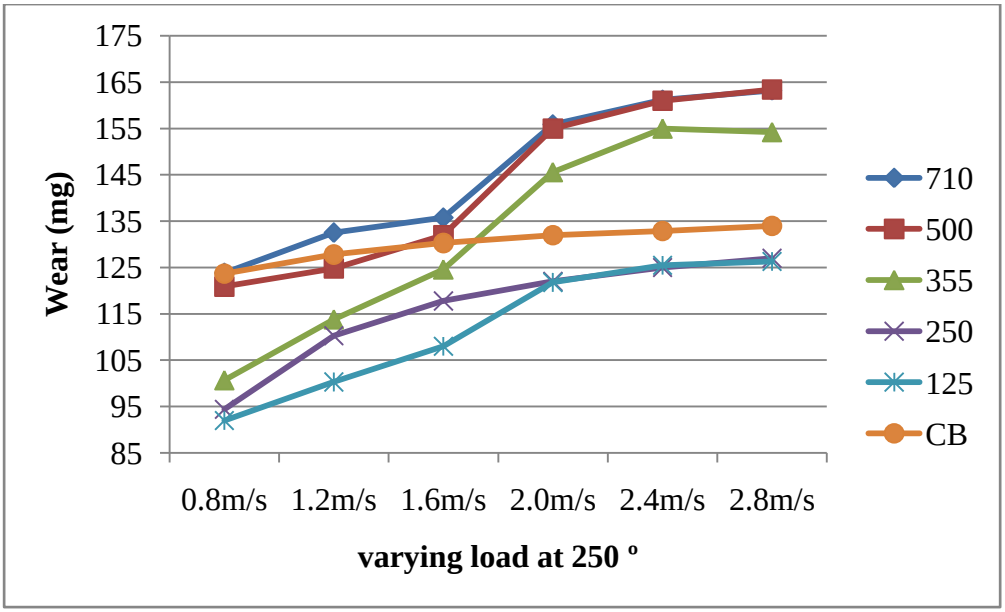

(a)Periwinkle shell and commercial brake pad.

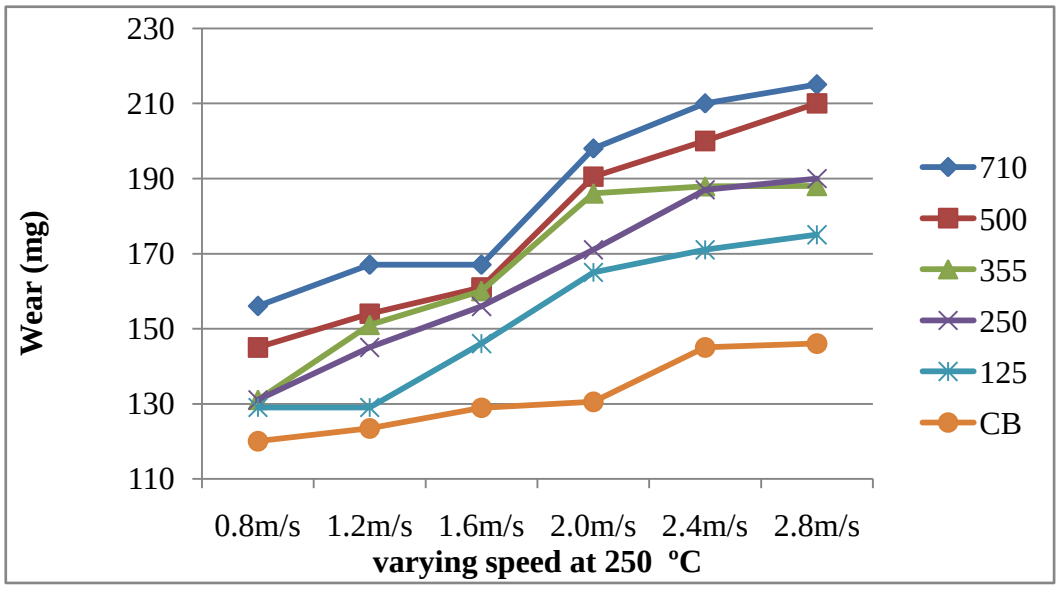

(b)Fan palm shell and commercial brake pad.

Figure 4.19: Effect of sliding speed on wear (mg) of developed fan palm shell brake and commercial brake pad at varying speed at constant load 120kg, time 45min at 250°C.

It can be seen that as the sliding speed, load and temperature increase, in wear of the developed brake pad also increased (see Figures 4.16to 4.19).The wear rate of the710µm particle size is more than that of the other samples for allsliding speeds, loads

andtemperatures.As the sliding speed and temperature increase the wear rate of the samples increases.However,the wear rate decreases with decrease in the particle sizeis due to higher bonding of the 125 µm with resin resulting in less plastic deformation which occurs by the plowing action. This is in agreement with Archads low which gives the relationship between wearvolume loss (Δ*V*), applied load (*L*,), sliding distance (*S*,) and hardness of the wearing surface (*H*) wear coefficient (K) (Jeong*et el.*,2001)

$$\Delta V = K.\frac{L.\ S}{H} \qquad 4.1$$

From Figures 4.14 to 4.17, a decrease in particles size reduces the wear rate. When the load applied is low; the wear loss is quite small, and increases with increase in applied load. This is because at higher loads, fracture of the reinforced particle in the matrix occurs. As a result, the mechanical property of the composite decreases, hence the wear rate of the composite increases.A similar trend was also observed independently for different wear distances as a function of load and speed by Aigbodion*et al.*,(2010). In addition, to the increase of wear with increase of loads, is wear mechanism (of the composite changes with loads as reported by Gul and Acilar(2004).The wear increases with particle size decreases may be attributed to better interfacial bonding between the reinforcement particles and the resin. This is in agreement with Kumar and Balasubramanian (2010).The size effect is also related to increase propensity for cracking of large particles as well as decreases in slip distance at fine particle sizes. This is becausesmaller particles serve as barriers to slip, small inter-particle distance reduce slip distance.

Sliding speed is another parameter which affects the wear behavior of brake pads. It has been reported that an increase in sliding speed causes an increase in wear and decrease in wear resistance of friction materialsNatarajanetal. (2006).This isbecause as the speed

increases, the interface temperature also increases resulting in; microthermal softening of the matrix material (Qin *etal.*,2008), oxide formation on the contact area (Menezes*etal.*,2011) and decrease in flow stress of the material.Temperature is another key factor that affects the wear of friction materials however, the effect of temperature on wear is similar phenomenon to the effect of sliding speed and load already discussed.

The decrease in wear rate of the periwinkle based brake pads compared to that of the fan palm brake pad composite may also be attributed to higher load bearing capacity of hard materials (CaO) and better interfacial bond between the particles and theresin as shown in (Plate 4.3 to 4.7) reducing the possibility of particle pull out which may result in lower wear in the periwinkle pads than in the fan palm pads. The improvement in wear resistance accompanying the presence of decreasing particle size of the periwinkle shell in the resin is due to an increase in average hardness values and compressive strength (see Figures 4.12to 4.13). The wear rates obtained for these periwinkle shell brake pads from 125 to 250µm size fall within the automotive standard ranges for the production of automotive brake pads Bhagwan, *et al.*,(2000).

4.9 FRICTION CHARACTERISTICS OF DEVELOPED AND COMMERCIAL BRAKE PADS

Figures 4.18to 4.21 and Tables A14 to A21 (Appendix A) show the effect of load and sliding speed on the co-efficient of friction of the developed and commercial pads at 150^{o}C and 250^{o}C.The co-efficient friction for both the developed and the commercial brakes pads decrease as applied loads, sliding speed and temperatures increasedand for the developed brake pad.

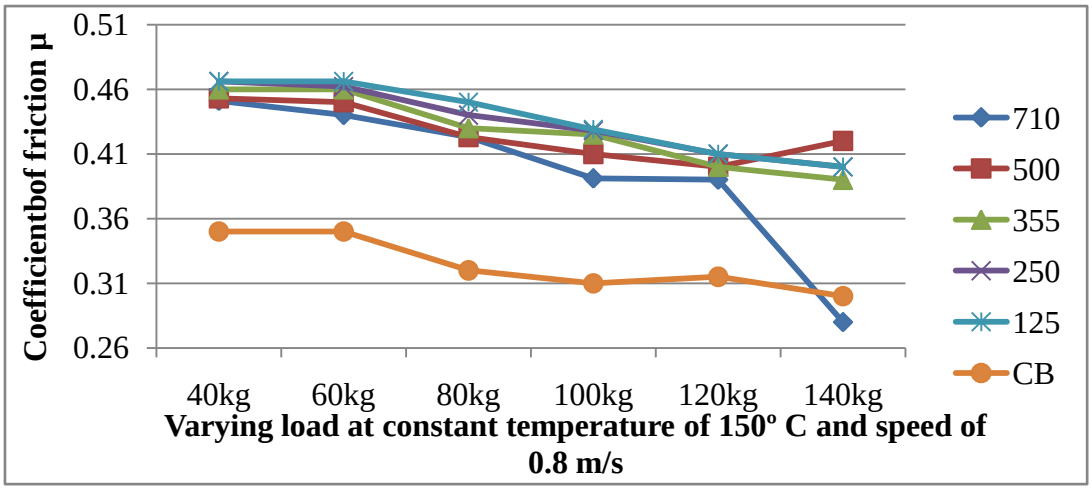

(a) Periwinkle shell and commercial brake pad

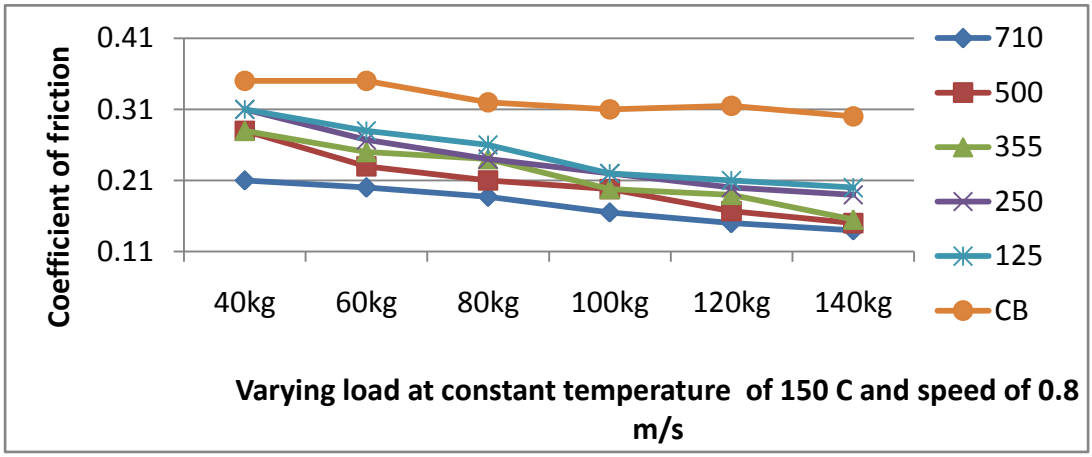

(b) Fan palm shell and commercial brake pad

Figure 4.20: Effect of load on coefficient of friction of developed periwinkle/ fan palm and commercial brake pads at constant speed and temperature for 45mins.

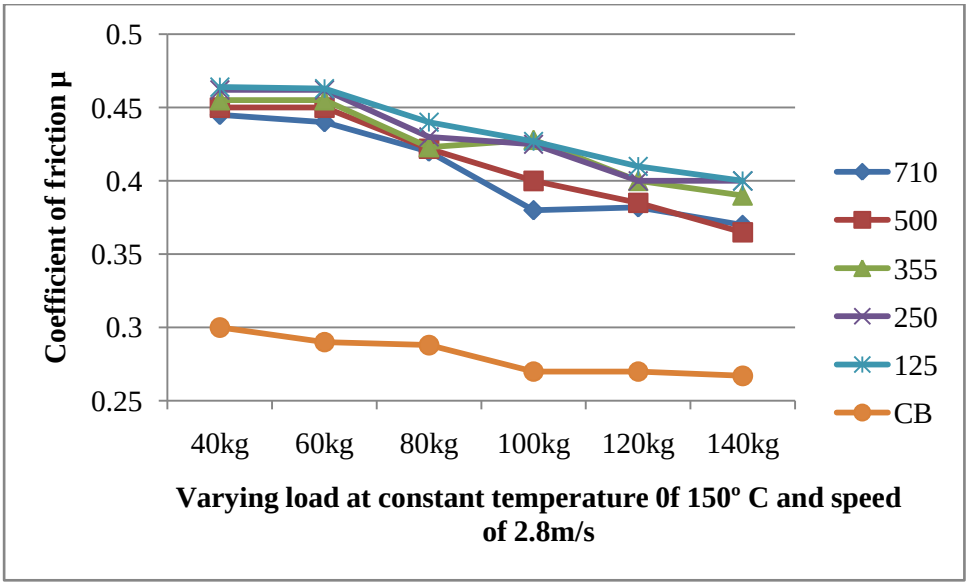

(a) Periwinkle shell and commercial brake pad

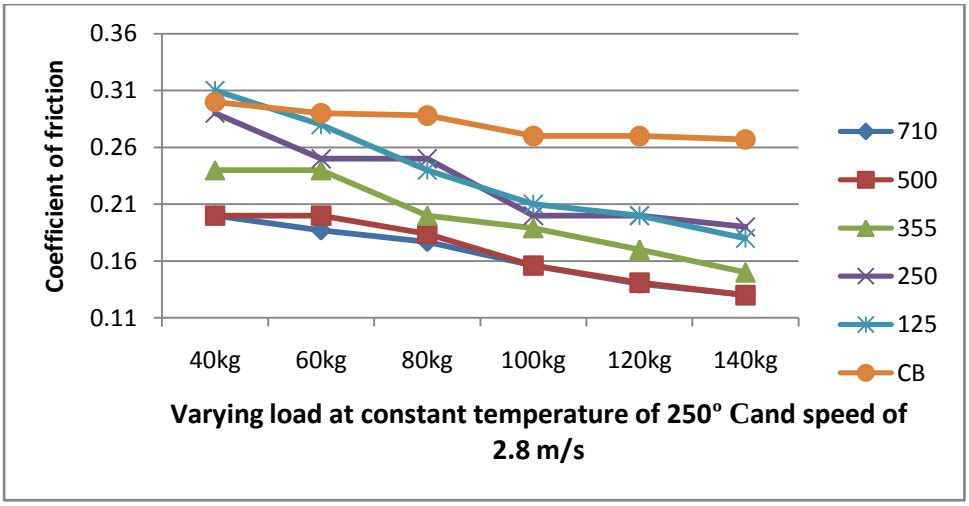

(b) Fan palm shell and commercial brake pad.

Figure 4.21: Effect of load on coefficient of friction of developed periwinkle/ fan palm and commercial brake pads at constant speed and temperature for 45mins.

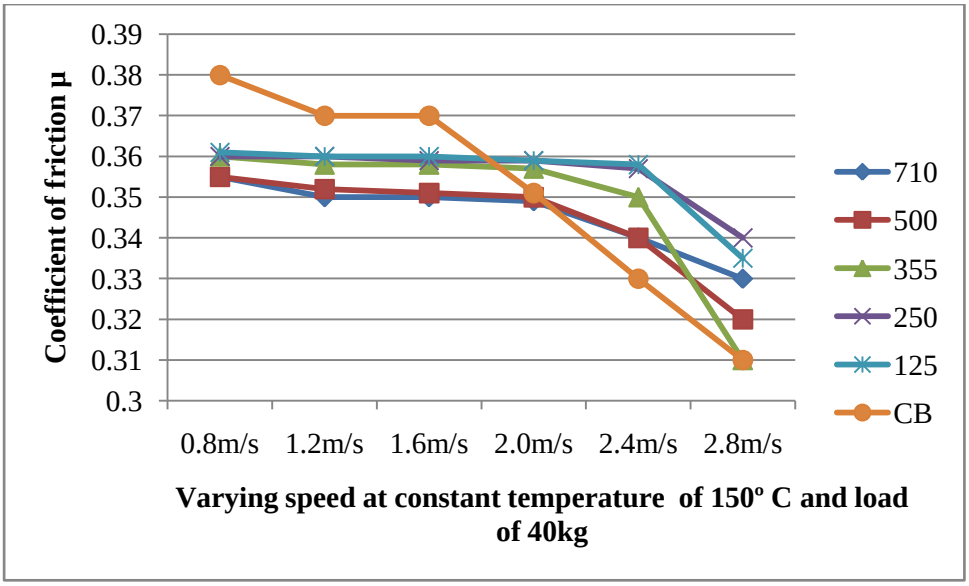

(a) Periwinkle shell and commercial brake pad

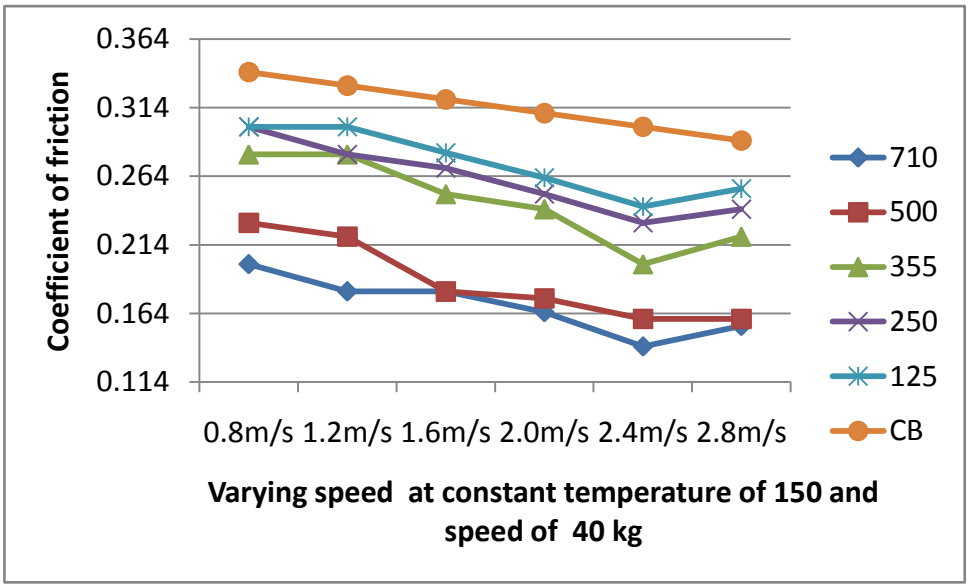

(b)Fan palm shell and commercial brake pad

Figure 4.22: Effect of sliding speed on coefficient of friction of developed periwinkle/ fan palm and commercial pad brakepads at constant load and temperature for 45mins.

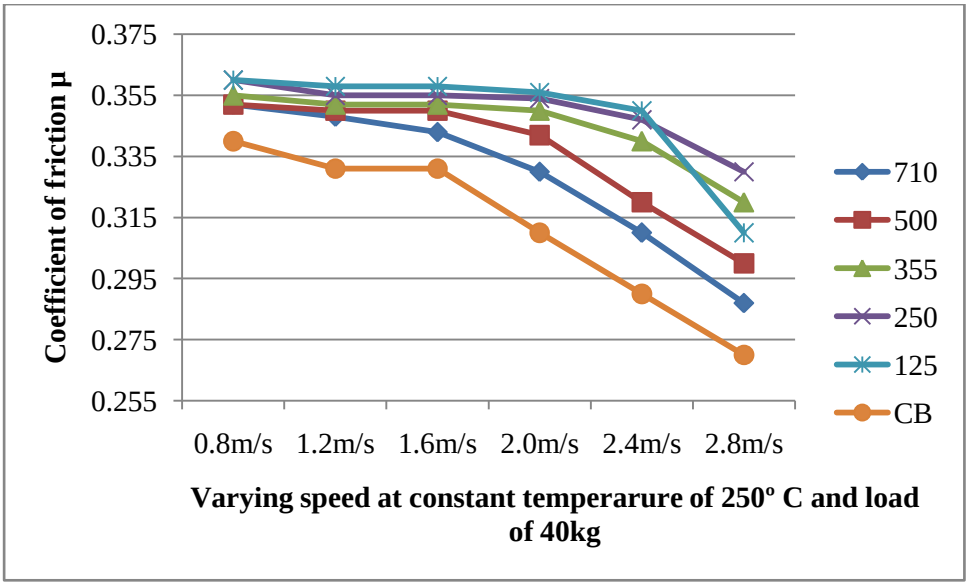

(a) Periwinkle shell and commercial brake pad

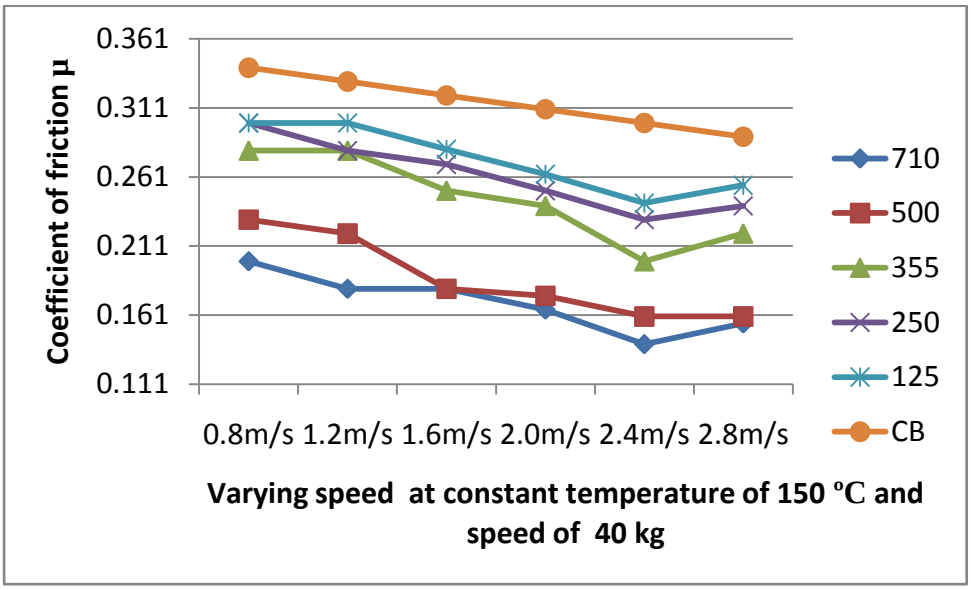

(b) Fan palm shell and commercial brake pad

Figure 4.23: Effect of sliding speed on coefficient of friction of developed periwinkle/ fan palm and commercial brake pads atconstant load and temperature for 45mins.

The coefficient of friction (μ) also decreases when applied loads, sliding speed and temperature increased. Thefluctuation of friction wasseen in allthe

stages.Slidingsurface irregularities, temperature, speed and applied load cause stick-slip oscillation as observed in frictional profiles. This decrease could be explained by the appearance of significant plastic deformation of the pin surface(Mahanty, 2007; George, 2007). Again the effect of particle size showed a marked effect as higher friction was recorded for brake pad composite particle sizes decreased. This marginally higher friction coefficient can be attributed to the high number of particles present in the brake pad composite.

From the result, the coefficient of friction of the periwinkle and fan palm based brake pads do not only fall within the industrial standard range of 0.3 to 0.45 for automotive brake pad systemsNicholson, (1995), but are better than the values obtained from the commercial brake pad.

4.10. THE STATISTICAL DESIGN AND DEVELOPED MATHEMATICAL MODEL FOR CO-EFFICIENT OF FRICTION OF THE DEVELOPED BRAKE PAD

The test results for periwinkle and fan palm shells were recorded against the standard order of sequence as shown in Tables (4.6 and 4.7) which were obtained through design expert software 6.0.8.the for involves in the use of the software have been outlined in section 3.7.1

Table 4.6Design layout and response data for Co-efficient of friction study of periwinkle shell brake pad

Standard	A:Speed m/s	B:Load kg	C:Temperature ^{o}C	D:particles sizeμm	Coefficient of friction periwinkles brake pad
1	2.80	140.00	250.00	710.00	0.37
2	2.80	140.00	250.00	710.00	0.37
3	0.80	40.00	150.00	125.00	0.361
4	0.80	140.00	150.00	125.00	0.4
5	2.80	40.00	250.00	710.00	0.475
6	2.80	140.00	250.00	125.00	0.4
7	0.80	140.00	250.00	125.00	0.4
8	2.80	40.00	150.00	125.00	0.335
9	2.80	40.00	150.00	710.00	0.445
10	0.80	40.00	250.00	125.00	0.466
11	2.80	40.00	250.00	125.00	0.464
12	0.80	40.00	150.00	710.00	0.454
13	2.80	140.00	150.00	125.00	0.4
14	0.80	140.00	250.00	710.00	0.28
15	2.4	40	250	710	0.464
16	0.80	140.00	150.00	710.00	0.28

Table 4.7 Design layout and response data for Co-efficient of friction study of fan palm shell brake pad

Standard	A:Speed m/s	B:Load kg	C:Temperature ^{o}C	D:particles size μm	Coefficient of friction(Fan palm brake pad
1	2.80	140.00	250.00	125.00	0.18
2	0.80	140.00	150.00	710.00	0.14
3	2.80	40.00	250.00	125.00	0.18
4	0.80	140.00	250.00	125.00	0.80
5	0.80	40.00	250.00	710.	0.80
6	2.80	40.00	250.00	710.00	0.2
7	2.80	140.00	150.00	125.00	0.18
8	0.80	40.00	150.00	125.00	0.255
9	0.80	40.00	250.00	125.00	0.295
10	0.80	40.00	150.00	710.00	0.21
11	2.80	140.00	250.00	710.00	0.13
12	0.80	140.00	250.00	710.00	0.21
13	0.80	140.00	150.00	125.00	0.21
14	2.80	40.00	150.00	125.00	0.255
15	2.80	40.00	150.00	710.00	0.2
16	2.80	140.00	150.00	710.00	0.13

Table 4.8 ANOVA of the coefficient of friction analysis for Periwinkles brake pad

Source	Sum of squares	DF	Mean square	F values	P values
Model	0.065	15	4.353E-003	22.91	0.0426
A	6.848E-003	1	6.848E-003	13.61	0.0663
B	9.361E-003	1	9.361E-003	34.56	0.0277
C	5.881E-004	1	5.881E-004	12.38	0.0721
D	4.389E-003	1	4.389E 003	34.56	0.0277
AB	5.256E-005	1	5.256E-005	14.73	0.0617
AC	3.053E-003	1	3.053E-00	15.55	0.0587
AD	9.361E-003	1	9.361E-00	31.86	0.0300
BC	5.881E-004	1	5.881E-004	27.91	0.0340
BD	7.014E-003	1	7.014E-003	35.57	0.0270
CD	8.603E-003	1	8.603E-003	20.80	0.0449
ABC	3.053E-003	1	3.053E-003	23.81	0.0395
ABD	4.556E-005	1	4.556E-005	25.71	0.0368
ACD	1.871E-003	1	1.871E-003	21.68	0.0416
BCD	8.603E-003	1	8.603E-003	24.6	0.033
ABCD	1.871E-003	1	1.871E-003	19.8	0.0378
Pure Error	0.000	0	Pure Error		
Cor Total	0.065	15	Cor Total		

Table 4.9ANOVA of the coefficient friction analysis for the Fan palm brake pad

Source	Sum of squares	DF	Mean square	F values	P values
Model	0.033	15	2.208E-003	48.98	0.0202
A	2.627E-003	1	2.627E-003	89.70	0.0110
B	7.877E-003	1	7.877E-003	127.63	0.0077
C	1.266E-004	1	1.266E-004	9.32	0.0926
D	9.752E-003	1	9.752E-003	0.035	0.0026
AB	3.516E-004	1	3.516E-004	13.92	0.0649
AC	6.891E-004	1	6.891E-004	0.12	0.3785
AD	9.766E-004	1	9.766E-004	1.26	0.3785
BC	1.702E-003	1	1.702E-003	0.36	0.6094
BD	3.516E-004	1	3.516E-004	3.63	0.1971
CD	1.266E-004	1	1.266E 004	0.93	0.4362
ABC	1.406E-005	1	1.406E-005	5.15	0.2420
ABD	2.627E-003	1	2.627E-003	2.70	0.2420
ACD	6.891E-004	1	6.891E-004	2.42	0.354
BCD	8.266E-004	1	8.266E-004	3.23	0.540
ABCD	4.389E-003	1	4.389E-003	3 67	0.412
Pure Error	0.000	0	Pure Error		
Cor Total	0.033	15	Cor Total		

Figures 4.24- 4.26 showed the estimated response surface for the co-efficient of friction as a function of, speed(A), load(B), temperature(C) and the particles size (D).

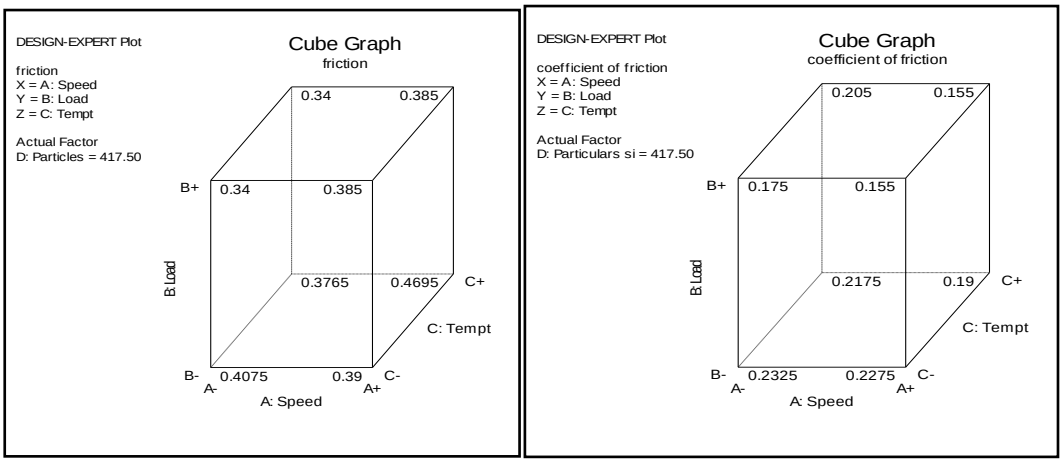

b)Fan palm brake pad

Figure 4.24: Cube map of the modeling process showing the interaction between load, sliding Speed and Temperature

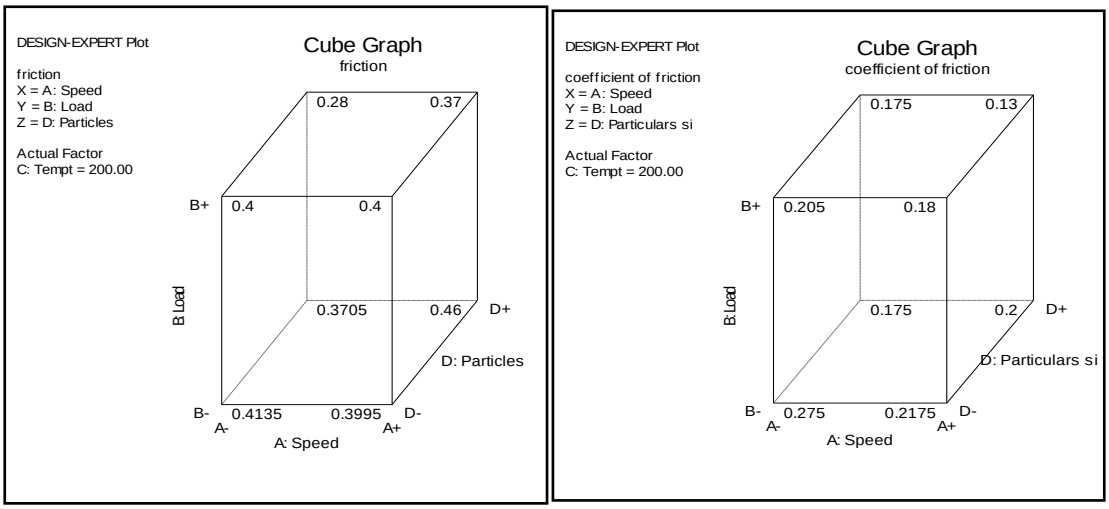

b)Fan palm brake pad

Figure 4.25: Cube map of the modeling process showing the interaction between load, sliding speed and particle size

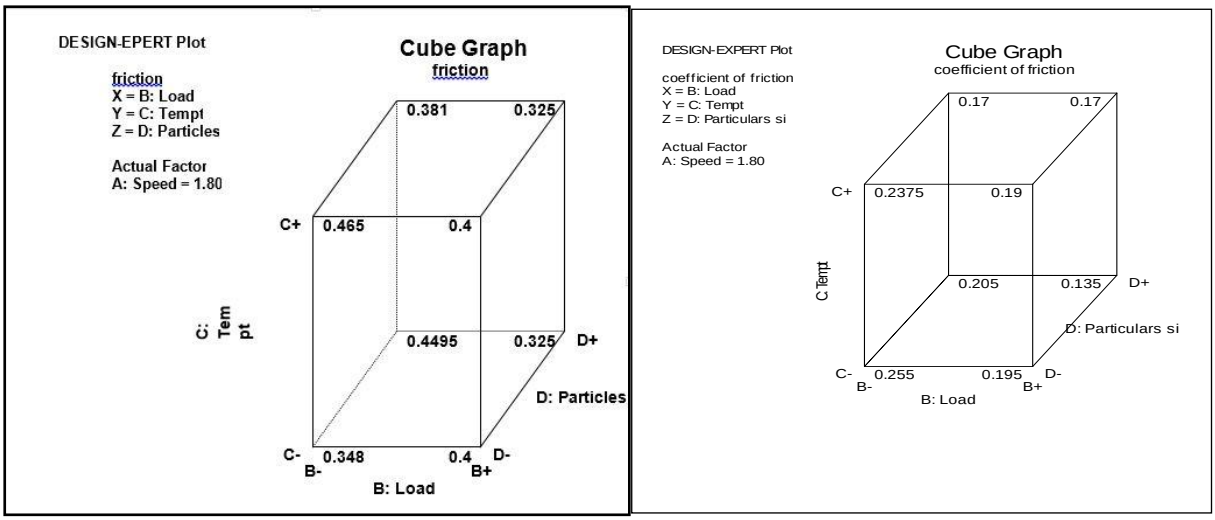

b)Fan palm brake pad

Figure 4. 26:Cube map of the modeling process showing the interaction between Temperatures, Load and particle size

It can be seen that the coefficent of friction is highly influenced by the speed, load, temperature and particles sizes content. For the particle size, the coefficient of friction increases with decrese in the particles size from 710 µm to 125 µm.

Tables 4.6 to 4.9obtained through design expert software, show the results of ANOVA for coefficient of friction. This analysis was evaluated at a confidence level of 95%, that is for significance level of α=0.05. The last column of Tables 4.8 and 4.9 shows the contribution (P) of each parameter on the response, indicating the degree of influence on the result. It can be observed from the results obtained in the Table 4.6, that periwinkle shell and fan palm shell size (D) was the most significant parameter having the highest statistical influence on the coefficientof the developed brake composites.

When the P-value for this mode is less than 0.05, then the parameter or interaction can be considered as statistically significant. From the analysis of the results obtained in Table 4.8, it is clear that the periwinkle shell particle size (D), the interaction effect of speed with particle size (A*D), effect of load with periwinkles shell particles size (B*D), effect of temperature with periwinkles shell particles size (C*D), the interaction effect of speed,

load with temperature (A*B*C), effectof speed, load with periwinkles size particles (A*B*D), effect of speed,temperature with periwinkle shell particles size (A*C*D), effect of load, temperature with periwinkle shell particle size (B*C*D) and effect of speed, load, temperature with periwinkle shell particle size (A*B*C*D) were significant model terms influencing friction coefficient of periwinkle brake pad composites. For fan palm brake pad, Table 4.9 A(speed), B(load) , C(Temperature), and D(Fan palm particles size) were significant model terms influencing thecoefficientfriction of fan palm brake pad composites, since they have P-values < 0.05(see Tables 4.6 to 4.9 and Figures 4.24 to 4.26).

Tables 4.6 to 4.7 obtained through design expert software, show the results of ANOVA for coefficientof friction from which the regression equations obtained in equations 4.2 to 4.3; establishes a correlation between the coefficient of friction with speed, load, temperature, particle size and their interactions. The regression equations developed for the coefficient of friction for periwinkle shell developed brake pad

= +0.39 +0.021*A- 0.024*B +6.062E-003*C -0.017*D +1.813E-00* A*B+0.014*A*C +0.024*A*D -6.062E-00*B*C -0.02*B*D - 0.023*C*D - 0.014*A*B*C -1.688E-003*A*B*D +0.011* A*C*D+0.023*B*C*D - 0.01*A*B*C*D(4.2)

Co-efficient of Friction for fan palm shell developed brake pad

= +0.19 - 0.013*A - 0.022 *B - 2.813E-003*C - 0.025*D - 4.687E-003*A*B - 6.562E-003*A*C +7.813E-003*A*D +0.010*B*C +4.688E-003*B*D +2.813E-003*C*D - 9.375E-004*A*B*C - 0.013*A*B*D +6.562E-003*A*C*D +7.187E-003*B*C*D -0.017*A*B*C*D(4.3)

The above equations (4.1 to 4.2) can be used to predict the friction coefficient of the developed brake pad composites. The coefficient associated with speed (B) in the regression equation (4.2) is negative and it indicates that as the temperature decreases, the coefficient of friction of the brake pad also increases. The coefficient associated with periwinkles shell particles size (D) in the regression equation (4.2) is negative and this

suggests that the coefficient of friction of the brake pad composite decreases with increasing periwinkles shell particle size. Also the coefficient associated with speed(A), load(B), temperature (C) of fan palm particle size in the regression equation (4.3) are negative and it indicates that as the, speed, load temperature and fan palm particle size increase, coefficientof friction of the brake pad decreases

4.11 VEHICLE LIVE TEST

Figure 4.27 shows the effect of speed on disc temperature which was carried out as described in section 3.11.The results indicate that as the speed increases, the disc temperature rises due to the conversion of kinetic energy to heat energy as the vehicle is brought to rest. The disc temperature rise is higher with the commercial brake pad than the developed brake pad. This may be dueto the good heat transfer properties of the developed brake pad. The consequence of high disc temperature rise is gradual heating of the hydraulic fluid which can lead to its boiling and loss of brakingefficiency Asley*etal.*,(997).

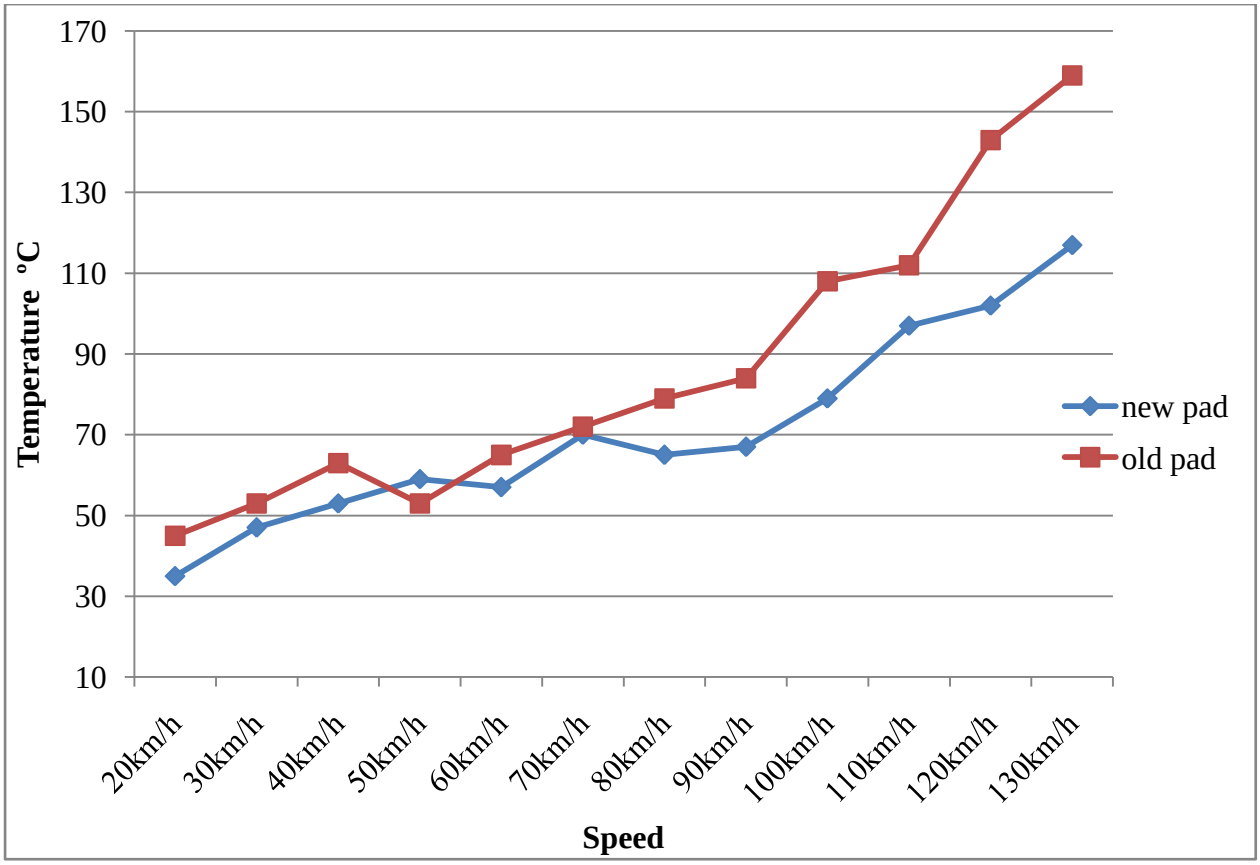

Figure 4.27: Variation of speed on disc temperature for the developed and commercial brake pad

4.12 LABORATORY TESTS

a.Variation of speed with stopping pressure

The variation of speed with stoppingpressure for both the commercial and the laboratory developed brake pads was determined. The test was carried out by applying brake at speeds of; 100rpm, 149rpm, 225rpm and 250 rpm till the system comes to rest while applied the stopping pressure was recorded. Figure 4.28 shows variation of speed with stopping pressure between the commercial and the developedbrake pads.

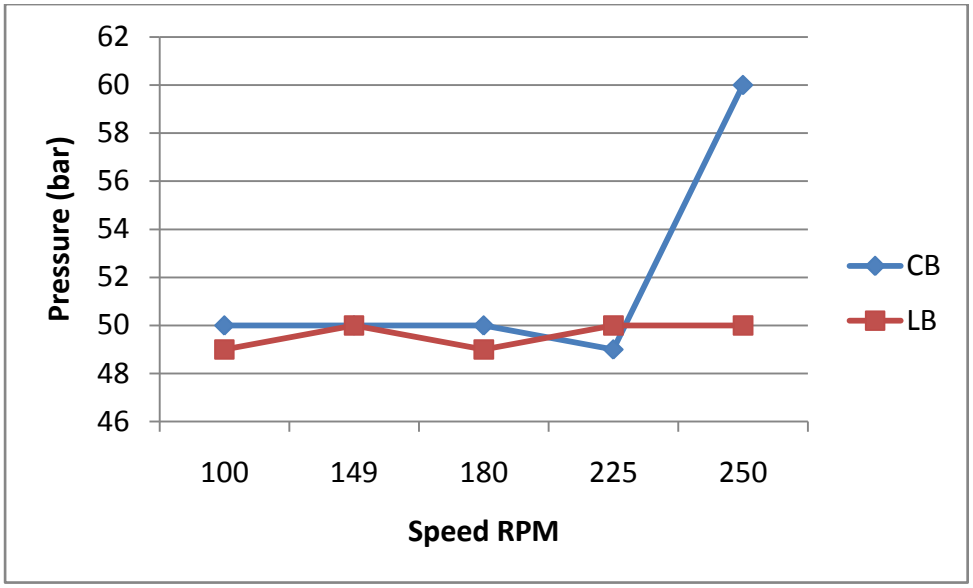

Figure 4.28: Variation of speed with stoppingpressure for developed and commercial brake pads

The results show that for the same speed, the laboratory developed brake pad requires less contact pressure to bring the system to a stop. This is because of its higher coefficient of friction.

b. Effect of speed on brake pad wear(lossin mass and thickness) at constant contact pressure of 10bar after average of 10 stops.

The effect of speed on brake pad wear(loss in mass and thickness) at constant contact pressure of 10bar after an average of 10 stops is shown in Figure 4.29 (aand b). This was achieved by applying a constant stopping pressure of 10bars at each of the test speeds of, 125rpm, 140rpm and 325rpm to bring the system to a stop. An averagepressure of 10bars was applied at each test speed. The tests show that at a constant line pressure, the mass loss and reduction in thickness of pad increase with theincrease in speed. However, the laboratory brake pad exhibits a low mass loss compared to the commercial brake pad. This is in agreement with the wear result in Figure4.16 to 4.19.

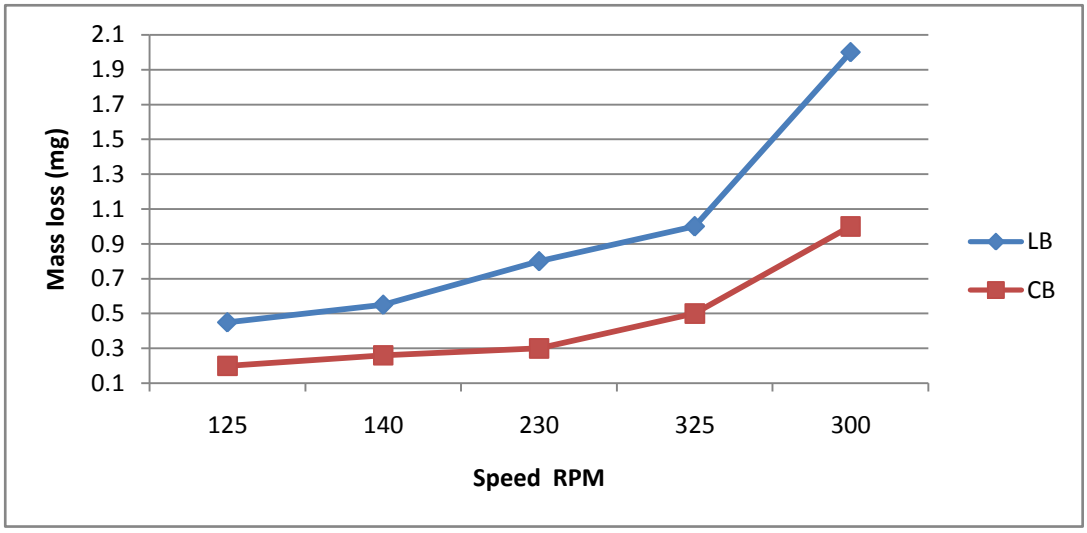

Figure 4.29a: Effect of speed on mass loss at constant contact pressureof 10bar after an average of 10 stops.

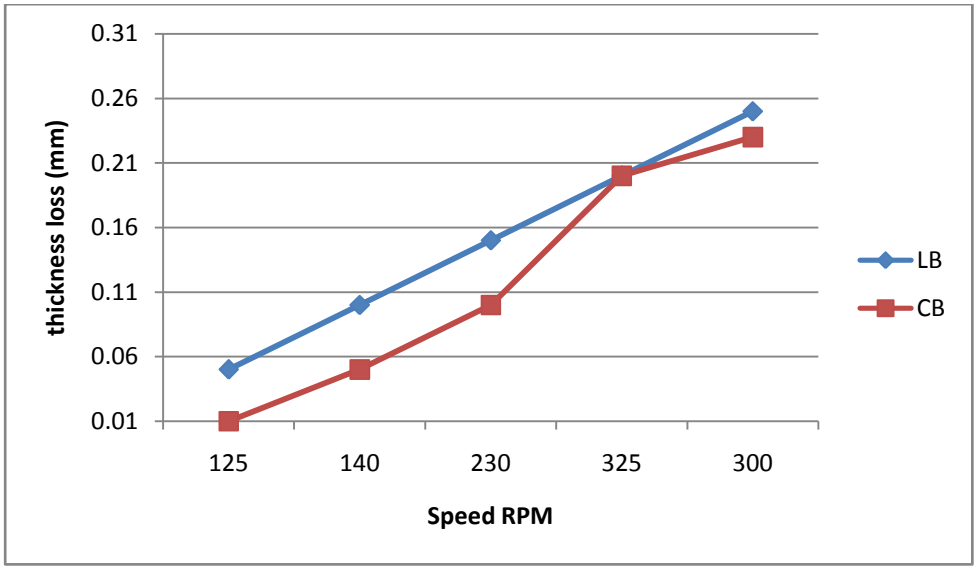

Figure 4.29b: Effect of speed on loss in thickness at constant contact pressure of 10bar after an average of 10 stops.

c. Effect of Speed on Average stopping time at constant pressure of 10bar

The effect of speed on average stopping time at constant pressure of 10bars for the developed and commercial brake pads wascarried out. This test was carried out by keeping the line pressure at 10 bar at various speeds of; 12 rpm, 140rpm, 230rpm, 300rpm and 325rpm while the stopping time at each of the speed was noted. Figure 4.30shows

that the average stopping time for both pads at constant pressure increased with increase in speed, with the laboratory pad having lower stopping time. The lower stopping time of the laboratory pad is due to its higher coefficient of friction when compared with the commercial brake pad as observed in section4.9.

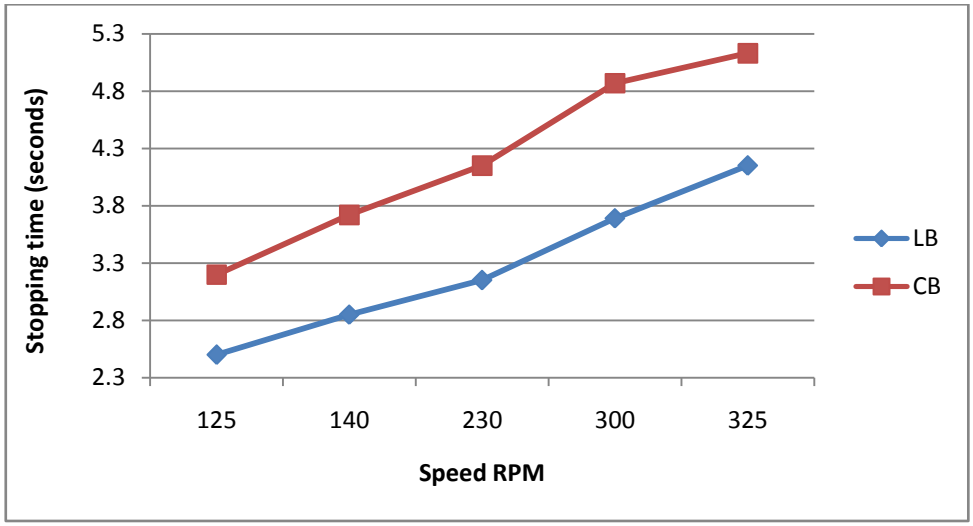

Figure 4.30: Effect of speed on average stopping time at constant pressure of 10bar for the developed and commercial brake pads

d. Effect of contact pressure on stopping time at constant speed of 325rpm

The effect of contact pressure on stopping time at constant speed of 325rpm for the developed and commercial brake pad was carried out. This was carried out by noting the average stopping time at applied pressure of; 8bar, 10bar, 12bar, 14bar, and 16bar while maintaining a constant speed of 325rpm.

The result showed that the stopping time decreased as the pressure increased as shown in Figure 4.31

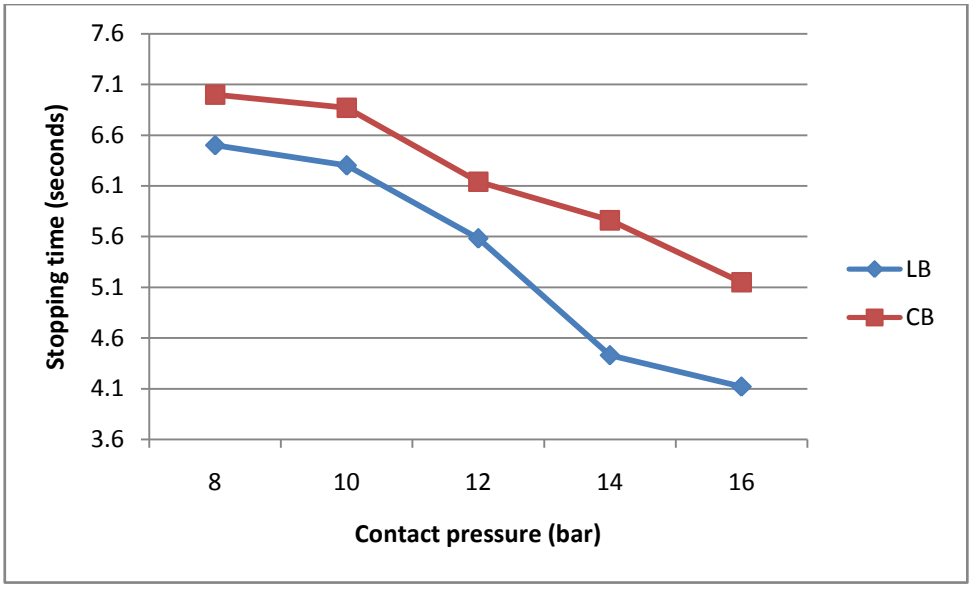

Figure 4.31: Effect of constant pressure on stopping time at constant speed of 325rpm for the developed and commercial brake pads

4.13 COMPARISON OF RESULTS

The results of this work indicate that samplesconsisting of 125µm particlesgave better properties than the commercial brake and other samples tested. Hence, a decrease in particle size leads to the best properties. The result of formulation of 125µm particle size was further compared with thosefrom palm kernel shell (PKS) and bagasse brake and commercial, pads as shown in the Table 4.10.

Table 4.10Comparison of properties of various pad materials

Pad Materials / Properties	Commercial brake pad (asbestos based) (Dagwaetal)	Laboratory formulation Palm kernel shell (Dagwaetal)	Laboratory formulation (Bagasse) (Aigbodionetel)	New Laboratory formulation (periwinkles shell at 125µm)	New Laboratory formulation (Fan palm shell at 125µm
Specific gravity(g/cm^3)	1.89	1.65	1.43	1.12	0.99
Friction coefficient	0.3-.0.4.	0.440	0.420	0.35-0.41	0.20-0.31
Thicknesses swell in water (%)	0.9	5.03	3.48	0.39	4.0
New Thickness swells in SAE oil (%)	0.30	0.44	1.11	0.37	4.56
Hardness values(HRB)	101	92.0	100.5	116.7	95.7
Compressive strength(N/mm^2)	110	103.5	105.6	147	92.9
Thermal resistance (%)	Charred ash 9%	Charred ash 46%	Charred ash 34%	Charred ash 5.6%	Charred ash 30%

The results show that the formulations using periwinkle shell pads produced higher friction coefficient, wear resistance, higher hardness and compressive strength than those of the commercial brake pads. Thepercentage of swelling in water and oil showed no significant difference between developed brake pads with periwinkle, fan shells particle and commercial brake pads. The results are in close agreement; hence asbestos free brake pads can be produced with these formulations. Brake pads produced from the 125µm particles are shown in Appendix A

CHAPTER FIVE

CONCLUSION AND RECOMMENDATIONS

5.1 CONCLUSION

From the results and discussions in this work the following conclusions can be made:

1. The physical and chemical properties of periwinkle and fan palm shells were determined using TGA, SEM and XRD characterization techniques and they compared favorably with those of commercial brake pads and of past related research works on asbestos free brake pad
2. The optimum particle size for the formulation was found to be of 125µm.
3. Taguchi method was employed to determine the optimal formulation of 65% periwinkle/ fan palm particles and 35% resin.
4. The automobile disk brake pad was developed from the best formulation
5. The oil/water soak, wear rate and amount of charring decreased with particle size.
6. The values of the coefficient of friction, hardness, compressivestrength, of the 125µm of periwinkle shellsas shown in Table 4.10were higher than those of commercial brake pads by 14.28% %, 15.5%, and 33.63% respectively, while the values of the density and the water swell were 40% and 56.67% lower than those of the commercial brake pad.
7. The results of research indicate that periwinkle shell and fan palm shell particles can be effectively used to development of an automobile disk brake pad

5.2 CONTRIBUTION TO KNOWLEDGE

1.Only two (2) materials;periwinkle shell and Resin, Fan palm and Resin instead of the 10 – 15 materials used in the production of brake pads and still achieve the recommend (0.3- 0.45) range of coefficient of friction

2.Produced lighter brake pads from periwinkle and fan palm shells having density of 1.12g/cm^3 and 0.99g/cm^3 against asbestos brake of density 2.8g/cm^3 and still attain the recommend values of hardness and compressive values of (92 to 120) and (130(N/mm^2 to 150 (N/mm^2)

2. Added value to periwinkle shells which was before now a nuisance are now valued at N5,000.00 per kg

5.3 RECOMMENDATIONS

The following recommendations have been made:

1. Periwinkle and fan palm shell brake pads can be tried for commercial purposes.
2. Periwinkle and fan palm shells may be used to develop of vehicle clutch plate
3. The National Automotive Council is requestedto support further development of these novel materials

REFERENCES

Adewuyi, A.P. and Adegoke, T. (2009), Exploratory Study of Periwinkle Shells as Coarse Aggregates in Concrete Works. *Journal of Applied Science Research*; 4(12): 1678 – 1681, 2008 Insinet publication,

Amaren S.G, Aku S.Y and Yawas D.S (2013); Effect of Peiwinkle Shell Particle Size on Wear Behaviour of Asbestos Free Brake Pad. Elsevier results in Physics 3 (3013) 109 - 114

Ahmet K. (2012).investigation of using natural zeolite in brake pad. Scientific Research and Essays Vol. 6(23), pp. 4893-4904, 16 October, 2011

Anderson.A. E. (1992),*Friction and Wear of Automotive Brakes*, in ASM Handbook, FrictionLubrication and Wear Technology, Volume 18, ASM International, Materials Park, Ohio, pp. 569-577

Aigbodion, V. Akande, U.,Hasssn, S. B. Asuke, F and Agunsoye, J. O (2010), Development of Asbestos- Free Brake Pad Using Bagasse. *Journal of Tribology in Industry*, Vol32.No.1, 2010.

Aigbodion. V.S. and J.O.Agunsoye(2010), Bagasse(Sugarcane waste): Non-Asbestos Free Brake Pad Materials, LAP Lambert Academic Publishing,Germany, ISBN 978- 3-8433-8194-9.

Anon Automotive Brake Repairs Trends and Safety Issues. http//ww.sirim.my/amtee/pm/brake.htm,2004

Aku S.Y, Yawas D.S, Madakson P.B, and Amaren S.G (2012); Characterization of aperiwinkle shell as Asbestos Free Brake Pad Materials. Pacific Journal of Science and Technology.Vol 13 Number 2 Novembr 2012

Allen, S.H,Alfred, B.H and Herman, G.M (2002), Theory and Problems of Machine Design, McGraw Hill Publishing companyLimited New Delhi. PP.113-130

Ashkey, F., Emery,P. and Joseph ,C.F (1997),Experimental study of Automobile Brake system temperature

Bhabani , K. S and Jayashree, B.(2006), Composite friction materials based on organic fibres: Sensitivity of friction and wear to operating variables Elsevier Volume 37, Issue 10, October 2006, Pages 1557–1567

Bert. B, and kartheinz H.C (2006), Brake technology Handbook SAE International pp. 1-9

BBU Chemie (1993), "Friction Additives," Product Literature, Arnoldstein, Germany.

Bhagwan, D.G,Steven,H.M, Patricia,A.M and Petet, J.G,(2000), Brake Wear Particulate Matter Emissions, Journal of Environmenta Science and Technology;2000,34, (21),pp4463 – 4469

Blau.P.J(2001), Compositions, Functions and Testing of Friction Brake Materials and their Additives.Being a report by Oak Ridge National Laboratory for U.S Dept. of Energy.www. Ornl.gov/-webworks/cppr/y2001/rpt/112956.pdf

Borden Packing and Industrial Products, Inc. (1994) Literature on modified resin products, Louisville,KY.*20*

Bush.H. D, Rowson DM, and WarrenS. E. (1972), The Application of Neutron Activation Analysis to the Measurement of the Wear of a Friction Material, *Journal Wear, 20,* pp. 21 l-225.

Chapman T. R., NieszD. E., Fox, R. T., and Fawcett, T. (1999),Wear-Resistant Aluminum-Boron CarbideCermetsfor Automotive Brake Applications, Journal Wear, 236, pp. 81-87.

Dagwa, I.M. and Ibhadode, A.O.A. (2005), Design and Manufacture of Experimental Brake Pad TestRig Nigerian Journal of Engineering Research and Development,Basade Publishing Press Ondo, Nigeria, Vol. 4, No. 3. 15-24.

Dagwa, I.M, and Ibhadode, A.O.A. (2006), Determination of Optimum Manufacturing Conditions for Asbestos-free Brake Pad Using Taguchi Method, Nigerian Journal of Engineering Research and Development 5 (4): 1-8.

Dillip, K.AnupK, andBijwe, J. (2008), Analysis of load Speed Sensitivity of Friction CompositesBased on Various Synthetic Graphite. *Journal of Wear,* Volume 2006 Issues 1-2, pp. 266-274.

El-Tayeb, N.S.M, and Liew, K. W. (2008),Effect of Brass Fibers in increasing amounts on the Friction and Wear Performance of Non-asbestos Organic (NAO) friction composites Wear *Journal. Volume* 256.Issues 1-2: 275-287.

Erik. O, Franklin D. J, Holbrook L. K, and Henry H. R (2004), Machinery Handbook, pp 2465 –2477.Industrial Press

Eriksson.M. and JacobsonS. (2000), Tribological Surfaces of Organic Brake Pads, Tribology International: 817-827, 2000." 33, pp. 817-827.

Elakhame, Z.U. Alhassan, O.A. and SamuelA.E. (2014); Development and Production of Brake Pads from Palm Kernel Shell CompositesInternational Journal of Scientific & Engineering Research, Volume 5, Issue 10, October-2014 735 ISSN 2229-5518

El Zahrea. F.L., Khasaba M.I., El-GlusyM.a., and Ali W.Y. (2003), □ Friction and wear of Asbestos Free Friction Material Tribology Journal vol. 50, pp.40-45

Fono-Tamo R.S.and KoyaO.A. (2013), Evaluation of Mechanical Characteristics of Friction Lining

from Agricultural Waste. International Journal of Advancements in Research & Technology, Volume 2, Issue 11, November-2013 ISSN 2278-7763

Festus, A. O., Oriyomi M. O., and Olatunji S. O. (2012),Assessment of the Suitability of Periwinkle Shell Ash (psa) as Partial replacement for Ordinary Portland cement (OPC) in Concrete. International Journal of Research & Reviews in Applied Sciences;2012, Vol. 10 Issue 3, p428

George, A. and Arnab, G. (2007), Asbestos free Friction Composition Brake LuningsBull. MatterScience Vol.31 pp.19-22

Gong K.-C, Cheng,Y. C. and Huang, Y.Y. (1985),The High temperature Resistance of Polymeric Brake Composites, *ASME Wear of Materials Conference Proc.,* ASME, New York, pp. 765- 770.

Ganguly, A. and George, R. (2008), Asbestos Free Friction Composition for Brake Linings".*Bull. Mat*. Sc, Vol 31, No 1, pp 19-22.

Gurunath P.V. and Bijwe J., (2009), Potential Exploration of Novel Green Resins as Binders for Non-Asbestos-Organic (NAO) Friction Composites in Severe Operating Conditions. *Wear Journal*. Volume 267, Issues 5-8: 789-796.

Gudmand-Hoyer. L, A. Bach, Neilsen,G. T. and Per, M. (1999),Tribological Properties of Automotive Disc Brakes with Solid Lubricants,*Wear Journal , 232,* pp. 168-175.

Gul.F. and Aciliar. M. (2004), Effect of the reinforced volume fraction on dry sliding behavior of Al-10 Si/SiCp composites produced by vacuum distillation. Composite science Technology 64(13-14); 1959-1970

Gopal. P.DHarani, L. R. and Frank D. Blum: Wear 174 (2003), 119–127.

Handa.Y. and T. Kato (1996),Effects of Cu Powder, $BaSO_4$, and Cashew Dust on the Wear and Friction Characteristics of Automotive Brakes, Tribology *Trans., 39,* pp. 246-353.

Harald , A.,Yosuke,.S.,Carlos,A.(2010); Brake Pads Standards for Safer Vehicles ISO Focus, www.iso.org/isofocus

Hooton N. A. (1969); Metal-Ceramic Composites in High-Energy Friction Applications," BendixTechnical Journal,Spring 1969, pp. 55-61. (concerning aircraft brakes)

Ibhadode A.O.A and Dagwa I.M (2008), Development of Asbestos – Free Friction Lining Material from Palm Kernel Shell. Journal of the Brazilian Society of Mechanical Science and Engineering. April –June 2008, Vol XXZ, No.3/173 pp 166-173.

Ikpambese, K.K, Gundu, D.T, and Tuleun L.T (2014), Evaluation of Palm Kernel Fibres (PKFs) for production of asbestos –free brake pads. Journal of King Saud University- Engineering Size.Doi: 10.1016/j.jksues.2014.02.001

Jang.H. and S. J. Kim (2000), "The Effects of Antimony Trisulfide and Zirconium silicate in the Automotive, Brake Friction Material," *Wear Journal vol, 239,* pp. 229-236.

Jayashree. B., Mukesh. K.,Guranath .P.V., Ynnic.D., and Degalix G. (2008),Optimization of Brass contents for best Combination of Tribo- Performance and Thermal Conductivity of Non-Asbestos Organic (NAO) Friction composites Journal *of Wear,* vol.265, no.5 pp.699-712.

Jia Xian and LingXiamen.(2003**),**Friction and Wear Characteristics of Polymer- Matrix Materials einforced with Brass Fibers.*Journal of Materials engineering and Performance*, 642, vol 13 (5)

Jeong .D.U, Palumbo .G, Aust .K..T and Erb . U. (2001) The Effect of Grain Size on Wear Properties of Electrodeposited Nano crystalline Nickel Coatings. Sripta Matter. 44 (2001) pp. 493 - 499

Joseph, E.S and Charles, R.M (1989), Mechanical Engineering Design, McGraw-Hill Book Company New York. PP. 668-677.

Kato, T and Soutome, H. (2001), "Friction Material Design for Brake Pads Using Database," *Tribology Transactions,* 44, pp. 137-141.

Khurmi R,S and Gupta J.K (20012) A Text book of Machine Design.Eurasia Publication House (PVT.) Ltd, Ram Nagar, New Delhi – 110 055 pp 777-787.

Keon H.C. Min, H, C.,Seong J.K. and Ho, J. (2008),Tribological Properties of Potassium Titanate in the Brake Friction Material; Morphological effects.Journal of Tribology.Volume 32. Issue 1; 59-66.

Kolapo.O. O. and Akaninyene. A. U (2012), Strength Characteristics of Periwinkle Shell Ash BlendedCement Concrete. International Journal of Architecture, Engineering and ConstructionVol 1, No 4, December 2012, 213-220

Kim S.J, Kim K.S. and Jang H. (2003),Optimization of Manufacturing Parameters for Brake Lining Using Taguchi MethodJ.*MaterialProcessing Technololgy*, 136 (2003), pp. 202–208

Kristoffer, K. and Zmago, S. (2007), Preparation and properties of C/C–SiCnano-composites (2007) *Journal of The European Ceramic Society* - J EUR CERAM SOC 01/2007; 27(2):1211-1216

Kuma.S. and Balasubramanian.V.(2010),Efect of reinforcement particle size and volume fraction on abrasive wear behavior of AA7075 Al/SiCp P/M composites – a statistical analysis.TribololgyInternational 43(1-20; 214-422

Kukutschova, J., Rouicek, K; Malchova, Z., Pavlickova, V., Holusa, J., Kubackova, V., Mickab, D.,Macrimmon, D., and Filip, P. (2009), Wear Mechanism in Automotive Brake Materials, Wear Debris and its Potential Environmental Impact. Journal of Wear.Volume 267.Issues 5-8.

Leman Z., Sapuan, S.M. Saifol, A.M. Maleque M.A. and Ahmad, M.M. (2008), Moisture absorption behaviour of sugar palm fibre reinforced epoxy composites' Short Communication, International Journal of Materials and Design 29 (8): 1666-1670.

Mahanty, S., andChugh, Y. P., (2007); Development of Fly Ash -based Automobile Brake lining Tribology International PP.1207-1224

MayowaA.,Abu-Bakro.KLawal. S.A. and Abdulkabir, R. (2015);experimentalinvestigationofpalmkernelshellandcow boner e i n f o r c e d polymercompositesfor brake paproduction.International Journal of Chemistry and Materials Research, 2015, 3(2): 27-40

Mathur, R. B., Thiyagsrjan, P., and Dhami, T. L., (2004), "Controlling the Hardnessand Tribologicalbehaviour of Non asbestos Brake Lining Materials for Automobiles". Journal of carbon science 5(1) (2004) pp. 6 – 11

Menezes, L.F. Figueiredo, L., Ramalho, A., Oliveira, M.C., (2011),Experimental study of friction in sheet metal forming. Wear, vol. 271, no. 9-10, p. 1651-1657, DOI:10.1016/j.

Mudd, S.C (1996), Technology for Motor Mechanics, Second Edition Ibadan.

Natarajan.N. Vijayaranagan.S. andRajendran.I.(2006), Wear behavior of A35/25SiCp Aluminum Matrix Composites Sliding against Automobile Friction material. Wear 26; 812-822.

Nicholson.G. (1995), Facts About Friction, P&W Price Enterprises, Inc., Croydon, P.A. Olerie, W.,Klob, H., Urban, I. and Dmitrie, A. I., (2007), Towards a Better Understanding of Brake Friction Materials. Journal of Wear. Volume 263, Issues 7-12, 01189-1201.

Nwafo,O.C, Ezeji, M.D, Nwaiwu, C.A, and Okoronkwo, C.A (2013), Effect Of Speed and Pressure on wear Rate of Automotive Brake Pad, International Journal of Engineering Mahanty, S., and Chugh, Y. P., (2007), Development of Fly Ash -based Automobile Brake lining Tribology International PP.1207-1224`

Mathur, R. B., Thiyagsrjan, P., and Dhami, T. L., (2004), "Controlling the Hardness and Tribological behaviour of Non asbestos Brake Lining Materials for Automobiles". Journal of carbon science 5(1) (2004) pp. 6 – 11

Mudd, S.C (1996), Technology for Motor Mechanics, Second Edition Ibadan.

Nicholson.G. (1995), Facts About Friction, P&W Price Enterprises, Inc., Croydon, P.A. Olerie, W., Klob, H., Urban, I. and Dmitrie, A. I., (2007), Towards a Better Understanding of Brake Friction Materials. Journal of Wear. Volume 263, Issues 7-12, 01189-1201.Vol.2, Issue 4. PP.72-76

Olufemi, I.A and Joel. M (2009), Suitability of Periwinkle Shell as a Partial Replacement for River Gravel in Concrete Leonardo Electronic Journal of Practices &Technologies; Jul2009, Issue 15, p59

Qin Q.D, Zha Y.D, and zhaou W (2008), dry sliding wear behavior of Mg_2Si/Al Composite against Automobile Friction Material. Wear 264(7-8); 654-661.

Rajiv. A,Ashok. A., Narandra B.D (2006), Material Science Manufacturing pp 26 Elsevier

Rhee S. K. (1974) "Wear Mechanisms for Asbestos-Reinforced Automotive Friction Materials," Wear,29, pp. 391-393.

Sasaki, Y. (1995), Development Philosophy of Friction Materials for Automobile Disc Brakes. The Eight International Pacific Conference on Automobile Engineering. Society of Automobile Engineers of Japan; Society of Automobile Engineer of Japan.407-412

Satapathy, B.K and Bijwe, J(2004), Performance of Friction materials Based on variation in nature ofOrganic Fibres**:** Wear Volume 257, Issues 5–6, September 2004, Pages 585–58

Shaoyang, B and Fuping, W. (2006),comparism of Friction and Wear Performances of Brake Material Dry Sliding Against Two Aluminium Matrix Composite reinforced with SiCParticles Journal of material processing Technology (Impact Factor; 2.24) 182(1-3) 122-127

Sloss Industries Corp. (1996), "PMF@ Fiber - The Preferred Reinforcement in Friction Products,"Product Literature, Birmingham, AL.

Spurr,. R. T. (1972), "Fillers in Friction Materials," *Wear Journal, 22*, pp. 367-409.

Seong J.K and Ho J.(2000), Friction and Wear of Friction Materials Containing Two Different Phenolic Resins Reinforced with Aramid Pulp. Journal of Tribology international, 33(7): 477 – 484.

Swapnil R. A and Bhaskar D.P (2014) Design and analysis of Disc Brake, International Journal of Engineering and Technology (IJETT) - volume 8 Feb 2014

Talib, R.J.; Azimah, M.A.B., Yuslina, J., Arif S.M. &Ramlan K. (2008),Analysis on theHardnessCharacteristics of Semi-Metallic Friction Materials.*Journal Solid StateScience & Technology*, Vol. 16, No. 1, pp. 124-129

Tatarzicki, Y. T. and. Webb, R. T (1992), Friction and Wear of Aircraft Brakes, ASM Handbook, Vol. 18, ASM International, Materials Park, Ohio, pp. 582-587

Tsang,.P. H. S., M. G. Jacko, and Rhee, S. K. (1985, Comparison of Chase and InertiaBrake Dynamometer Testing of Automotive Friction Materials, ASME Wear of Materials, pp. 129- 137.

Zamri B.Y, Shamsul B.J, amun M.M (2011),Potential OF Palm Oil Clinkeras ReinforcementinAluminiumMatrix CompositesforTribologicalapplications. international Journal of Mechanical and Materials Engineering (IJMME), Vol.6(2011), No.110-17

APPENDIX A

Table A1: Results of Density of the developed brake pad

Sieve Size (µm)	Readings	Mass in Air (gm)	Vol (cm^3)	Density(gm/cm^3)
710	Periwinkle shell	27.3	27.5	0.99
	Fan palm shell	27.4	27.64	0.88
500	Periwinkle shell	27.4	27.6	0.993
	Fan palm shell	33.1	33.39	0.90
355	Periwinkle shell	32.1	32.2	1
	Fan palm shell	26.1	26.35	0.94
250	Periwinkle shell	27.8	27.9	1
	Fan palm shell	26.8	27.06	0.96
125	Periwinkle shell	27.5	24.5	1.12
	Fan palm shell	21.1	21.30	0.99

Table A2: Results of Thickness swelling in water of the developed brake pad

Sieve Size(µm)		Wet in Air	Weight after Water (24hrs)	% Water Absorption (24hrs)
710	Periwinkle shell	34.0	36.5	7.371
	Fan palm	34.0	39.68	16.70
500	Periwinkle shell	31.2	33.5	7.37
	Fan palm	35.0	38.8	10.90
355	Periwinkle shell	27.1	27.2	0.59
	Fan palm	28.8	31.36	8.90
250	Periwinkle shell	27.9	28	0.36
	Fan palm	30.1	32.17	6.89
125	Periwinkle shell	25.71	25.8	0.39
	Fan palm	27.80	29.07	4.56

Table A3: Results of Thickness swelling in oil of the developed brake pad

Sieve Size(μm)	material	Wet(gm) in Air	Weight (gm) in oil after (24hrs)	% Oil Absorption (24hrs)
710	Periwinkle shell	27.4	28.74	4.9
	Fan palm	28.8	31.05	7.80
500	Periwinkle shell	31.8	32.8	3.15
	Fan palm	30.60	32.74	7.00
355	Periwinkle shell	34.4	34.8	2.034
	Fan palm	36.50	38.95	6.70
250	Periwinkle shell	27.8	27.9	037
	Fan palm	27.0	28.23	4.56
125	Periwinkle shell	27.4	27.5	0.37
	Fan palm	26.7	27.77	4.00

Table A4: Results of Hardness values of the developed brake pad

Periwinkles shell				
Size(μm)	I	II	III	AV.(HRB)
125	115	120	115	116.7
250	110	100	95	101.7
355	100	97.5	100	99.2
500	95.0	95.0	96.0	95.3
710	85.0	87.0	84.5	85.5
Fan palm				
125	95.0	95.0	96.0	95.7
250	85.0	87.0	84.5	85.8
355	70.5	70.00	68.9	69.8
500	65.89	63.00	64.5	64.46
710	55.9	54.8	53.0	54.56

Table A5: Results of Compression strength of the developed brake pad

Periwinkles shell			
µm	Cross sectional Area (A_o) mm	Maximum. Load Sustained (N)	Maximum. Compressive Strength (N/mm^2)
125	510.705	75,000	147
250	10.705	69,000	135
355	510.705	56,700	111
500	510.705	54,800	107
710	510.705	51,500	101
Fan Palm			
125	450.00	41805	92.9
250	500.00	40950	81.9
355	456.00	34241	75.09
500	550.00	37345	67.90
710	500.000	30025	60.05

Table A6: Wear (mg) at varying load at constant speed 2.4m/s, time 45min at 150^{o}C(periwinkles brake pad)

Load (kg) / Sieve Size (µm)	40kg	60kg	80kg	100kg	120kg	140Kg
710	102.5	112.8	129.5	139.0	143.9	145
500	99.7	101.3	121.0	126.9	132.4	134
355	86.7	96.8	100.4	112.7	124.2	133
250	76.9	79.0	97.9	101.3	112.7	115.2
125	76.3	80.4	96.9	100.7	112.0	114.1
CB	123.5	135.7	401	143.9	145	147.2

Table A7: Wear rate(mg) at varying load at constant speed of 2.4m/s, time 45min at 250^{o}C(periwinkles brake pad)

Load / Sieve Size(µm)	40kg	60kg	80kg	100kg	120kg	140kg
710	156.7	173.0	189.9	190.6	200.2	202.1
500	156.0	167.8	185.0	185.9	190.3	196
355	123.0	134.6	147.9	167.0	177.9	180.2
250	100.2	121.9	134.6	145.7	156.2	167.21
125	99.6	121.2	132.7	145.0	155.7	157
CB	135.6	137.7	143.8	148.9	150.7	155.4

Table A8: Wear (mg) at varying speed at constant load of 120kg, time 45min at 250^{o}C (periwinkles brake pad)

Speed / Sieve Size(μm)	0.8m/s	1.2m/s	1.6m/s	2.0m/s	2.4m/s	2.8m/s
710	123.8	132.5	135.8	155.9	161.2	163.2
500	120.9	124.8	132.0	155.0	161.0	163.4
355	100.7	113.8	124.6	145.6	155.0	154.23
250	94.4	110.3	117.8	122.0	125.0	127
125	92.0	100.3	108.0	121.8	125.5	126.3
CB	123.7	127.8	130.3	132	132.9	134

Table A9: Wear(mg) at varying speed at constant load 120kg, time 45min at 150^{o}C(periwinkles brake pad)

Speed / Sieve Size(μm)	0.8m/s	1.2m/s	1.6m/s	2.0m/s	2.4m/s	2.8m/s
710	87.2	90.1	97.6	97.8	100.3	102
500	79.9	89.5	90.1	91.7	100.0	101.9
355	65.7	78.0	76.3	80.7	92.6	93.1
250	55.7	64.6	67.9	76.9	79.2	81.1
125	55.9	61.9	68.9	75.0	80.6	82.3
CB	120	123.4	128.9	130.5	145	146

Table A10: Wear (mg) of fan palm at varying load at constant speed 2.4m/s, time 45min at 150^{o}C

Load / Sieve Size(μm)	40kg	60kg	80kg	100kg	120kg	140kg
710	156.7	170.5	200.7	220	220	222.1
500	155.7	170	196	200	220	223
355	155	168.4	180	200	215	217
250	150	145	148	189	200	206.4
125	150	138.9	145	176	176.8	179.1
CB	135.6	137.7	143.8	148.9	150.7	155.4

Table A11Wear mg) of fan palm at varying load at constant speed of 2.4m/s, time 45min at 250°C

Sieve Size(μm)	40kg	60kg	80kg	100kg	120kg	140kg
710	156.7	170.5	200.7	220	220	222.1
500	155.7	170	196	200	220	223
355	155	168.4	180	200	215	217
250	150	145	148	189	200	206.4
125	150	138.9	145	176	176.8	179.1
CB	135.6	137.7	143.8	148.9	150.7	155.4

Table A12: Wear (mg) of fan palm at varying speed at constant load of 120kg, time 45min at 250°C

Speed / Sieve Size(μm)	0.8m/s	1.2m/s	1.6m/s	2.0m/s	2.4m/s	2.8m/s
710	148.9	155.7	160.5	175	178.9	177.0
500	145	145	156.7	175	175	176.5
355	134.5	145	155	168	174	176
250	126	126	148	165	173	175
125	124	129	143	155	164	169.3
CB	123.7	127.8	130.3	132	132.9	134

Table A13 Wear(mg) of fan palm at varying speed at constant load 120kg, time 45min at 150°C

Speed / Sieve Size(μm)	0.8m/s	1.2m/s	1.6m/s	2.0m/s	2.4m/s	2.8m/s
710	156	167	167	198	210	215
500	145	154	161	190.5	200	210
355	131	151	160	186	187.9	188
250	131	145	155.9	171	187	190
125	129	129	146	165	171	175
CB	120	123.4	128.9	130.5	145	146

Table A14 Coefficient of friction at varying load at constant speed of 0.8m/s, time 45min at 150^{o}C(periwinkles brake pad)

Load / Sieve Size(μm)	40kg	60kg	80kg	100kg	120kg	140kg
710	0.451	0.440	0.423	0.391	0.390	.28
500	0.453	0.450	0.423	0.410	0.400	.42
355	0.460	0.460	0.430	0.425	0.400	0.39
250	0.466	0.462	0.440	0.428	0.410	0.4
125	0.466	0.466	0.450	0.429	0.410	0.4
CB	0.35	0.35	0.32	0.31	0.315	0.3

Table A15 Coefficient of friction at varying load at constant speed of 2.8m/s, time at 250^{o}C(periwinkles brake pad)

Load / Sieve Size(μm)	40kg	60kg	80kg	100kg	120kg	140kg
710	0.445	0.440	0.420	0.380	0.382	0.37
500	0.450	0.450	0.422	0.400	0.385	0.365
355	0.455	0.455	0.423	0.428	0.400	0.39
250	0.462	0.462	0.430	0.425	0.400	0.4
125	0.464	0.463	0.440	0.427	0.410	0.4
CB	0.3	0.29	0.288	0.27	0.27	0.267

Table A16 Coefficient of friction at varying speed at constant load of 40kg, time at 150^{o}C (periwinkles brake pad)

Speed / Sieve Size(μm)	0.8m/s	1.2m/s	1.6m/s	2.0m/s	2.4m/s	2.8m/s
710	0.355	0.350	0.350	0.349	0.340	0.33
500	0.355	0.352	0.351	0.350	0.340	0.32
355	0.360	0.358	0.358	0.357	0.350	0.31
250	0.360	0.360	0.359	0.359	0.357	0.34
125	0.361	0.360	0.360	0.359	0.358	0.335
CB	0.38	0.37	0.37	0.351	0.33	0.31

Table A17 Coefficient of friction at varying speed at constant load of 40kg, time at 250^{o}C (periwinkles brake pad)

Speed / Sieve Size(μm)	0.8m/s	1.2m/s	1.6m/s	2.0m/s	2.4m/s	2.8m/s
710	0.352	0.348	0.343	0.330	0.310	0.287
500	0.352	0.350	0.350	0.342	0.320	0.3
355	0.355	0.352	0.352	0.350	0.340	0.32
250	0.360	0.355	0.355	0.354	0.347	0.33
125	0.360	0.358	0.358	0.356	0.350	0.31
CB	0.34	0.331	0.331	0.31	0.29	0.27

Table A18Coefficient of friction of fan palm at varying load at constant speed 0.18m/s, time at 150^{o}C

Load / Sieve Size(μm)	40kg	60kg	80kg	100kg	120kg	140kg
710	0.21	0.2	0.187	0.165	0.15	0.14
500	0.28	0.23	0.21	0.198	0.167	0.15
355	0.28	0.25	0.24	0.198	0.19	0.155
250	0.31	0.267	0.24	0.22	0.2	0.19
125	0.31	0.28	0.26	0.22	0.21	0.2
CB	0.35	0.35	0.32	0.31	0.315	0.3

Table A19 Coefficient of friction of fan palm at varying load at constant speed of 2.8m/s, time at 250^{o}C

Load / Sieve Size(μm)	40kg	60kg	80kg	100kg	120kg	140kg
710	0.2	0.187	0.177	0.156	0.14	0.13
500	0.2	0.2	0.184	0.65	0.141	0.13
355	0.24	0.24	0.2	0.189	0.17	0.15
250	0.29	0.25	0.25	0.2	0.2	0.19
125	0.31	0.28	0.24	0.21	0.2	0.18
CB	0.3	0.29	0.288	0.27	0.27	0.267

Table A20 Coefficient of friction of fan palm at varying speed at constant load of 40kg, time at 150^{o}C

Speed / Sieve Size(μm)	0.8m/s	1.2m/s	1.6m/s	2.0m/s	2.4m/s	2.8m/s
710	0.2	0.18	0.18	0.165	0.14	0.155
500	0.23	0.22	0.18	0.175	0.16	0.16
355	0.28	0.28	0.251	0.24	0.2	0.22
250	0.3	0.28	0.27	0.251	0.23	0.24
125	0.3	0.3	0.281	0.263	0.242	0.255
CB	0.34	0.33	0.32	0.31	0.3	0.29

Table A21 Coefficient of friction of fan palm at varying speed at constant load of 40kg, time at 250^{o}C

Speed / Sieve Size(μm)	0.8m/s	1.2m/s	1.6m/s	2.0m/s	2.4m/s	2.8m/s
710	0.2	0.171	0.17	0.154	0.15	0.14
500	0.2	0.185	0.18	0.155	0.154	0.14
355	0.22	0.21	0.2	0.22	0.19	0.18
250	0.291	0.29	0.261	0.245	0.24	0.22
125	0.295	0.29	0.281	0.278	0.255	0.24
CB	0.38	0.37	0.37	0.351	0.31	0.30

Table A22 Effect of speed on brake pad wear at constant contact pressure of 10bar after an average of 10 stops

Effect of speed on brake pad wear at constant contact pressure of 10bar after an average of 10 stops				
brake disk in (RPM)	commercial brake (CB)		laboratory brake pad (LB)	
	Mass(kg)	thickness (mm)	Mass(kg)	thickness (mm)
125	0.45	0.05	0.2	0.01
140	0.55	0.1	0.26	0.05
230	0.8	0.15	0.3	0.1
325	1	0.2	0.5	0.2
300	2	0.25	1	0.23

Table A23Average stopping time at constant pressure of 10 bar at varying speed

AVERRAGE STOPPING TIME AT CONSTANT PRESSURE OF 10 BAR AT VARYING SPEED			
S/N	DISC SPEED (RPM)	STOPPING TIME (SEC)	
		LABORATORY BRAKE PAD	COMMERCIAL BRAKE PAD
1	125RPM	2.5	3.2
2	140RPM	2.85	3.72
3	230RPM	3.15	4.15
4	300RPM	3.69	4.87
5	325RPM	4.15	5.13

Table A24Average stopping time at constant speed of 325 rpm at varying pressure

AVERAGE STOPPING TIME AT CONSTANT SPEED OF 325 RPM AT VARYING PRESSURE			
S/N	CONTACT PRESSURE (BAR)	STOPPING TIME (SEC)	
		LABORATORY BRAKE PAD	COMMERCIAL BRAKE PAD
1	8BAR	6.5	7
2	10BAR	6.3	6.87
3	12BAR	5.58	6.14
4	14BAR	4.43	5.76
5	16BAR	4.12	5.15

Table A 25Physical and Mechanical Properties of Periwinkle Shells

	Property	Value
1	Average length L (mm)	47.13
2	Average thickness t (mm)	1.1
3	Average volume (mm^3)	2,851.08
4	Average mass (kg)	0.08
5	Moisture content (%)	0.54
6	Hardness	45.4
7	Compressive strength (N/mm^2)	163
8	Specific gravity	2.73
9	Density g/cm^3	1.9

Source; National Metallurgical Development Centre,Jos2009

TABLEA 26 Physical and Mechanical Properties of Fan palm Shells

	Property	Value
1	Diameter (mm)	79.3
2	Thickness t (mm)	3.80
3	Volume (mm^3)	208,843.09
4	Mass (kg)	0.042
4	Moisture content (%)	12.25
6	Hardness	64.9
7	Compressive strength (N)	1100
8	Specific gravity	1.44
9	Density g/cm^3	0.99

Source; National Metallurgical Development Centre, Jos2009

Table A 27 Elemental composition of periwinkle shell

Compound	%
Al_2O_3	8.0%
SiO_2	24%
P_2O_5	0.8%
SO_3	1.0%
K_2O	2.3%
CaO	5.27%
TiO_2	2.36%
V_2O_5	0.08%
Cr_2O_3	0.61%
MnO	0.35%
Fe_2O_3	44.8%
NiO	0.16%
CuO	0.85%
ZnO	0.49%
ZnO	ND
Br	0.02%
SrO	0.76%
BaO	0.08%
MgO	1.54%
Na_2O	0.10%

Source; National Metallurgical Development Centre, Jos 2009

Table A 28Elemental composition of fan palm shell

COMPOUND	%
Al_2O_3	5.5%
SiO_2	19.9%
P_2O_5	0.78%
SO_3	0.87%
K_2O	1.61%
CaO	4.48%
TiO_2	1.96%
V_2O_5	0.18%
Cr_2O_3	0.67%
MnO	0.84%
Fe_2O_3	55.9%
GeO_2	3%
Ag_2O	3.57%
BaO	0.50%
NiO	0.16%
CuO	0.85%
ZnO	0.49%
Y_2O_3	0.26%
ZrO_2	0.42%
RuO_2	7.22%
WO_3	0.07%
Re_2O_7	0.2%
Au	0.34%

Source; National Metallurgical Development Centre, Jos 2009

Photograph of the Developed Brake Pad for Mercedes Benz 230E

APPENDIX B

PUBLICATIONS

1. Characterization of Periwinkle Shell as Asbestos – Free Brake Pad Material. The Pacific Journal of Science and Technology. Volume 13, Number 2 November 2012.
2. Evaluation of the Wear and Thermal Properties of Asbestos Free Brake Pad using Periwinkle shell Particles. Usak University Journal of Material Sciences
3. Morphology and Properties of Periwinkle Shell Asbestos – free Brake pad. Journal of King Saud University – Engineering Sciences. Engineering Sciences (2013) XXX XXX
4. Effect of Periwinkle Shell Particle size on the Wear Behaviour of Asbestos free Brake pad. Elsevier- Results in Physics